

**COASTAL EVOLUTION OF PACIFIC ISLANDS IN RESPONSE TO SEA LEVEL  
CHANGE DURING THE MID-HOLOCENE**

A DISSERTATION SUBMITTED TO THE GRADUATE DIVISION OF THE UNIVERSITY  
OF HAWAI'I AT MĀNOA IN PARTIAL FULFILLMENT OF THE REQUIREMENTS FOR  
THE DEGREE OF

**DOCTOR OF PHILOSOPHY**

**IN**

**EARTH AND PLANETARY SCIENCES**

MAY 2019

By

Haunani Hi'ilani Kane

Dissertation Committee:

Charles H. Fletcher, Chairperson

Craig R. Glenn

Henrietta Dulai

Ralph M. Moberly

David W. Beilman

Keywords: sea level rise, stratigraphy, sedimentology, carbonate, climate change, atoll,  
foraminifera, Pacific Islands, Samoa, Majuro



## ACKNOWLEDGEMENTS

### **He pūko‘a kani ‘āina**

*A coral reef that grows into an island.*

A person beginning in a small way gains steadily until she becomes firmly established.

For islanders across the globe, your strength and resilience does not go unnoticed. This work was accomplished with you in mind.

I would to thank my committee first. Chip Fletcher, your guidance over the past nine years as a graduate student has enabled me to proudly view the world through a geological lens. Ralph Moberly, thank you for digging deep into your photographic memory to help me identify my thin sections whenever I got stumped. Craig Glenn, mahalo for introducing me to the world of carbonate sedimentology. Dave Beilman, your guidance and assistance in the world of radio carbon dating has been invaluable. Henrietta Dulai, you are an amazing scientist, and an inspiration to young and aspiring female scientists.

To the past and present coastal geology nerds; Shellie, Tiff, Matt, Kammie, Anna, Kristian, Korey, Cuong, and Alisha, you have been my ‘rocks’, my friends, and my colleagues. Mahalo nui from the bottom of my heart for your help in the field and for all of the laughs in the office. Bruce Richmond (BR), SeanPaul, Brent, and the rest of the USGS Santa Cruz team thank you for allowing me to tag along and teaching me to interpret tsunami deposits.

To my family, thank you for always supporting me and seeing the value in receiving an education. Clifford, thank you for helping me shape my story into one that I can be proud of. Native Hawaiian Student Services, Kahuewaiola, Kuaana, Maile SOEST mentoring program, NHSEMP, Kamehameha Schools, Rosie, Anela, Aurora, Ku‘umealoha, Lelemia, Kealoha, Kanoe(s), Aloha, Lauren, Christian, Lisa, Geo and all of the other kānaka on campus it is with pride that I say I am a product of YOU. Mahalo for reminding us kānaka that we are worthy of PhD degrees in any field we choose. My Nā Kama Kai ohana, thank you for the endless love and support. Mahalo for giving me the opportunity to learn from you and your children.

Mahalo nui Pua Lincoln for sharing wā 14 of the Kumulipo with me and for explaining that Hina was established after all the stars were born. From Hina came our corals and the foundations of island building. I believe our kūpuna knew that one day we would be ready to relearn their

stories. If by chance some young kanaka reads my dissertation, the words below were created by our kūpuna and translated by our Queen Lili‘uokalani with you in mind.

1901. Lu ka 'ano'ano Makali'i, 'ano'ano ka lani
1902. Lu ka 'ano'ano akua, he akua ka la
1903. Lu ka 'ano'ano a Hina, he walewale o Lonomuku
1904. Ka 'ai a Hina-ia-ka-malama o Waka
1905. I ki'i [i]a e Wakea a Kaiuli
1906. A kai ko'ako'a, kai ehuehu
1907. Lana Hina-ia-ka-malama he ka
1908. Kaulia a'e i na wa'a, kapa ia Hina-ke-ka ilaila
1909. Lawe [i]a uka, puhuluholu ia
1910. Hanau ko'ako'a, hanau ka puhi
1911. Hanau ka inaina, hanau ka wana
1912. Hanau ka 'eleku, hanau ke 'a
1913. Kapa ia Hina-halako'a ilaila

Strewed the seeds, finest seeds of stars in the heavens;  
Strewed fine seed of gods, the sun became a god,  
Strewed the seeds from Hina; Lonomaku was formed like jelly,  
The food on which subsisted Hinahanaikamalama or Waka,  
Sought for by Wakea in the deep blue sea,  
In the coral mound, 'mongst rough waves,  
Causing Hinaiakamalama to float, a sprig,  
'Twas flung into his canoe, she was thereby called Hina the sprig;  
Taken ashore and warmed by the fire.  
Corals were born and eels were born,  
Sea-urchins were born, sea-eggs were born.  
Blackstone was born, volcanic rocks were born,  
Whereby she was named Hinahalakoa.

Finally, mahalo Hōkūle‘a for teaching me to observe the world through the eyes and senses of my kūpuna. You have been my biggest teacher, and you have taught me to love Hawai‘i. To my brothers and sisters of the sea, thank you for deciding to go on this journey with me.

-Haunani

## ABSTRACT

Understanding the timing and influence of past examples of sea level change is important for discerning coastal sediment dynamics, interpreting early human migration and guiding decision making related to future sea level rise (SLR). The mid-Holocene sea level highstand is now well documented across the equatorial Pacific, with peak sea level values reaching from 0.25-3.00 m above present mean sea level between 1,000-5,000 yr BP. Interpretations of the composition and age of buried island sediment and fossil reefs were used to characterize the response of high volcanic islands and low lying atolls to sea level change.

At eastern ‘Upolu, a volcanic high island in Sāmoa (Chapter 2) we find that a sea level fall of 0.3-1.0 m, approximately 1899–2103 cal yr BP (calendar years before present), triggered the burial of the fossil beach as the coastal plain expanded towards the sea. A millennium of coastal plain development was further required before post mid-Holocene drawdown in regional sea level produced coastal settings that were morphologically attractive for human settlement.

In Chapter 3, a 5,000 year record of ecosystem response to mid- to late- Holocene sea level change is interpreted from fossil-reef cores and atoll island sediment. Emergence of a foraminifera dominant atoll reef-island required (1) the formation of a low porosity, limestone platform by reef-flat infilling and diagenesis, and (2) sea level regression and decreased hydrodynamic energy to activate a highly productive *Calcarina* foraminifer dominated reef-flat.

Chapter 4 couples the geologic record and future projections of SLR to derive place based sea level thresholds and time frames to anticipate rapid island evolution in response to future SLR within the Republic of the Marshall Islands. Under all sea level projections reef-islands will actively evolve within this century as SLR exceeds threshold values conducive with former island building. Impacts are further expedited due to loss of groundwater, accelerating

SLR, and infrastructure damage. SLR threatens the cultural identify of atoll nations and as such will require adaptable planning methods, reflective of multidisciplinary research, and open minded, multi-world views.

## Table of Contents

ABSTRACT.....	v
LIST OF TABLES.....	ix
LIST OF FIGURES.....	x
LIST OF EQUATIONS.....	xi
CHAPTER 1. INTRODUCTION.....	1
1.1 Mid- to late-Holocene sea level dynamics.....	2
1.2 Island evolution in response to mid- to late-Holocene sea level change.....	5
1.3 Goals and dissertation structure.....	8
CHAPTER 2. COASTAL PLAIN STRATIGRAPHY RECORDS TECTONIC, ENVIRONMENTAL, AND HUMAN HABITABILITY CHANGES RELATED TO SEA LEVEL DRAWDOWN, ‘UPOLU SĀMOA.....	9
Abstract.....	9
2.1 Introduction.....	10
2.2 Regional Setting.....	13
2.2.1 Subsurface stratigraphy of the carbonate plain.....	16
2.2.2 Vertical shifts in island elevation.....	18
2.2.3 The role of tsunamis and storms in reworking coastal plain sediments.....	19
2.3 Methods.....	21
2.3.1 Cores (sample collection).....	21
2.3.2 Topographic Data.....	23
2.3.3 Sedimentology, age, and composition of the coastal plain.....	23
2.4 Results.....	24
2.5 Discussion.....	30
2.5.1 Improving the interpretation of coastal plain evolution.....	32
2.5.2 Implications of coastal evolution upon past and future societies.....	34
2.6 Conclusion.....	35
CHAPTER 3. INTERPRETING BIO-GEOLOGIC LINKAGES FROM A WINDWARD REEF-ISLAND SYSTEM, BOKOLLAP ISLAND, MAJURO.....	38
Abstract.....	38
3.1 Introduction.....	39

3.2 Methods.....	40
3.2.1 Field setting.....	40
3.2.2 Reef-island stratigraphy.....	41
3.3 Results and discussion .....	43
3.3.1 Modern island-building components .....	43
3.3.2 Bio-geologic linkages recorded in the fossil record.....	46
3.3.3 Future reef-island resiliency is dependent upon sediment infilling and reef ecology.....	60
3.4 Conclusion .....	62
CHAPTER 4. RETHINKING REEF-ISLAND STABILITY IN THE REPUBLIC OF THE MARSHALL ISLANDS.....	64
Abstract.....	64
4.1 Introduction.....	65
4.1.1 The now .....	65
4.1.2 The recent past .....	66
4.1.3 The geologic record .....	66
4.2. Methods.....	68
4.2.1 Modeling island formation.....	68
4.2.2 Sea level threshold.....	73
4.3 Observations of reef-island formation .....	74
4.4 Reef-islands will actively evolve under all sea level scenarios this century.....	78
4.5 Discussion.....	80
4.5.1 Sea level thresholds in the context of previous studies.....	80
4.5.2 Other considerations for the future stability of reef-islands under elevated sea level .....	83
4.5.3 Resiliency of island nations to the rising tide will require shifts in world views.....	85
REFERENCES .....	86
Appendix 1. Carbonate Identification.....	96

## LIST OF TABLES

Table 2.1.....	20
Table 2.2.....	28
Table 3.1.....	47
Table 3.2.....	53
Table 3.3.....	59
Table 4.1.....	71
Table 4.2.....	73
Table 4.3.....	78
Table 4.4.....	81

## LIST OF FIGURES

Figure 1.1.....	3
Figure 1.2.....	6
Figure 1.3.....	7
Figure 2.1.....	13
Figure 2.2.....	15
Figure 2.3.....	16
Figure 2.4.....	22
Figure 2.5.....	26
Figure 2.6.....	31
Figure 3.1.....	42
Figure 3.2.....	45
Figure 3.3.....	49
Figure 3.4.....	50
Figure 3.5.....	56
Figure 3.6.....	57
Figure 3.7.....	61
Figure 4.1.....	75
Figure 4.2.....	76
Figure 4.3.....	79
Figure 4.4.....	82

## LIST OF EQUATIONS

Equation 2.1.....	18
Equation 3.1.....	42
Equation 4.1.....	69

## CHAPTER 1. INTRODUCTION

Inundation and erosion related to sea-level rise (SLR) threatens the habitability of critical coastal ecosystems, and the existence of coastal communities. Understanding the timing and influence of past examples of sea level change is important for discerning coastal sediment dynamics, interpreting early human migration and occupation histories and guiding decision making related to future SLR. Interpretations of the composition and age of buried island sediment and fossil reefs were used in this dissertation to characterize the response of high volcanic islands (e.g. Sāmoa) and low lying atoll (e.g. Majuro atoll) reef-islands to sea level change. Here we refer to high volcanic islands as those islands that are of volcanic origin, have well developed mountains, and carbonate sediment is limited to the coastal margins. In contrast atolls are typically composed of a ring shaped reef that encircles a central lagoon. Reef-islands are low lying accumulations (typically less than 3 m in elevation) of unconsolidated sand and rubble that is derived entirely from the nearshore coral reef ecosystem and deposited upon carbonate platforms (i.e. fossil reefs) located within atoll lagoons, atoll rims, or mid-ocean reefs (Woodroffe et al., 1999). The overarching goal of this dissertation was to elucidate how changes in mid- to late-Holocene sea level influenced the formation and evolution of Pacific high islands and low lying atoll reef islands.

The ‘ōlelo no‘eau (Hawaiian proverb) *ka wā ma mua, ka wā ma hope* describes from a Hawaiian perspective the value of referencing the past to better understand current and present day dilemmas. When translated literally, “ka wā ma mua” means “the time in front” however in Hawaiian thinking, it describes the time that came before the present (Ching, 2003). Furthermore, “ka wā ma hope” literally means “the time in back” or from a Hawaiian perspective the time which follows this time in which we live (Ching, 2003). According to Kame`eleihiwa (1992) “it

is as if the Hawaiian stands firmly in the present, with his back to the future, and his eyes fixed upon the past, seeking historical answers for present day dilemmas.” Following this line of thought, my research uses a Hawaiian way of thinking to investigate past changes in sea level during the mid- to late-Holocene to better understand how islands and island people will be impacted by future SLR.

### **1.1 Mid- to late-Holocene sea level dynamics**

In order to understand how Pacific islands respond to SLR, it is important to first understand the geophysical processes that triggered mid- to late-Holocene sea level change. Reconstructing a global or relative sea level history is a very complex process because it calls upon a number of different fields of science and is thus an interdisciplinary approach. SLR is a function of both surface processes (melting of land ice and thermal expansion of water) and solid earth dynamics (elastic deformation of the ground surface). These processes result in rates and patterns of sea level change that are not uniform globally (Spada et al., 2013). To better understand coastal impacts of surface and solid earth processes, sea level dynamics are discussed in the context of elastic (instantaneous) and postglacial ( $10^3$  to  $10^5$  yr) time scales (Conrad, 2013) (**Figure 1.1**).

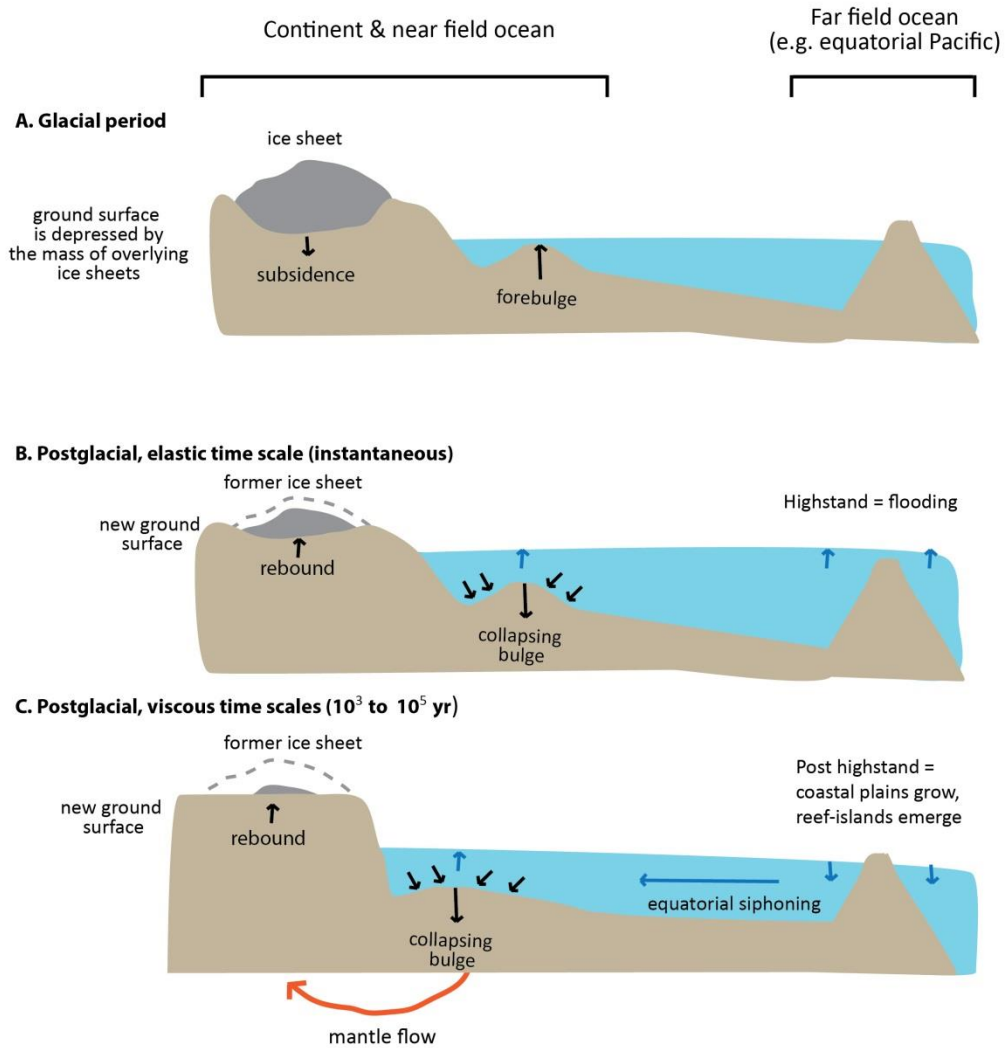


**Figure 1.1** A) During glacial periods ice sheets impose a large enough load to depress the underlying ground surface, and create a forebulge at the adjacent seafloor. B) As the earth warms, the instantaneous response to deglaciation is eustatic sea level rise in both the near field region and the far field region. C) Over viscous time scales ( $10^3$  to  $10^5$  yr) the solid Earth's response to deglaciation is sea level rise in the near field, and sea level fall in the far field regions.

The solid earth deforms instantaneously in response to the collapse of ice sheets (**Figure 1.1B**). First the direct addition of meltwater to the ocean results in eustatic SLR, with the exception of near-field regions (Polar Regions located at and near long-term sources of ice). In the near field region, melting ice reduces the mass or load on the ground surface, and causes the land formerly covered in ice to uplift. The nearby seafloor or ocean basins are subsequently depressed as they gain mass from additional water that is added as ice sheets melts (Conrad, 2013). A secondary impact in the nearfield area is related to a decreased gravitational attraction of seawater to land ice and a subsequent decline in the near field sea surface (Grossman et al., 1998).

On the time scales of  $10^3$ - $10^5$  years, the solid Earth's viscous response to deglaciation begins to impact relative sea level experienced in the near and far field (Conrad, 2013). During glacial periods ice sheets impose a large enough load to depress the underlying ground surface, and create a flexural bulge on the lithosphere in front of the load (of ice sheets) (**Figure 1.1A**). The sea-floor adjacent to continents uplifts, and creates a feature known as a forebulge. As the Earth warms and ice sheets continue to melt, the load upon land diminishes and the viscous response of the Earth's surface is a collapse in the forebulge (**Figure 1.1C**). An increased volume in the seafloor triggers "equatorial syphoning", a processes by which a flux of meltwater from far-field equatorial regions migrates towards the near field deglaciated areas (**Figure 1B**). The resulting impact is enhanced SLR in the nearfield and local relative sea level fall in far field regions. The collapse in the Last Glacial Maximum induced forebulge and subsequent "equatorial ocean siphoning" (Mitrovica and Peltier, 1991) resulted in the mid-Holocene highstand in the equatorial Pacific region.

## 1.2 Island evolution in response to mid- to late-Holocene sea level change

Sea level change during the mid- to late- Holocene played a critical role in the development of coastal plains at high Pacific Islands, and the emergence of low lying reef-islands. The mid-Holocene sea level highstand is documented across the equatorial Pacific with peak sea level values ranging from 0.25-3.00 m above present mean sea level (MSL) between 1,000-5,000 yr BP (Fletcher and Jones, 1996; Grossman et al., 1998; Dickinson, 2003; Woodroffe et al., 2012). Previous studies (Grossman et al., 1998; Kayanne et al., 2011; Yamano et al., 2014) estimate mid-Holocene sea level by identifying and dating emergent paleoshoreline features that formed within a restricted elevation range relative to the sea surface (Dickinson, 2001). Intertidal corals such as microatolls are believed to be the most precise sea level indicators with an indicative range as low as 3 cm (e.g., Smithers and Woodroffe, 2000). Beachrock is often used as a mid- to late-Holocene tidal range indicator, and uncertainty can be reduced to half the tidal amplitude if the deposit can be referenced to the upper or lower intertidal zone (Mauz et al., 2015).

The sedimentological record of high Pacific Islands can be used to infer the geomorphic response and environmental consequences of coastal evolution in response to changes in sea level and local tectonics. At high islands, coastal plain formation and development is linked to sea level regression following a highstand (**Figure 1.2**) (Calhoun and Fletcher, 1996). Whereas at low lying reef-islands, island emergence has been documented during mid-Holocene SLR (pre-highstand) (Kench et al., 2005, 2014b), during the highstand (Kayanne et al., 2011), and as sea level fell in the recent 1,000-2,000 years (post-highstand) (Woodroffe and Morrison, 2001; Mckoy et al., 2010) (**Figure 1.3**).

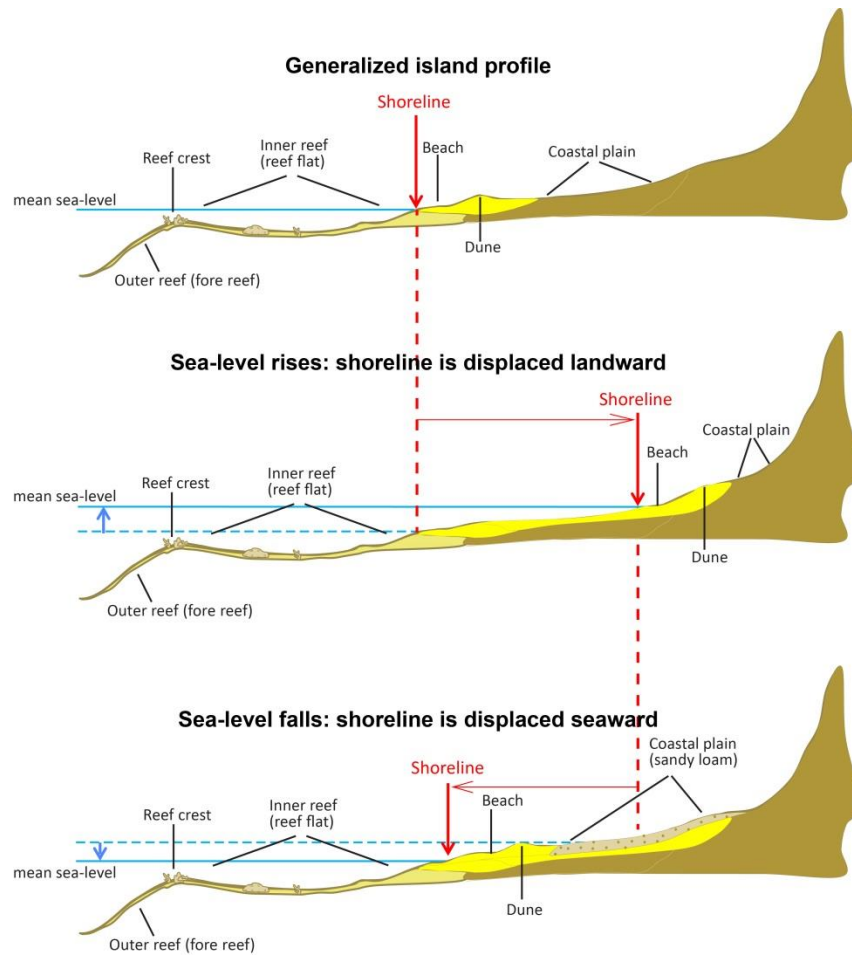


**Figure 1.2** Generalized high island profile and coastal plain evolution in response to sea level change.

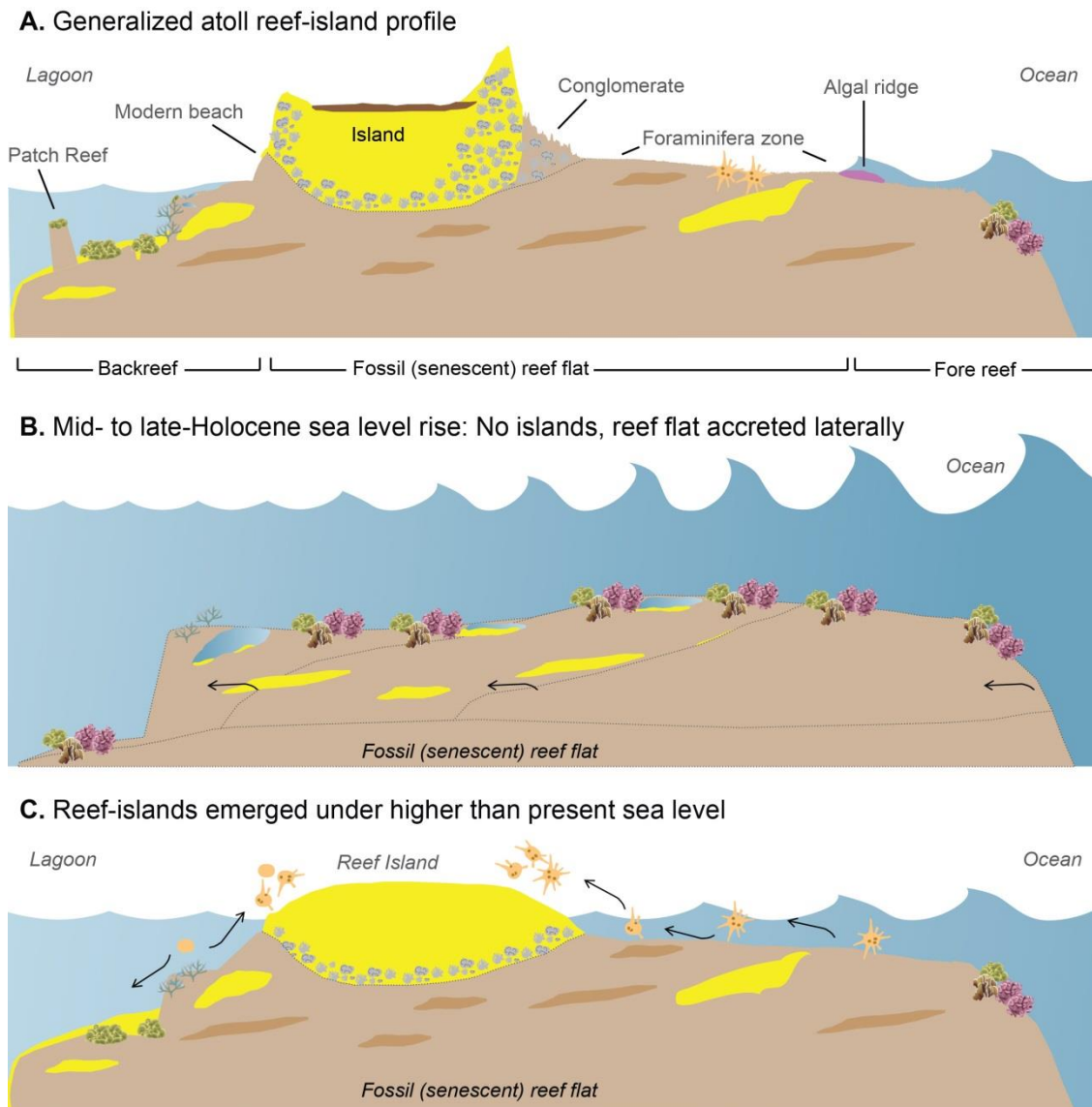


**Figure 1.3** A.) Generalized atoll reef-island profile. B.) During mid- to late-Holocene sea level rise reef islands did not exist. This was a time when coral-algal ecosystems dominated and laterally accreted across the fossil reef flat. C.) Reef island emergence is documented under rising sea-level, during the highstand, and following the highstand. Unconsolidated sand and rubble derived from the adjacent coral reef ecosystem accumulated, and rapid island formation followed.

### **1.3 Goals and dissertation structure**

The overarching goal of this dissertation was to elucidate how changes in mid-Holocene sea level influenced the formation and evolution of Pacific Islands. Three projects compose this dissertation. Chapter 2 characterizes coastal plain evolution of eastern ‘Upolu, a volcanic high island in Sāmoa. The primary objective of Chapter 2 was to assess the impact of mid-Holocene sea level change upon the habitability of a narrow coastal plain. Here we find that a sea level fall of 0.3-1.0 m, approximately 1899–2103 cal yr BP (calendar years before present), triggered coastal plain progradation. However a millennium of coastal plain development was further required before buried anthropogenic deposits indicative of the first human population of Sāmoan people were established.

Chapter 3 and 4 characterize the role sea level played in the emergence and evolution of low lying reef-islands. In Chapter 3 atoll reef-islands are described as bio-geologically linked systems such that reef-islands are composed entirely of unconsolidated sand and rubble derived from the adjacent reef-flat. Furthermore a series of fossil-reef cores and island sediment are used to interpret a 5,000 year record of ecosystem responses to mid- to late- Holocene sea level change. Chapter 4 couples the geologic record and future projections of SLR to derive place based sea level thresholds and time frames to anticipate rapid island evolution in response to future SLR within the Republic of the Marshall Islands.

**CHAPTER 2. COASTAL PLAIN STRATIGRAPHY RECORDS TECTONIC,  
ENVIRONMENTAL, AND HUMAN HABITABILITY CHANGES RELATED TO SEA  
LEVEL DRAWDOWN, ‘UPOLU SĀMOA**

*Published:* Kane, H.H., Fletcher, C.H., Cochrane, E.E., Mitrovica, J.X., Habel, S., and Barbee, M. (2017), Coastal plain stratigraphy records tectonic, environmental, and human habitability changes related to sea level drawdown, Upolu, Samoa: *Quaternary Research (United States)*, v. 87, doi:10.1017/qua.2017.2.

**Abstract** - Coastal plain stratigraphy is often over looked in paleo sea level reconstructions because carbonate sediments do not precisely constrain former sea level. Pacific Island sedimentology provides an invaluable record of geomorphic and environmental consequences of coastal evolution in response to changes in sea level and local tectonics. A series of coastal auger cores obtained from eastern ‘Upolu reveal a subsurface carbonate sand envelope predominately composed of coral and coralline algae derived from the reef framework. Coupling the sedimentological record with geophysical models of Holocene sea level we identify a critical value (0.3-1.0 m) during the falling phase of the sea level highstand (1899-2103 cal yr BP) that represents the transition from a transgressive to a regressive environment, and initiates coastal progradation. Correlating the critical value with time we observe nearly a millennium of coastal plain development is required before a small human population is established. Our findings support previous studies arguing that Sāmoa was colonized by small and isolated groups, as post mid-Holocene drawdown in regional sea level produced coastal settings that were morphologically attractive for human settlement. As future sea level approaches mid-Holocene

highstand values, lessons learned from Pacific Island sedimentological records may be useful in guiding future decisions related to coastal processes, and habitat suitability.

## **2.1 Introduction**

Understanding the timing and influence of the mid-Holocene highstand is important for discerning coastal evolution of Pacific Islands, interpreting early human migration and occupation histories (Allen, 1998; Rieth et al., 2008; Cochrane et al., 2013), and guiding decision making related to future SLR (Dickinson, 2003; Goodwin and Grossman, 2003). Holocene sea level change in the far field region was initiated by eustatic SLR (Lambeck et al., 2002) associated with the addition of glacial meltwaters and thermal expansion of seawater following the last ice age. In the Northern hemisphere melting ended approximately 5,000-6,000 cal yr BP (Alley and Clark, 1999) and, assuming no additional meltwater was added to the oceans, Earth continued to deform viscously on time scales of 1,000-100,000 yr (Conrad, 2013). The solid Earth's viscous response to deglaciation produced emergent coastal systems in areas formerly occupied by ice sheets, and submergent coastal systems in the region of the peripheral forebulge (Mitrovica and Milne, 2002; Conrad, 2013). Far field locations such as the equatorial Pacific Islands experienced a mid- to late- Holocene drawdown in sea level (termed 'equatorial ocean syphoning', Mitrovica and Peltier, 1991) as seawater migrated to the near field and filled growing oceanic basins related to the collapsing forebulge (Mitrovica and Peltier, 1991) and the ocean load induced by levering of continental margins (Mitrovica and Milne, 2002).

The highstand is documented across the equatorial Pacific with peak sea level values ranging from 0.25-3.00 m above present mean sea level (MSL) between 1,000-5,000 yr BP (Fletcher and Jones, 1996; Grossman et al., 1998; Dickinson, 2003; Woodroffe et al., 2012).

Woodroffe et al., (2012) argues that Holocene sea level oscillations of a meter or greater are likely to have been produced by local rather than global processes. Thus the timing and magnitude of the high-stand varies between island settings due to localized uplift, or subsidence (Dickinson, 2014) and distance from continental margins (Mitrovica and Milne, 2002). Previous studies estimate mid-Holocene sea level by identifying and dating emergent paleoshoreline features that formed within a restricted elevation range relative to the sea surface (Dickinson, 2001). Intertidal corals such as microatolls are believed to be the most precise sea level indicators with an indicative range as low as 3 cm (e.g., Smithers and Woodroffe, 2000). Beachrock is often used as a paleo tidal range indicator, and uncertainty can be reduced to half the tidal amplitude if the deposit can be referenced to the upper or lower intertidal zone (Mauz et al., 2015).

Coastal plain sedimentology is often overlooked in mid-Holocene sea level studies because carbonate sediments alone are not indicative of a precise relationship to former sea level (Goodwin and Grossman, 2003). However, the subsurface sedimentological record of high Pacific Islands is of value because it can be used to infer the geomorphic response and environmental consequences of coastal evolution in response to changes in sea level and local tectonics. Prior research has shown that as sea level falls following a highstand, carbonate sediment is stranded along the coastal plain and later buried by terrigenous sediment as the coastal plain progrades seaward (Calhoun and Fletcher, 1996). The subsurface carbonate unit thus preserves a record of the landward extent of marine transgression, supplementing prior estimates of highstand sea level.

Pacific archaeologists have had a long-standing interest in the effects of sea level drawdown and environmental habitability along coastal plains as exemplified by analyses at Tikopia, Solomon Islands (Kirch and Yen, 1982), Manu‘a Islands, Sāmoa (Kirch, 1993), Ha‘apai group, Tonga (Dickinson et al., 1994), Aitutaki, Cook Islands (Allen, 1998), and Mo‘orea (Kahn et al., 2014). Early in the drawdown phase of the highstand some coastal landforms may have been less conducive to large populations and productive forms of staple food crops such as wetland taro (*Colocasia esculenta*) (Kirch, 1983; Spriggs, 1986; Quintus et al., 2015). Continued sea level fall, however, eventually led to the expansion of sandy coastal flats characterized by increased size of coastal lowlands, eased coastal access, and low sloped environments more suited to larger human populations (Rieth et al., 2008; Cochrane et al., 2016). Building upon prior archaeological studies, we provide a geological reconstruction of ‘Upolu, Sāmoa’s (-14° 1.2’ S, -171° 26.0’ W; **Figure 2.1**) coastal plain because of the unique potential to assess the impacts of differential subsidence and local variability of sea level across a single island. We define the value below which sea level must fall for a carbonate coast to prograde seaward, as the critical value of sea level (**Figure 2.3A**). The critical value initiates a regressive phase of island evolution, enabling the development of coastal landforms for a variety of human uses and settlement.

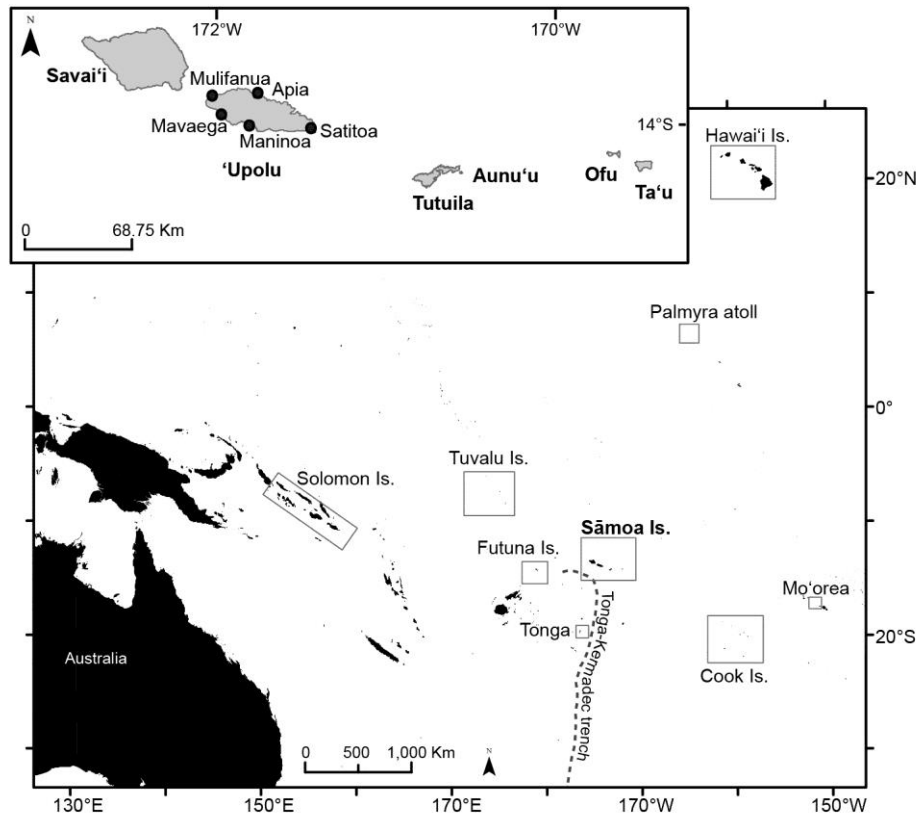


**Figure 2.1:** The Central Pacific Island group of Sāmoa consists of three large, high volcanic islands (Savai'i, 'Upolu, and Tutuila) and several smaller islands that are bordered in the southwest by the Tonga-Kermadec trench. Previous sea level assessments in Sāmoa have focused largely on 'Upolu island, while the majority of relevant archaeology, paleoclimate, tropical cyclone, and tsunami assessments have been conducted at neighboring Pacific islands.

## 2.2 Regional Setting

The Sāmoan archipelago consists of three large, high volcanic islands (Savai'i, 'Upolu, and Tutuila) and several smaller islands (**Figure 2.1**) that formed as the Pacific Plate moved west

over a stationary hotspot. Currently the hotspot is located beneath Vailulu‘u, a seamount east of Tutuila, however post erosional volcanism has occurred as recently as AD 1905-1911 on Sava‘i (Terry et al., 2006). We chose Satitua village ( $14^{\circ} 1.73' S$ ,  $171^{\circ} 25.96' W$ ), located along the southeastern coast of ‘Upolu, as the focus of this study because modelled subsidence rates are negligible (Dickinson, 2007), and tropical cyclone and tsunami impacts are well documented in this region (Jaffe et al., 2011; McAdoo et al., 2011; Richmond et al., 2011).

Satitua is characterized by a relatively broad coastal plain (up to 300 m in width) bordered on one end by a gradually ascending alluvial slope and on the other by a wide, shallow ( $< \sim 5$  m) fringing reef (Richmond et al., 2011; **Figure 2.2**). The eastern and southern coasts of ‘Upolu are characterized by regionally thicker coastal deposits due to exposure to the dominant southeasterly trade winds, well-developed and sediment-rich fringing reef complexes, and relatively high wave energy (typical 1.3-2 m wave heights may exceed 10 m during severe cyclones) (Richmond et al., 2011). A rock revetment protects the coastal Satitua community and prevents the formation of a modern beach.

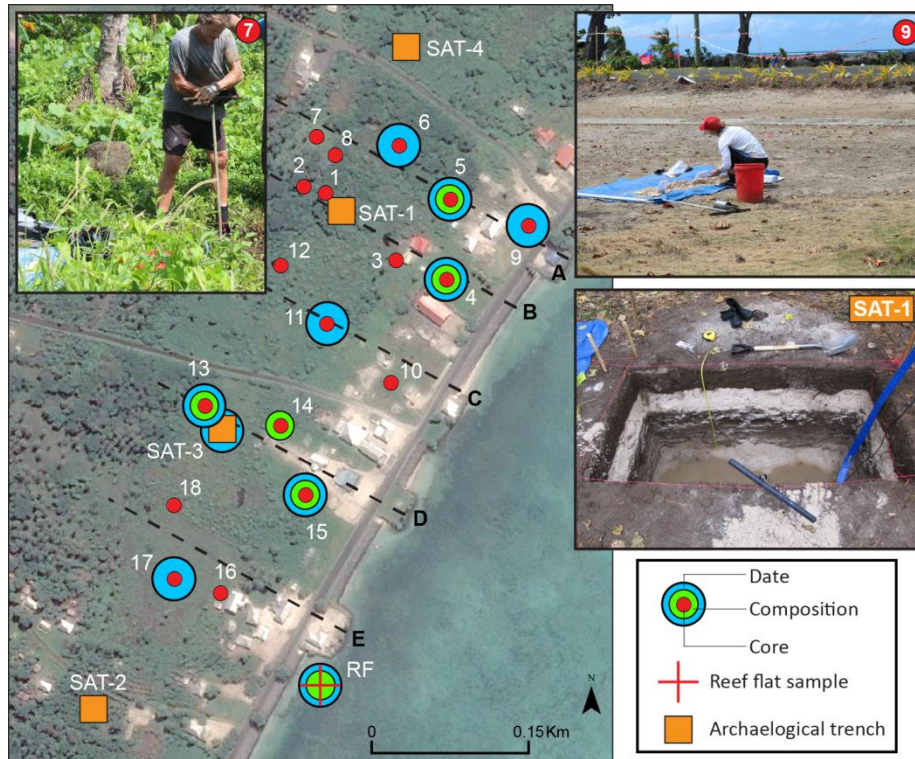


**Figure 2.2:** Satitua, ‘Upolu is characterized by a relatively broad coastal plain (up to 300 m in width bordered on one end by a gradually ascending alluvial slope and on the other by a wide, shallow (<~5 m) fringing reef. The location of cores, archaeological trenches, dated carbonate samples, and samples analyzed for composition are identified along the coastal plain. The rock wall revetment that borders the coastline was breached by the 2009 South Pacific tsunami and a remnant carbonate sand apron is still visible at the surface near core 9. Moving inland a loam or clay surface develops and supports dense vegetation at core 7. Archaeological trench 1 (SAT-1) is located near core 1 and depicts the distinct boundaries between carbonate and terrigenous layers of sediment (described in Cochrane et al., 2016).

### 2.2.1 Subsurface stratigraphy of the carbonate plain

Two studies on the island of ‘Upolu, Sāmoa focused on the post mid-Holocene highstand sedimentary sequence. Mulifanua (northwestern ‘Upolu; **Figure 2.3B**), the oldest known Sāmoan settlement site (2880–2750 cal yr BP), was discovered submerged approximately 115 m offshore (Dickinson and Green, 1998; Petchey, 2001). A cultural midden layer was deposited upon a thick (4.58 m thick) sandy beach that originally lay above sea level during the highstand. Following the highstand, local subsidence outpaced sea level fall, and the surface of the beach became cemented into beachrock within the intertidal zone. Beachrock (0.75 m thick) currently extends up to the modern lagoon floor, preserving the underlying carbonate sand and cultural midden unit.

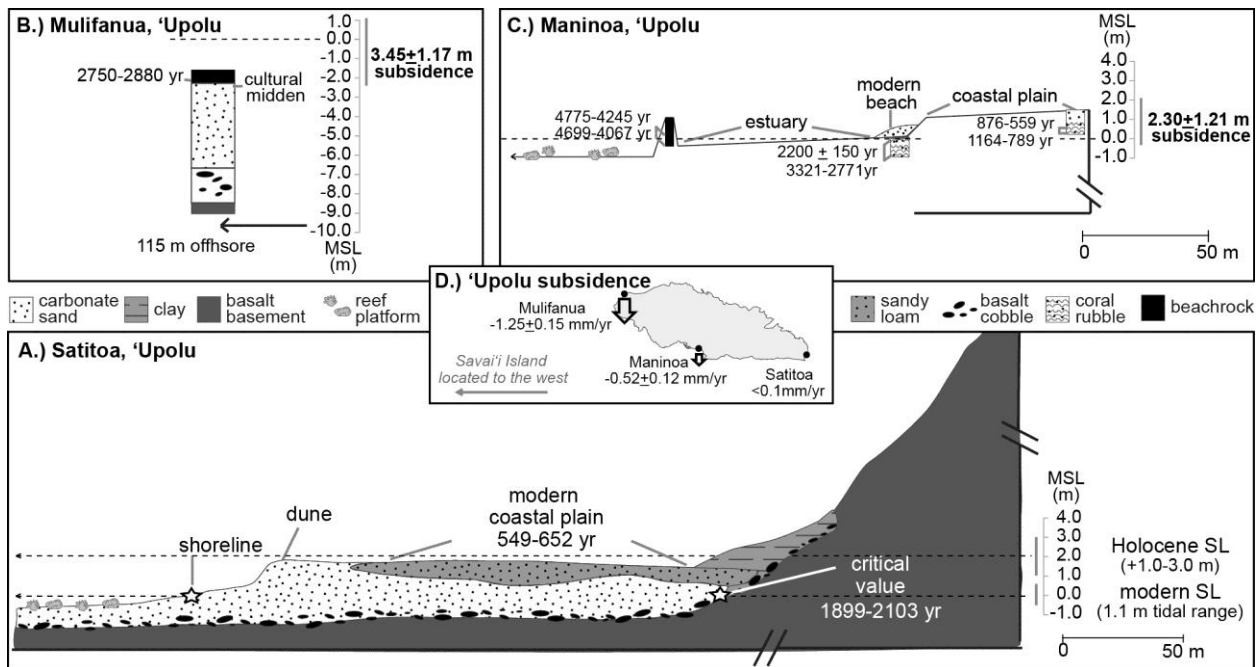


**Figure 2.3:** ‘Upolu Island coastal stratigraphy interpreted at Mulifanua (after Dickinson & Green, 1998), Maninoa (after Goodwin & Grossman, 2003), and Satitua (this study) as a function of Holocene sea level change, and local tectonics. All ages are reported as calendar years before present (cal yr BP). A.) We define the value below which sea level must fall for a carbonate coast to prograde seaward, as the critical value of sea level. Following the 1-3 m modelled mid-Holocene highstand, coastal progradation at Satitua was initiated as sea level fell beneath a critical value of 0.3-1.0 m (approx. 1899-2103 cal yr BP), and the coastal zone switched from a transgressive to a regressive environment. B.) The general stratigraphy at Mulifanua reveals paleobeachrock that formed as beach sands were cemented within the intertidal zone approximately 2750-2880 cal yr BP. The entire unit is now a submerged feature approximately 115 m offshore due to local subsidence ( $3.45 \pm 1.17$  m total subsidence). C.) Offshore paleobeachrock formed at Maninoa prior to 4000 cal yr BP and subsided ( $2.30 \pm 1.21$  m) to its current position within the modern intertidal zone. The coast prograded 50-100 m in response to a slight lowering in relative sea level between 300-700 cal yr BP. D.) Differential subsidence rates were calculated for ‘Upolu based upon the elevation and age of beachrock at Mulifanua and Maninoa (Dickinson 2007).

Building upon the work of Dickinson and Green (1998), Goodwin and Grossman (2003) analyzed coastal sedimentology along a shore perpendicular transect at Maninoa, southern ‘Upolu (**Figure 2.3C**). Offshore, stranded beachrock is interpreted as a former carbonate beach that formed around the time of the mid-Holocene highstand (4699-4067 cal yr BP) (Goodwin and Grossman, 2003). Because the offshore beachrock is not emergent and instead is located within the modern intertidal zone, the author’s concluded that southern ‘Upolu subsided since the

highstand. In addition the region is believed to have experienced expansive coastal plain progradation (50-100 m) between approximately 300-1000 cal yr BP in response to a slight lowering in relative sea level (Goodwin and Grossman, 2003).

### 2.2.2 Vertical shifts in island elevation

Accounting for vertical shifts in island elevation in response to local or regional tectonism is necessary to accurately reconstruct paleo sea level (Dickinson, 2001). Over time, shorelines may be vertically displaced due to a volcanic load creating lithospheric flexure (Pirazzoli and Montaggioni, 1988; Muhs and Szabo, 1994). For example, subsidence rates of the island of ‘Upolu (Mulifanua and Maninoa) (**Figure 2.1**) were re-estimated (Equation 2.1) by Dickinson (2007) based upon the elevation and age of beachrock (interpreted as a paleoshoreline indicator) at each site, and a correction for ice age sea level change (Mitrovica and Peltier, 1991) across each respective time period.

$$\text{Subsidence rate } \left( \frac{\text{mm}}{\text{yr}} \right) = \frac{\text{Elevation of dated beachrock (mm)} + \text{Sea-level (mm)}}{\text{Age (yr BP)}} \quad (2.1)$$

However, Dickinson (2007) underestimated the uncertainty associated with subsidence because his analysis only accounted for the  $^{14}\text{C}$  error associated with the dated material and ignored the vertical error associated with beachrock formation. In the absence of cement and facies analysis, beachrock error can be approximated by the local tidal range (Mauz et al., 2015). Dickinson’s (2007) subsidence estimates were updated in this study by incorporating the median tidal range value of 1.1 m observed at Apia, ‘Upolu (Goodwin and Grossman, 2003) into the uncertainty analysis. Mulifanua was modeled to be subsiding at  $1.25 \pm 0.43$  mm/yr and Maninoa, located approximately 30 km from Mulifanua, was modeled as subsiding at  $0.52 \pm 0.28$  mm/yr (**Figure**

**2.3D).** Subsidence rates at Mulifanua and Maninoa were compared with the modeled pattern of flexural subsidence known for Hawai‘i (Moore et al., 1996) and it was concluded that differential subsidence related to distance from the central volcanic load at Savai‘i was a viable option for explaining the local sea level history. Furthermore, the model implies that the lowest subsidence (<0.1 mm/yr) rates would be found on the far eastern end of ‘Upolu.

### **2.2.3 The role of tsunamis and storms in reworking coastal plain sediments**

The tropical Pacific is characterized by a high frequency of tropical cyclones and tsunamis. Although distinguishing amongst tsunami and storm deposits is a growing field, it was not the purpose of this study and rather we acknowledge that both events are mechanisms of carbonate deposition and erosion within the subsurface coastal plain. The historical record of storms and tsunamis should be investigated so that correlations between the sedimentological record and these catastrophic saltwater events may be made or ruled out. For example in the region surrounding ‘Upolu, Sāmoa, five tsunamis with a maximum water height of three meters or greater (Richmond et al., 2011) and eight category two cyclones or greater have been documented since 1868 (Diamond et al. 2011; Table 2.1). In both Sāmoa and Tuvalu (**Figure 2.1**), cyclone banks as large as 2-3 m high, 50 m wide and 2 km long formed by large storm waves that dredged coral debris from the fore reef and reef crest and deposited them as far as 10-20 m shoreward onto the reef-flat (Rearic, 1990) where they were reworked and moved shoreward by subsequent wave action. In addition, both tsunamis and storm waves can transport and deposit coral boulders along the coastal plain (Goto et al., 2010; McAdoo et al., 2011; Richmond et al., 2011).

Table 2.1. Historical tsunamis and cyclone record for Sāmoa.

Historical Tsunamis <sup>a</sup>							
Year	Observation location	Max water height (m)		Max inundation distance (m)		Tsunami source	
1868	Apia, 'Upolu	3				Earthquake (8.50)	
1907	Matautu, 'Upolu	3.6		110		Volcano <sup>b</sup>	
1917	Apia, & S. coast 'Upolu	12.2				Earthquake (8.3) <sup>b</sup>	
1960	Apia, 'Upolu	4.9				Earthquake (9.5)	
2009	Samoa	17.59		620		Earthquake (8.0) <sup>b</sup>	

Historical Cyclones <sup>c</sup>							
Name	Year	Pressure (mbar)		Wind speed (km/h)		Closest approach to Satitōa (km)	Max Cyclone category
		min	ave	max	ave		
Tusi	1987	955.0	969.0	156.5	131.0	295.1	2
Ofa	1990	925.0	944.4	186.3	169.0	203.7	3
Val	1991	940.0	943.5	185.2	167.9	35.1	3
Ron	1998	925.0	956.4	188.7	140.9	295.1	3
Heta	2004	909.3	920.7	218.0	204.3	235.2	3
Olaf	2005	907.3	915.7	226.9	213.8	140.5	4
Rene	2010	945.0	984.6	157.4	85.4	102.5	2
Evan	2012	960.0	972.5	166.7	128.8	4.6	2

<sup>a</sup>Tsunami data was updated from Richmond et al. (2011) and historical cyclone data was

provided by Southwest Pacific Enhanced Archive of Tropical Cyclones (Diamond et al., 2011).

<sup>b</sup>indicates Sāmoa or Kermadec-Tonga trench source.

<sup>c</sup>Historical cyclones are defined as category 2 or greater tropical cyclones that tracked within 300 km of Apia, 'Upolu.

Because Holocene sea level studies typically extend beyond the historical record, an understanding of the potential for paleotsunamis and paleostorms is pertinent for interpretation of coastal stratigraphy. A recent study at Futuna Island (~ 600 km west of Sāmoa; **Figure 2.1**) identified two Holocene paleotsunamis believed to have originated from the Tonga-Kermadec

trench region (**Figure 2.1**) around 1860-2000 cal yr BP, and 470 cal yr BP (Goff et al., 2011). In addition, fossil corals provide high-resolution reconstructions of tropical Pacific climate and a 1,100 year  $\delta^{18}\text{O}$  monthly resolved coral record from Palmyra atoll (**Figure 2.1**) reveals significant changes in El Niño Southern Oscillation (ENSO) (Cobb et al., 2003), indicative of a highly variable tropical Pacific climate throughout the late Holocene (Mayewski et al., 2004). Time periods characterized by ‘El Niño like conditions’ generally have an increased probability for extreme weather events such as tropical cyclones for island countries within the South Pacific region (Cai et al., 2012).

## **2.3 Methods**

### **2.3.1 Cores (sample collection)**

Eighteen cores were sampled along five shore perpendicular transects (labeled A-E; **Figure 2.4**) to record the spatial coverage, composition and age of the subsurface carbonate unit. A t-handle bucket auger recovered successive units of sediment until refusal, typically at depths of 1 to 2 m. Field descriptions such as texture, depth of sediment horizons, and the presence of datable coral clasts were recorded at each core location. Two surface grab samples were recovered from the Satitua reef-flat (RF), and the modern beach (MB) face at Taufua beach (~2.20 km to the southwest). This project was completed in conjunction with an archaeological study that excavated four test pits next to the geologically focused auger cores (Cochrane et al., 2015).

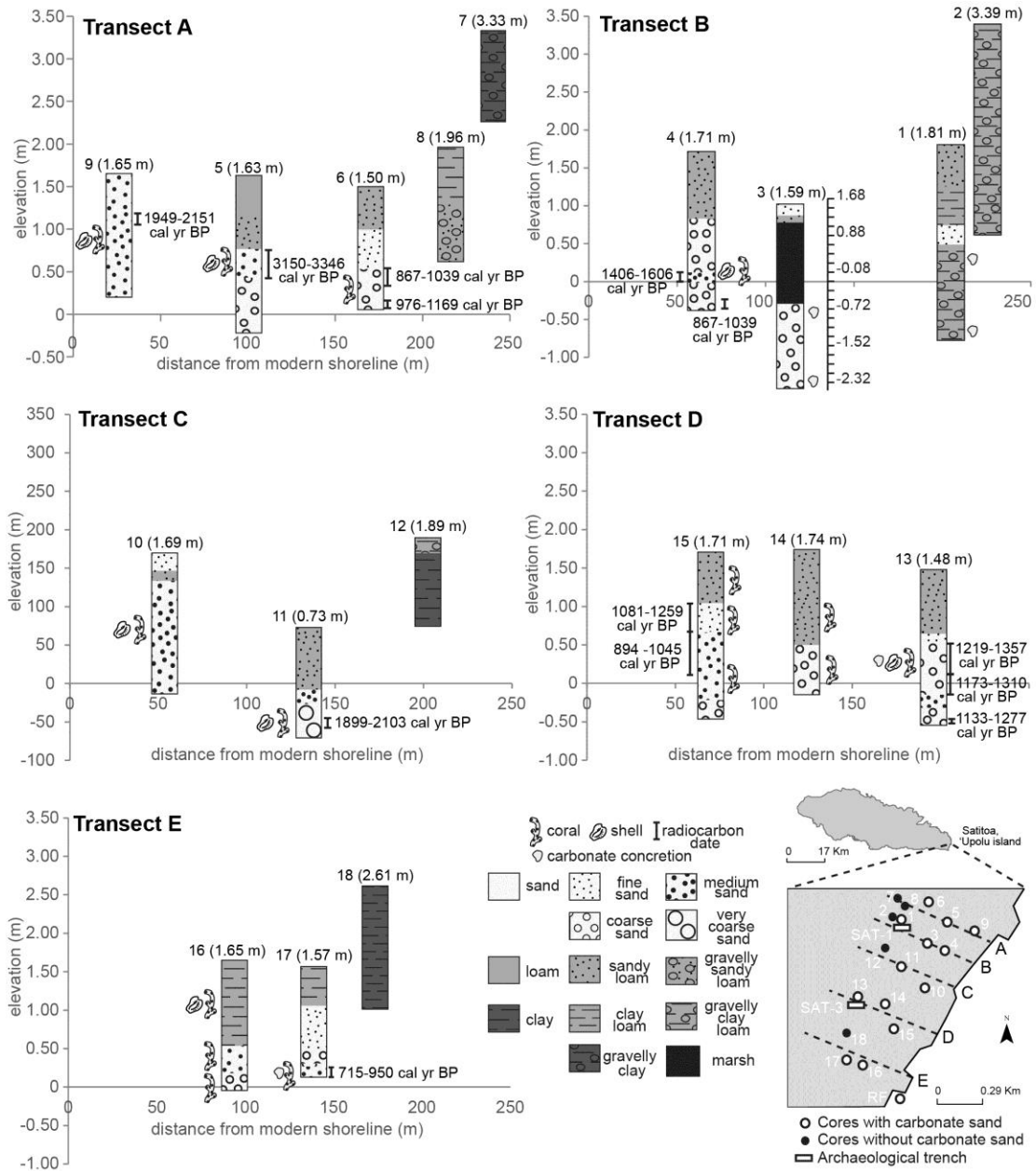


**Figure 2.4** Stratigraphic cross sections of 18 cores depicting dominant sedimentological units, location of carbonate clasts, and calibrated age ranges (cal yr BP) of dated material at Satittoa, eastern ‘Upolu. Elevation is referenced to mean sea level, and distance from the modern shoreline is based upon the mapped position of the low water mark during the time of data collection. Calibrated age ranges are reported at the 95.4% ( $2\sigma$ ) confidence interval. In general,

the stratigraphy of the coastal plain consists of a carbonate sand layer overlain by a loam. The coastal plain transitions into a terrigenous unit at the furthest inland extent of the study area.

### **2.3.2 Topographic Data**

A digital elevation model (DEM) of the study area was created from topographic point data collected with a Leica TS12 robotic total station on September 2-7, 2014. The reference survey points were adjusted to geographic coordinates and ellipsoid heights relative to World Geodetic System 1984 (WGS84) using an Ashtech LOCUS survey grade integrated L1 Global Positioning System (GPS) receiver/antennae base station. Because the tidal relationship between the Satitua Village study site and the Apia tide gauge is not established, the surveyed elevations were referenced to local low water observed at the toe of the Satitua shoreline. Low water positions were adjusted to MSL using the average low tide recorded at the Apia Tide station on the days that topographic data was collected (<http://www.ioc-sealevelmonitoring.org/>: accessed 2/3/16). A triangular irregular network (TIN) was derived from the topographic point data and interpolated into a DEM using the nearest neighbor method.

### **2.3.3 Sedimentology, age, and composition of the coastal plain**

Similar to Harney et al. (2000) carbonate sand samples were sieved through eight grain-size classes according to the Wentworth (1922) scale and mean grain size and sorting index were calculated using Folk and Ward (1957). Coral clasts and two surface sediment samples were submitted to the National Ocean Sciences Accelerator Mass Spectrometry Facility at Woods Hole Oceanographic Institution for  $^{14}\text{C}$  radiocarbon dating. Coral clasts selected for dating had uniform characteristics; minimal recrystallization, spatial representation of the study area, and

constrained the top and base of the cored carbonate layer. Coral clasts were pre-treated for dating with ultrasonic washing and acid etching and radiocarbon ages were corrected for the regional marine reservoir effect using CALIB version 7.1, and the Marine13 calibration dataset (Reimer et al., 2013; Stuiver and Braziunas, 1993; <http://calib.qub.ac.uk/calib/calib.html>: accessed 10/24/2016).

A compositional analysis of the carbonate sand layer was performed to determine the origin and relative percentage of skeletal, non-skeletal and unidentifiable grains (Harney et al., 2000). Skeletal grains included coral, coralline algae, *Halimeda*, mollusk, benthic foraminifera, and echinoderm fragments. Non skeletal sediment includes intraclasts and crystalline/volcanic grains. Carbonate sediments were embedded in epoxy, thin sectioned, and a petrographic microscope was used to classify a minimum of 300 identifiable grains for cores 4, 5, 13, 14, 15, and the surface sediment samples collected at the reef-flat and beach.

## 2.4 Results

In general, the stratigraphy of the coastal plain reveals an abrupt contact between the surface loam and underlying carbonate sand (**Figure 2.4**). Carbonate sand extends inland as far as 200 m and is typically found between 1.34 m to  $-0.71$  m relative to MSL. Thickness varies from 0.58 m to 1.80 m, however due to difficulty in coring, most cores were not able to fully penetrate the sandy carbonate unit. The basal carbonate units typically did not contain rip-up clasts, included both intact and fragmented marine shells, and were thicker (0.48-1.51 m) than both the modern tsunami deposits recorded at 'Upolu, and paleostunami deposits of Futuna Island. Three cores (3, 9, 10) encountered a second carbonate layer (<25 cm thick) at the surface of the core which may be interpreted as a deposit of the 2009 South Pacific tsunami. The

landward cores of each transect are typically composed entirely of loam or clay, with the exception of transect D which is bordered on the landward extent by a thickly vegetated marsh. Surface sand content diminishes in the south (transect E) and cores are capped with clay loam.

The subsurface carbonate unit generally fines upward (66.7% of cores) and contains poor to very poorly sorted, coarse to very coarse sand at the base. The seaward cores (9, and 10), and core 17 are an exception. Cores 9 and 10 contain a massive medium sand layer that is moderately well to poorly sorted, while core 17 fines upward with the exception of a very poorly sorted medium sand layer at the base of the core. Cores 3, 9, and 10 have a second carbonate sand unit at the surface that is characterized by moderately well to poorly sorted, fine to medium sand. Modern beach and reef-flat sediment samples are characterized by coarse sand that is moderately well and poorly sorted, respectively.

Cored sands contained isolated coral clasts, marine shells (*Monetaria moneta*), and carbonate concretions. The subsurface carbonate unit was dominated by skeletal grains, with unidentifiable grains accounting for 2-12% of total composition (**Figure 2.5**). Coral and coralline algae derived from the reef framework are the dominant source of sediment, representing  $\leq 42.0\%$  of total composition. Core 13 was found to have a lower relative percentage of reef derived components and a higher combined percentage of in situ calcareous organisms such as benthic foraminifera, *Halimeda*, mollusks, and echinoderms.

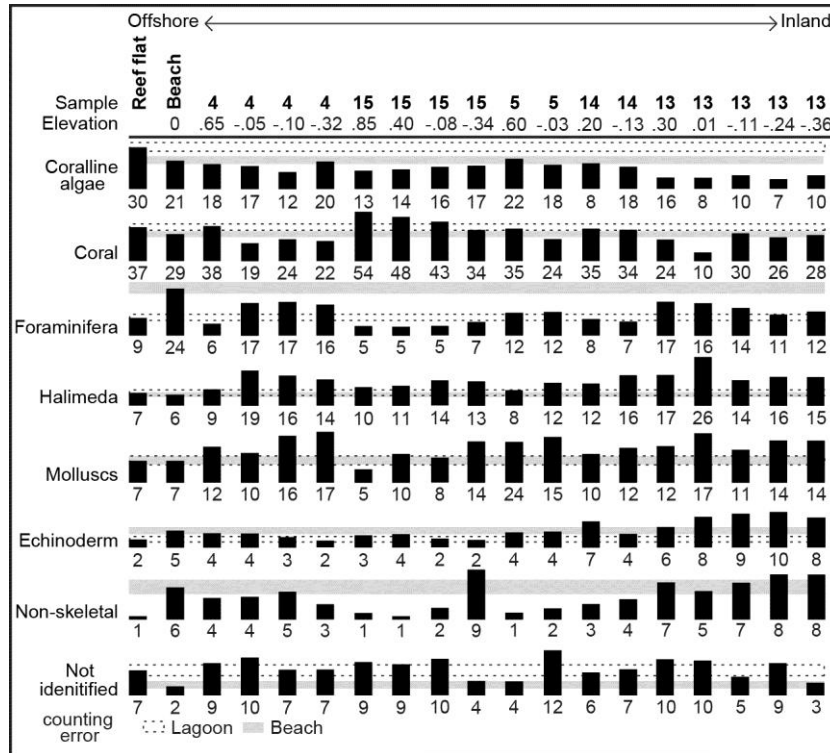


**Figure 2.5** Relative percentage of reef derived skeletal sediment, nonskeletal sediment, and unidentifiable materials (origin could not be determined). Surface samples were collected within the reef-flat (RF), and Taufua beach (MB), while subsurface carbonate samples were obtained from cores 4, 5, 13, 14, and 15.

All calibrated  $^{14}\text{C}$  ages presented in **Table 2.2** may be referenced with respect to distance from the shoreline and elevation relative to MSL. Core 5 (3150-3346 cal yr BP) and core 9 (1949-2151 cal yr BP) contain the two oldest dates and are found near the surface of the carbonate layer and relatively close to the modern shoreline. There is a general trend of increasing age with depth for those samples collected 150-200 m from the modern shoreline. The remaining coral clasts and surface sediment samples cluster around 838-1518 cal yr BP, however these samples do not depict a relationship with depth or distance from shoreline.

Because the base of the carbonate unit was not penetrated reported ages of basal sediments may underestimate the initiation of coastal progradation.

**Table 2.2** Radiocarbon dates of cored material.

Lab ID	Site	Distance from shoreline (m)	MSL elevation (m)	Material dated <sup>a</sup>	<sup>14</sup> C age ( <sup>14</sup> C yr BP)	<sup>14</sup> C error ( <sup>14</sup> C yr)	95.4% (2σ) cal age ranges (cal yr BP)
TMB	MB	0	0	CS	475	± 20	905-1056
SML	RF	-27.8	0	CS	1880	± 25	1306-1500
P105-D3	5	100.56	0.43-0.77	CC	3410	± 20	3150-3346
P106-D4	6	170.35	0.33-0.53	CC	1420	± 20	867-1039
P106-D6	6	170.35	0.06-0.15	CC	1550	± 20	976-1169
P109-D4	9	26.29	1.04-1.19	CC	2450	± 20	1949-2151
SAT1-S5	SAT1	192.90	0.33-1.05	CC	1380	± 15	799-963
P104-D6	4	63.71	-0.02- 0.12	CC	1990	± 20	1406-1606
P104-D9	4	63.71	-0.37- -0.27	CC	1420	± 20	867-1039
P111-D5	11	135.42	-0.60- -0.49	CC	2400	± 20	1899-2103
P113-D5	13	196.24	0.08-0.51	CC	1760	± 20	1219-1357
P113-D6	13	196.24	-0.07- 0.08	CC	1720	± 20	1173-1310

SAT3-D7	SAT3	196.24	-0.53- -0.50	CC	1670	± 15	1133-1277
P115-D4	15	70.47	0.67-1.04	CC	1640	± 20	1081-1259
P115-D5	15	70.47	0.12-0.67	CC	1440	± 20	894-1045
P117-D7	17	138.89	0.12-0.27	CC	1320	± 20	750-915
							612-619 (2%)
SAT1 <sup>b</sup>	SAT1	192.90	1.13-1.30	Cnn	523	± 20	512-554 (93.4%)
	Core 8	192.90	1.07-1.52	UIC	607	± 20	580-652 (75.3%)
Core8 <sup>b</sup>							549-571 (20.1%)

<sup>a</sup>Material dated: CS = carbonate sand, CC = coral clast, Cnn = *Cocos nucifera* nutshell, UIC = unidentified charcoal

<sup>b</sup>samples SAT1 (1.13-1.30 m depth), and Core 8 were originally published in Cochrane et al. (2015) and were found in a cultural loam layer that sits upon the subsurface carbonate unit.

## 2.5 Discussion

Numerous studies throughout the central Pacific equatorial region provide evidence of emergent shorelines formed by the mid-Holocene highstand (Calhoun and Fletcher, 1996; Fletcher and Jones, 1996; Allen, 1998; Grossman et al., 1998; Dickinson, 2001), yet coastal plain sedimentology is often overlooked because coral clasts and sands are not indicative of a precise relationship to former sea level (Goodwin and Grossman, 2003). The true value of the subsurface carbonate unit is that it records the landward extent of marine transgression and when correlated with time using modeled sea level curves we can determine a timeline for shoreline regression. For example, at Satitua the coastal plain prograded seaward approximately 200 m beginning as early as 2000 cal yr BP. Holocene sea level curves for ‘Upolu (**Figure 2.6**) were computed using a theory of ice age sea level change (Alley and Clark, 1999) that incorporates the full deformational, gravitational and rotational perturbations to the Earth system driven by ice melt and ocean meltwater loading (Kendall et al., 2005). The calculations require, on input, models for the ice history across the last glacial cycle, and the depth variation of viscosity within the Earth model. The following published pairings of ice history and mantle viscosity were adopted: the ICE5G ice history and VM2 viscosity model (Peltier and Fairbanks, 2006); the ICE6G ice history and VM5 viscosity model (Argus et al., 2014); and the ice history described by Lambeck et al. (2014), which is referred to as ANU, together with the viscosity model favored in their analysis (henceforth, the “LM” model). Variations in modeled ice history and viscosity impact the timing and amplitude of the highstand. For example, the viscosity models VM2 and VM5 are characterized by a relatively weak lower mantle ( $<3 \times 10^{21}$  Pa s), significantly lower than the value in model LM ( $2 \times 10^{22}$  Pa s). Thus coupling the sedimentary record with the modeled sea level curves does not confirm the accuracy of the geophysical record but rather we can conclude

that coastal progradation at Satittoa occurred nearly two to four millennia after the mid-Holocene highstand. As sea level fell below a critical sea level value of 0.3-1.0 m, the rate of deposition of marine sediments exceeded the rate of erosion along the coast.

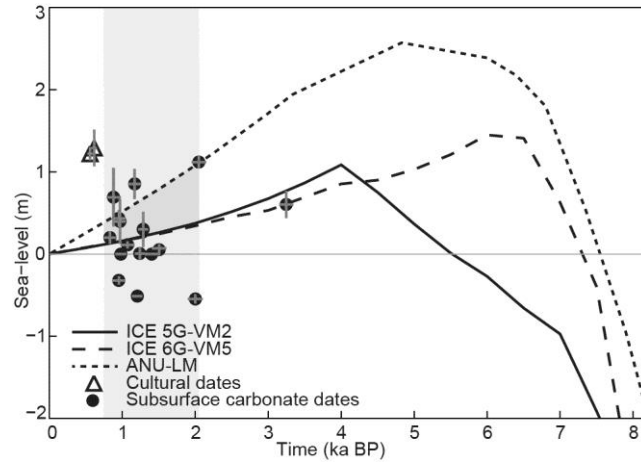


**Figure 2.6:** Dated core material is plotted together with three Holocene sea level curves computed using the coupled ice history and mantle viscosity models: ICE 5G-VM2, ICE 6G-VM5, and ANU-LM (see text). Cultural dates were obtained from the sandy loam cultural layer described by Cochran et al. (2015), while all other dates originate from subsurface coral clasts, or surface carbonate sand. The sedimentary record is plotted here with the modeled sea level curves not to confirm the accuracy of the modeled sea level record or to reconstruct Holocene shoreline migration but rather to constrain a time period for the initiation and growth of the sandy coastal plain. Coastal plain progradation initiated 1899-2103 cal yr BP and continued until approximately 549-652 cal yr BP when the unit became buried by the cultural loam layer. Because the base of the carbonate unit was not dated, the reported dates may represent a minimum age for coastal progradation.

An understanding of the vertical shifts in island elevation in response to local or regional tectonism is necessary to accurately account for the magnitude of sea level change, as well as the timing of subsequent coastal evolution. We argue that differential subsidence rates at ‘Upolu result not only in variations of relative sea level but also the timing at which the coastal plain recovers from an erosive state and begins to prograde seaward. Expansive coastal plain progradation has also been observed along the southern coast of ‘Upolu, but occurred later between 300-1000 cal yr BP and is originally believed to have been linked to increased sediment production and coral growth in response to a slight relative lowering of sea level (Goodwin and Grossman, 2003). Thus a lag in seaward growth along the southern coast may be related to higher relative sea level due to greater subsidence rates with closer proximity to the volcanic load on Savai‘i Island (**Figure 2.3D**).

### **2.5.1 Improving the interpretation of coastal plain evolution**

Based upon the age of carbonate clasts and presence of date inversions, we conclude that the subsurface carbonate architecture was heavily influenced by periodic, high-energy events such as tsunamis and cyclones. Prior high intensity events are known to remove and transport large sediment loads (silt size to coral boulders) from the reef crest to the beach and coastal plain (McAdoo et al., 2011; Richmond et al., 2011). We acknowledge periodic redeposition by high energy events as a research problem and call upon the importance of analyzing both the instrumental record and geologic record of tsunami and tropical cyclones when interpreting the stratigraphic record of Pacific Islands. For example the 1860-2000 cal yr BP paleotsunami recorded at nearby Futuna Island, could have eroded and deposited sediment at the base of our carbonate unit, while the younger 470 cal yr BP event could have reworked sediment near the

surface. High-energy punctuated events could also be responsible for our two oldest dates, which we interpret as outliers. Core 9 (1949-2151 cal yr BP) represents the closest core to the present marine environment, and core 5 (3150-3346 cal yr BP) is at least 1,000 years older than any other dated material.

Dated bulk surface sediments from the beach and reef-flat suggest that coastal sand-sized sediment may remain in transport for approximately 900-1500 years, which is not uncommon for Pacific Islands (Moberly and Chamberlain, 1964; Harney et al., 2000; Resig, 2004). In bioclast rich environments there inherently is a temporal uncertainty associated with radiocarbon ages because beach sediment originates from the progressive destruction of reef framework limestone and calcifying organisms. In future experiments the age of the coastal plain can more accurately be constrained by dating individual, delicate or spiny foraminifera such as *Calcarina* and *Baculogypsina spaerulata* as the ages of these specimens are more reflective of deposition and burial soon after death (Kayanne et al., 2011; Ford and Kench, 2012).

The Holocene sea level models incorporated in this study assume lateral uniformity in mantle viscosity, and as a result continental margins and mid-ocean environments are described by the same mantle rheology parameters. We acknowledge this as a flaw in the current state of these models due to the limited distribution of island data as well as the poor resolution of depth dependence of viscosity for islands (Lambeck et al., 2014). Following conventional practice, we attempt to account for uncertainty by employing a suite of the most widely accepted ice history and viscosity models (Peltier and Fairbanks 2006; Toscano et al., 2011; Argus et al., 2014; Lambeck et al., 2014), thus producing a range of predicted sea level values that encompass both the Holocene highstand as well as the subsequent fall in sea level. Coupling the sedimentary

record with the modeled sea level curves does not confirm the accuracy of the modeled sea level record but rather constrains a time period for the initiation and growth of the sandy coastal plain. Interpreting the shape of the sea level curves is imperative to interpreting coastal plain evolution. The slopes of the three curves are comparable for the period of sea level drawdown, resulting in a similar rate (0.8-.9 mm/yr) of sea level fall. The LM model implies that coastal progradation started when sea level was around 0.5 m higher than the other two curves.

### **2.5.2 Implications of coastal evolution upon past and future societies**

Coastal plain evolution is of particular interest to the permanent settlement and migrations of the first Pacific Island peoples because no single factor has influenced coastal environments more than sea level fluctuations (Allen, 1998). Prior studies have argued that due to the low gradient of most coastal plain environments, the rate of future SLR impact will rapidly accelerate once the height of the sea surface exceeds a critical elevation (Kane et al., 2015). Using this same logic, we reason that habitable coastal environments may not evolve until sea level falls below a critical value that allows for the rapid development of suitable coastal flats. For example, at the nearby Sāmoan islands of Tutuila and Aunu‘u it has been argued that permanent settlement prior to approximately 2500 cal yr BP was limited due to the lack of suitable sandy coastal flats related to less settlement space, coastal access, and higher slope under elevated sea level (+2.0 m) (Rieth et al., 2008). A cultural layer with sparse anthropogenic deposits found directly on top of the carbonate sands at Satitōa, ‘Upolu was dated and provides a *terminus ante quem* of 549-652 cal yr BP for the marine carbonate unit (Cochrane et al., 2016). Thus it is not until ~500 cal yr BP (Cochrane et al., 2016), more than a millennium after coastal progradation began, that the coastal zone stabilized and anthropogenic deposits indicative of a

small population along eastern ‘Upolu appear. Our findings support previous studies that suggest that post mid-Holocene drawdown in regional sea level produced coastal settings that were morphologically attractive for human settlement (Dickinson, 2001; Rieth et al., 2008; Cochrane et al., 2013; Burley and Addison, 2015).

A better understanding of coastal plain evolution since the fall of the mid-Holocene sea level highstand may guide decisions related to coastal communities impacted by future SLR. The Intergovernmental Panel on Climate Change (IPCC) Fifth Assessment Report predicts by the end of the century, under a worst case scenario (RCP8.5), Equatorial Pacific regions may experience sea level values 10-20% above the global mean of  $0.74 \pm 0.23$  m (Church et al., 2013). Coastal plain evolution recorded in the sedimentary record of volcanic islands reveal the timing and extent of marine transgression as Holocene sea level approached values similar to future projections. In addition, model projections also forecast increased South Pacific Convergence Zone migration, and increased extreme El Niño, and La Niña events in response to global warming (Cai et al., 2012, 2014, 2015). Thus, overlaid on the long-term rise in sea level, may be periods of increased probability for extreme weather events such as tropical cyclones. The impacts of short term catastrophic events such as storms and tsunamis will be further exacerbated by future SLR.

## **2.6 Conclusion**

Coastal plain stratigraphy is often over looked in paleo sea level reconstructions because carbonate sediments do not precisely constrain former sea level. Here we show that Pacific island sedimentology provides an invaluable record of geomorphic and environmental consequences of coastal evolution in response to changes in sea level and local tectonics.

Coastal evolution in response to prior changes in sea level is of particular interest because the late-Holocene fall in sea level is believed to have played a dominant role in the availability of suitable coastal habitats where early human populations were typically found. A series of auger cores obtained from eastern 'Upolu reveal that as sea level falls following a highstand, carbonate sediment derived from the destruction of the offshore reef framework is stranded along the coastal plain and subjected to periodic erosion and redeposition by punctuated high-energy events such as tsunamis and tropical cyclones. When interpreting coastal sediments it is important to have some understanding of the historical context of the timing and impacts tropical cyclones and tsunamis so that uncertainties related to interpretations of the sedimentological record may be reduced. In addition, to accurately reconstruct the magnitude of relative sea level and the timing of coastal progradation across larger volcanic islands it is necessary to account for vertical shifts in island elevation in response to local or regional tectonism. For example, we show that a lag in seaward growth along the southern coast of 'Upolu may be related to higher relative sea level rates resulting from increased subsidence rates closer to the volcanic load on Savai'i.

Coupling the sedimentological record with geophysical models of mid- to late- Holocene sea level we identify a critical value (0.3-1.0 m) during the falling phase of the sea level highstand (1899-2103 cal yr BP) that represents the transition from a transgressive to a regressive environment, and initiates coastal progradation. By correlating the critical value with time we observe that nearly a millennium of coastal plain development is further required before a small population is established. The framework by which a critical value of sea level may be used to better constrain the timing and development of morphologically attractive coastal settings

for human settlement is relevant throughout the far-field Pacific as the mid-Holocene sea level highstand was a regionally prominent geophysical event that shaped the coastal plain of thousands of islands. Thus we conclude that as SLRs into the future, approaching mid-Holocene highstand values, lessons learned from the Pacific Island sedimentological record may be useful in guiding future decisions related to coastal processes, and habitat suitability. Future SLR will once again exceed a critical value and the rate and extent of flooding will rapidly accelerate across the coastal plain. By coupling future SLR models with local topography, decision makers may begin to develop a timeframe by which they may plan for the largest impacts of SLR.

### **CHAPTER 3. INTERPRETING BIO-GEOLOGIC LINKAGES FROM A WINDWARD REEF-ISLAND SYSTEM, BOKOLLAP ISLAND, MAJURO**

*To Be Submitted To: Geology*

**Abstract** – The future existence of atoll islands is of global concern, as entire island nations and highly evolved ecosystems are projected to become uninhabitable due to sea level rise (SLR) by the mid-21<sup>st</sup> century. Atoll reefs and islands are bio-geologically linked such that islands are composed entirely of unconsolidated sand and rubble that is derived from the nearshore coral-reef ecosystem. Limited research has been invested into understanding the bio-geologic linkages that characterize these systems. Furthermore no study has compared ecological shifts in dominant island-building constituents recorded in the stratigraphic record of reef-islands and adjacent reef-flats. Analysis of fossil-reef cores and island sediment from a windward reef-island at Majuro atoll provides a 5.0 kyr record of ecosystem response to mid- to late- Holocene sea level change. The fossil record reveals a 2.5 kyr delay in island building following the completion of lagoonward reef-flat accretion. A prerequisite for island emergence was the formation of a low-porosity limestone platform by lithification of unconsolidated sediment coupled with the binding of coral rubble by encrusting foraminifera and calcareous algae. Sea level fall and the establishment of a highly productive *Calcarina* reef-flat enabled the accumulation of a foraminifer-dominant island, characteristic of most Pacific atolls. Future resiliency of reef-islands to SLR is dependent upon (1) ecological shifts that enable reactivation of coral growth along the fossil-reefplatform to accommodate lagoonal accretion of the reef-flat, and (2) sediment deposition rates comparable to the rate of SLR that foster both infilling of the reef-flat and island-building.

### 3.1 Introduction

Atoll reefs and islands are bio-geologically linked such that islands are composed entirely of unconsolidated sand and rubble that is derived from the nearshore coral-reef ecosystem (Woodroffe et al., 1999). Reef-islands form upon carbonate platforms located within atoll lagoons (Kench et al., 2005; Perry et al., 2013), atoll rims (Woodroffe et al., 1999; Kayanne et al., 2011; Kench et al., 2014b), or mid-ocean reefs (Yamano et al., 2000; Woodroffe and Morrison, 2001; Kench et al., 2014c). In this context shallow coral reefs and reef-flats serve as biological sediment sources (Perry et al., 2011) and reef-islands as sediment sinks. Pacific reef-islands are predominately composed of benthic foraminifera (Emery et al., 1954; Fujita et al., 2009; Mckoy et al., 2010). Reef-island composition and emergence is related to the formation of tidally emergent reef-flats that serve as the preferred habitat for benthic foraminifer communities (i.e. *Calcarina*, *Baculogypsina*, *Amphistegina*, and *Marginopora*).

Under current sea level, coarse sand (0.5-1.0 mm) size sediments (foraminifera, calcareous algae, and coral fragments) are preferentially transported during the majority of the tidal cycle by wave-generated currents from the reef-flat and deposited at the perimeter of reef-islands (Yamano et al., 2000). Transport of coarser sediment (i.e. gravel-size, 2-64 mm) is limited to the highest tides (Dawson and Smithers, 2014) or restricted to storm events (Kench et al., 2014a). Increased water levels related to sea level rise (SLR) may impact reef-island stability in two ways. Firstly, reef-flat ecology may shift to a coral-algal dominant system as greater (vertical) accommodation space enables increased coral growth and colonization (Scopélitis et al., 2011; Van Woesik, R. et al., 2015; Saunders, M.I. et al., 2016; Chen et al., 2018). Secondly, increased wave energy across reef-flats related to SLR (Storlazzi et al., 2011; Becker et al., 2014;

Cheriton et al., 2016) may shift island composition to coral gravel (Yamaguchi et al., 2009; Kench et al., 2014b) as higher energy environments retain finer sediment in the water column.

Improved understandings of the bio-geological linkages of reef-island systems are crucial for understanding how islands naturally respond (i.e. erode, accrete, or remain unchanged) to longterm variations in sea level. Previous studies have looked specifically at the role of key ecosystem shifts conducive for island building (Kench et al., 2005; Yasukochi et al., 2014) and maintenance. No study to date has compared ecological shifts in dominant island-building constituents recorded in both the stratigraphic record of reef-islands and the fossil record of adjacent reef-flats. Analysis of fossil-reef cores and island sediment from a windward reef-island at Majuro atoll provide a 5,000 year record of ecosystem response to environmental shifts and mid- to late- Holocene sea level change. Here we hypothesize that the fossil reef record will reveal the timing and type of ecosystem changes conducive for the emergence of a foraminifer-dominant island. Moreover this study provides potential for implementing better practices to manage reef-island communities through improved understandings of the bio-geologic factors that influence production, transport, and deposition of dominant island sediment components.

## **3.2 Methods**

### **3.2.1 Field setting**

The Republic of the Marshall Islands (RMI) comprises of a double chain of 29 atolls and 5 mid-ocean reef platform islands between 4°34' to 14°43'N and 160°48' to 172°10'E. Our study focused upon Bokollap, a windward reef-island at Majuro atoll (**Figure 3.4**). Light north easterly trade winds ( $6.32 \text{ ms}^{-1}$ ) predominate for most of the year. Moderate tradewind swell persists throughout the year, with larger swell ( $<2.3 \text{ m}$ ) during winter and spring months (Bosselle, 2015). Typically the largest wave-run up events coincide with king tides (highest

tides of the year) and have been associated with inundation, coastal erosion, and temporary salinization of groundwater aquifers (Storlazzi et al., 2018).

### 3.2.2 Reef-island stratigraphy

Island and reef-flat surface reconstructions were derived from total station survey points and drone Digital Elevation Model (DEM; 2 cm resolution) derived elevations. Elevations were reduced to mean sea level based upon an automated water-level data-logger deployed within coring location G1, and then compared with MAJURO-C tide station (<http://www.iocsealevelmonitoring.org/station.php?code=marsh>). Total station-derived survey points have a horizontal accuracy of  $\pm 1.0$  m, and vertical accuracy of  $\pm 0.03$  m.

Eight shallow cores 5.08 -7.62 mm in diameter were drilled in 2016, and 2017 along two shore transects at a tidally emergent reef-flat (**Figure 3.1**). Coring was conducted using a hand-held gas-powered drill. Each core sample was sliced longitudinally, photographed, lithological units were described, and fossil corals were identified to the species levels (Vernon, 2000; Humblet et al., 2015). Following Hongo and Kayanne (2009), in situ corals were distinguished from coral rubble larger than the core diameter by the lack of severe surface abrasion and rounding, and the upward orientation of well-preserved corallites and acroporid branches. Reef-flat cores were described based upon composition of bioclasts, and cement mineralogy and texture. A minimum of 200 identifiable skeletal grains were point counted for reef grainstone (n=6), and comparisons were made to unconsolidated biogenic sediment collected from the reef-flat surface (n=28) and island subsurface (n=28).

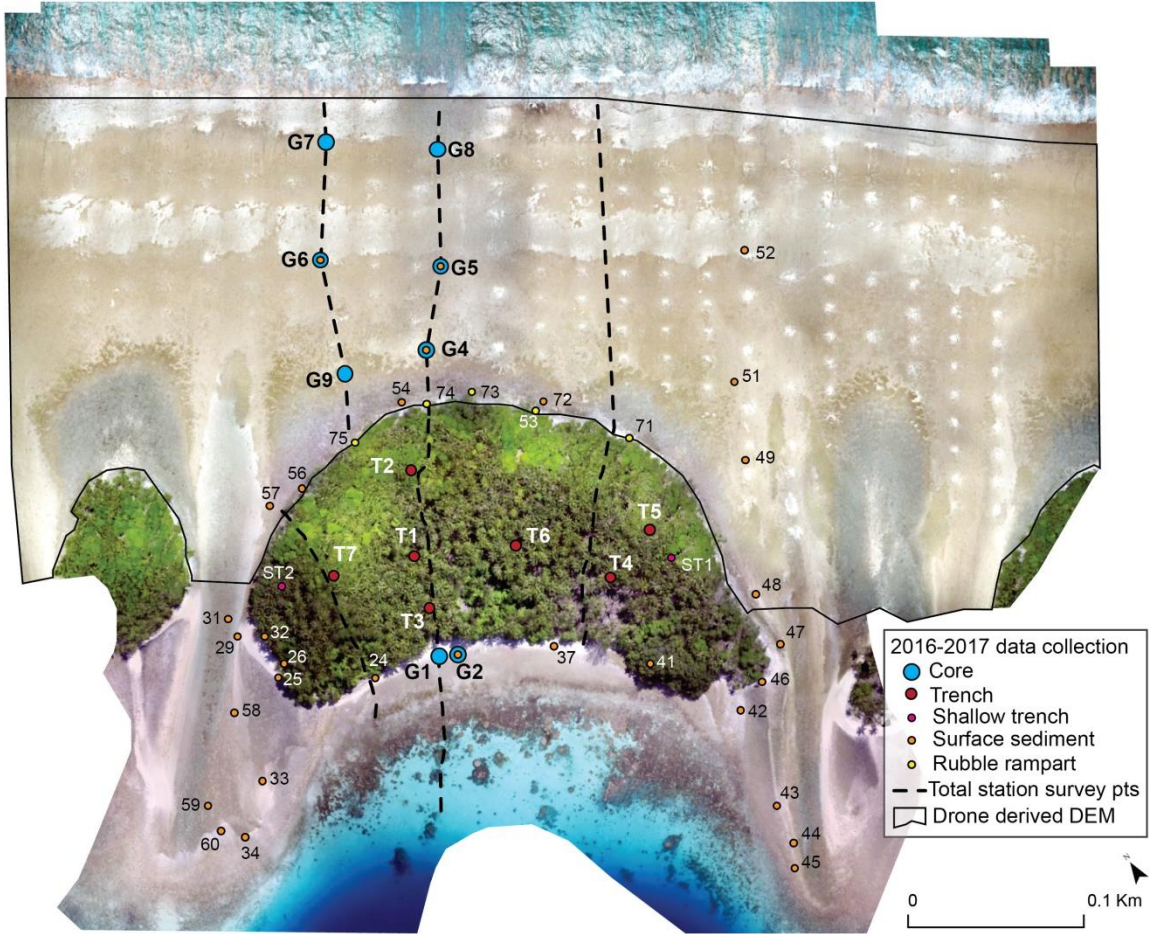


**Figure 3.1** Location and type of data collected at Bokollap island, Majuro.

Island age and composition was determined at seven geologic trenches. A spine ratio metric was also calculated (Equation 3.1) to account for abrasion of *Calcarina* tests (minimum of 200 total) collected from reef flat surface and the interior of the island. Spine ratio values are used to track sediment transport (Yasukochi et al., 2014) such that *Calcarina* spine ratios decrease with distance from their modern environment.

$$\text{Spine Ratio (\%)} = (A+B) / (A+B+C) \quad (3.1)$$

Grade A *Calcarina* had complete spines, grade B had some spines, and grade C had no spines. Because *Calcarina* spines are highly vulnerable to abrasion during transport, class A and B *Calcarina* are recommended for dating (Ford and Kench, 2012). Dating spiny *Calcarina* decreases the potential lag time between removal from the modern environment and incorporation into island sediments.

The timing of reef-island morphology is based on Radiocarbon ages from in situ coral samples from the fossil-reef flat (n=7), coral rubble from the seaward rubble rampart (n=1), and *Calcarina* foraminifera (Grade A and B; Ford and Kench, 2012; Yasukochi et al., 2014a) bulk island sediment that still had spicules attached (n=18) (**Table 3.1**). All samples were visually inspected under the microscope analysis to avoid recrystallization and impurities. X-ray diffraction analyses at the X-ray Atlas Diffraction Laboratory revealed that the majority of coral samples are composed of Aragonite and are appropriate for dating, however further analyses are required to quantify the relative percentages of Aragonite and Calcite. All Radiocarbon ages were determined by DirectAMS Radiocarbon Dating Service. Radiocarbon ages were recalibrated for the regional marine reservoir effect using CALIB version 7.1 (Stuiver et al., 2019) and Marine13 calibration dataset (Reimer et al., 2013; Stuiver and Braziunas, 1993; , with a marine reservoir correction ( $\Delta R$ ) of  $-30 \pm 25$  years for Majuro atoll (Kayanne et al., 2011).

### **3.3 Results and discussion**

#### **3.3.1 Modern island-building components**

The main reef-flat is an intertidal, fossil limestone platform that is subaerially exposed at low tide. Benthic foraminifera, *Calcarina* and *Amphistegina* sediment production is greatest on the surface of *Halimeda* living in inter-island passages ( $20 \pm 20 \times 10^{-3} \text{ m}^3 \text{ yr}^{-1} \text{ m}^{-2}$ ,  $1.3 \pm 1.1 \times 10^{-}$

$^3 \text{m}^3 \text{yr}^{-1} \text{m}^{-2}$  respectively) and within the algal turf zone ( $22.39 \pm 11 \times 10^{-3} \text{m}^3 \text{yr}^{-1} \text{m}^{-2}$ ,  $2.48 \pm 0.22 \times 10^{-3} \text{m}^3 \text{yr}^{-1} \text{m}^{-2}$ ) on the seaward margin of the reef-flat (Fujita et al., 2009) (**Figure 3.2**).

*Calcarina* constitute approximately  $63.2 \pm 13.8\%$  of modern reef-flat sediment. Spine ratios data reveal that wave generated currents preferentially transport *Calcarina* to the lagoon and perimeter of island spits throughout the tidal cycle via inter island passages, and across the reef-flat at high tide. Pristine *Calcarina* tests (class A & B) constitute approximately  $83.2 \pm 18.8\%$  of sediment deposited upon the seaward and inter-channel (nearshore) reef-flat. The lagoonal beach and spits are dominated by severely abraded tests ( $32.5 \pm 7.1\%$  class A & B). Majuro reef-islands are located on the lagoonal margin of the reef-flat and are bio-geologically connected to reef-flat sediment sources only at the island's perimeter.

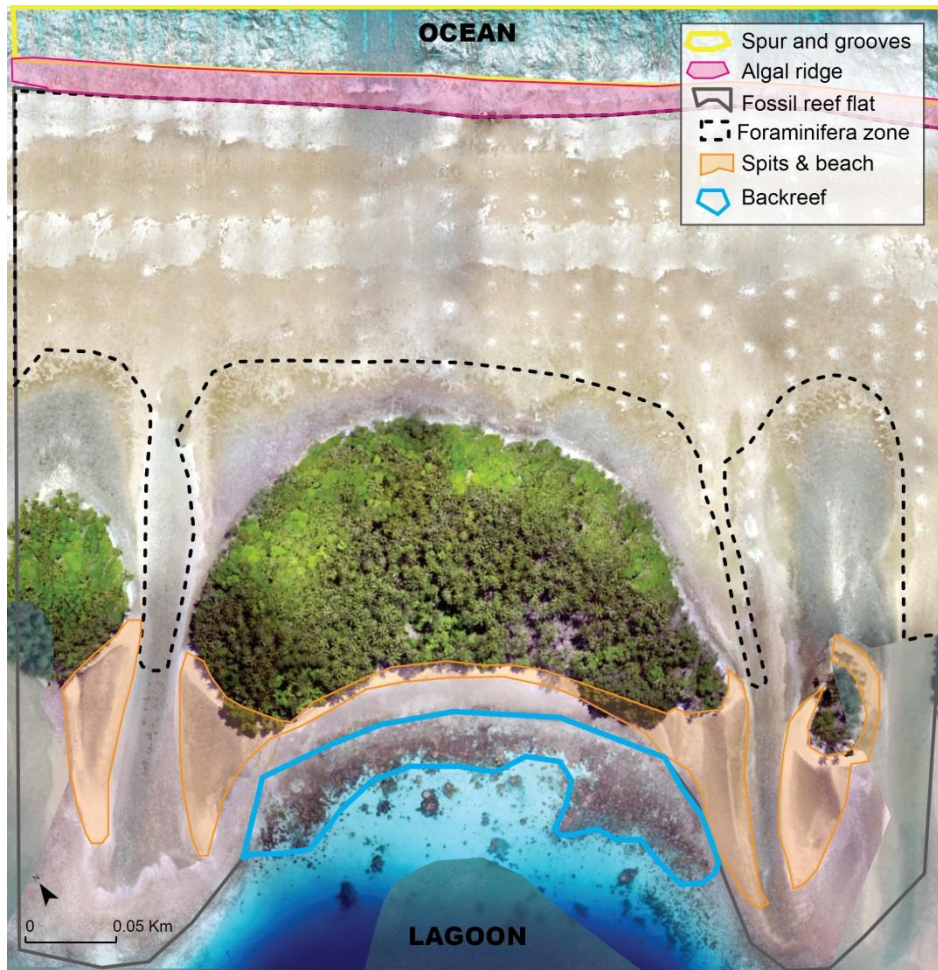


**Figure 3.2** This figure depicts the major zones of reef-island building components. Starting from the ocean extent of the reef-island system, coral-algal ecosystems are well established on reef spurs, and reef derived sediment accumulates in the reef grooves. The algal ridge is a high energy environment composed largely of encrusting and branching crustose coralline algae. *Calcarina*, the single most important island sediment is found largely on the tidally emergent reef flat, and at the inter-island channels. Currently subaerial sediment deposition is limited to island spits, and the lagoon beach. The backreef environment is composed of living coral and is currently being infilled by modern sediment derived from the reef flat.

In addition to lagoonal transport, sediment is also transported seaward off the reef-flat through a well-developed spur-and-groove system that extends from the modern calcareous algae ridge down the reef slope (**Figure 3.2**). The grooves serve as conduits of sediment export and are generally covered by a veneer of sand, gravel and boulders. The coral-algal spurs are occupied by *Halimeda*, calcareous red algae (*Porolithon gardineri*), submassive and branching *Acropora*, *Heliopora*, and *Pocillopora* and encrusting and massive *Montipora*, *Porites*, and *Favia*. The lagoonal reef-flat surface becomes increasingly porous with distance from the reef-island. The reef-flat surface transitions from delicate *Montipora digitata*, to plate and branching *Porites* habitat at the perimeter of the backreef (**Figure 3.2**). The shallow lagoon is occupied by branching and massive *Porites* patch reefs surrounded by abraded *Calcarina* rich lagoonal sediment.

### **3.3.2 Bio-geologic linkages recorded in the fossil record**

The seaward margin of the windward reef-flat reached MSL approximately 5.05 cal kyr B.P. (**Table 3.1; Figure 3.3**) and laterally accreted in the lagoonal direction at 228.3 m/kyr over the next century as sea level increased water levels across the reef-flat from 0.50 to 1.0 m. Active accretion of the reef-flat “turned off” at approximately 3.79 kyr and coral growth along the main reef-flat is currently in a senescent state (**Figure 3.4A**).

**Table 3.1** Geochronology of reef-island formation

Location	Site	MSL (m)	Material dated <sup>a</sup>	Lab ID	<sup>14</sup> C age (year BP)	Years cal BP (2σ)	Median (year cal BP)
Reef-flat	G1	-0.68 - -0.69	<i>Heliopora coerulea</i>	D-AMS 029828	3800 ± 27	3901-3671	3786
Reef-flat	G1	-1.37 - -1.42	<i>Heliopora coerulea</i>	D-AMS 029829	3879 ± 26	4020-3772	3894
Reef-flat	G1	-1.68--1.75	<i>Calcarina</i>	D-AMS 021239	3388 ± 29	3391-3179	3294
Reef-flat	G4	-0.73 - -0.77	<i>Acropora</i>	D-AMS 029830	4405 ± 28	4778-4500	4616
Reef-flat	G4	-1.82 - -1.92	<i>Calcarina</i>	D-AMS 021240	4251 ± 33	4766-4613	4805
Reef-flat	G6	-0.60 - -0.63	<i>Acropora</i>	D-AMS 029834	4721 ± 40	5203-4856	5006
Reef-flat	G8	-1.64 - -1.69	<i>Porites</i>	D-AMS 029831	4733 ± 29	5088-4941	5023
Reef-flat	G8	-2.66 - -2.68	<i>Pocillopora</i>	D-AMS 029832	4747 ± 30	5229-4900	5051
Reef-flat	G9	-1.22 - -1.27	<i>Montipora</i>	D-AMS 029835	4354 ± 28	4677-4415	4536
Rubble Rampart	RR72	1.42-1.44	<i>Acropora</i>	D-AMS 020170	814 ± 28	533-415	479
Island	T1	1.13-1.26	<i>Calcarina</i>	D-AMS 020171	1404 ± 28	1081-903	985
Island	T1	0.13-0.02	<i>Calcarina</i>	D-AMS 020172	1380 ± 29	1059-885	962
Island	T2	0.94-1.06	<i>Calcarina</i>	D-AMS 020173	1373 ± 25	1049-885	954
Island	T2	0.24-0.39	<i>Calcarina</i>	D-AMS 020174	1566 ± 23	1251-1068	1170
Island	T3	0.93-0.97	<i>Calcarina</i>	D-AMS 020175	1322 ± 23	976-795	904
Island	T3	-0.43	<i>Calcarina</i>	D-AMS 020176	1518 ± 30	1220-1000	1113
Island	T4	1.62-1.68	<i>Calcarina</i>	D-AMS 020177	1020 ± 34	686-537	624
Island	T4	0.64-0.71	<i>Calcarina</i>	D-AMS 020178	1192 ± 24	873-684	767
Island	T5	1.48-1.55	<i>Calcarina</i>	D-AMS 020179	1086 ± 29	757-615	676
Island	T6	2.0-2.13	<i>Calcarina</i>	D-AMS 020180	1333 ± 34	1015-793	915
Island	T6	0.92-1.02	<i>Calcarina</i>	D-AMS 020181	1436 ± 26	1123-926	1017

Island	T7	1.38-1.42	<i>Calcarina</i>	D-AMS 024740	1276 ± 29	935-755	853
Island	T7	-0.26- -0.21	<i>Calcarina</i>	D-AMS 024741	1466 ± 43	1171-934	1054
					modern		
Lagoon	LBF37	Beach	<i>Calcarina</i>	D-AMS 020182	*(102.86 ± 0.27)	-	-
					modern		
Lagoon	LBF60	Beach	<i>Calcarina</i>	D-AMS 020183	*(105.17 ± 0.31)	-	-
					modern		
Lagoon	LBF45	Beach	<i>Calcarina</i>	D-AMS 020184	*(103.18 ± 0.32)	-	-

\*Fraction of modern <sup>14</sup>C (pMC ± 1 σ error )

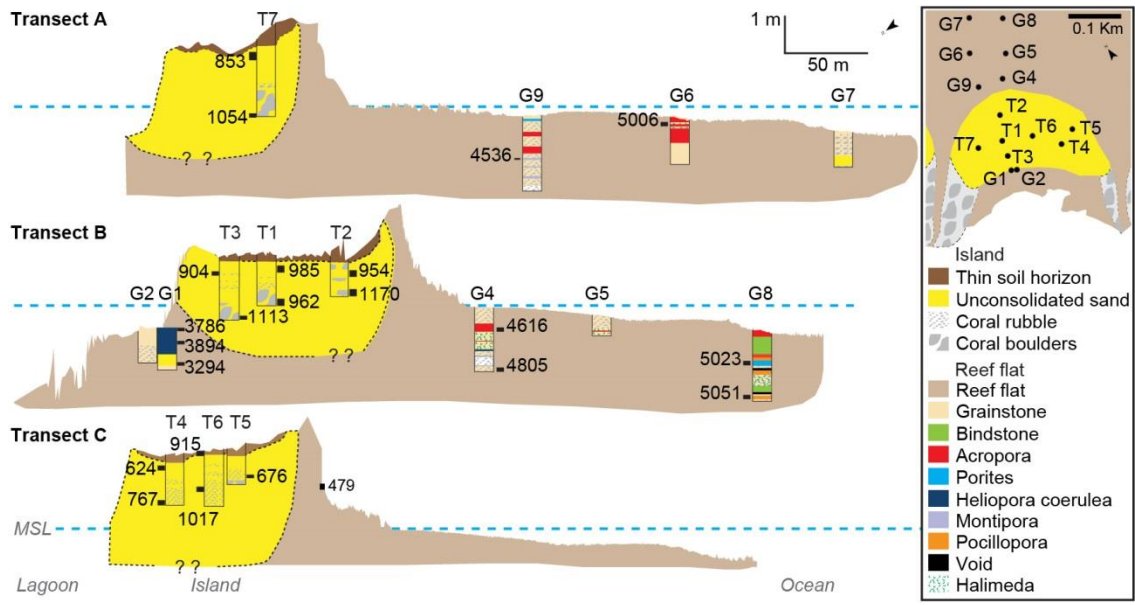


**Figure 3.3** Reef-island stratigraphy interpreted from reef cores and island trenches. Ages are median values depicted in cal yr B.P.

Rapid island building coincides with falling sea level (0.75-0.40 m). Island building initiated in the northwest (T1-3, 6-7) between 1.17–0.85 kyr and extended towards the southeast (T4 & 5) between 0.77–0.62 kyr (**Figure 3.3; Figure 3.4B**). A coral rubble basal unit was deposited first, followed by coarse, *Calcarina* ( $75.6 \pm 8.6\%$ ) dominant sand (**Figure 3.3; Figure 3.4C**). Abrasion of *Calcarina* increased towards the surface of the island symbolic of foraminiferal habitat transitioning seaward and an increased lag time between transport across the reef-flat and deposition during the final stages of island building. The base of the southeast region of the island is the only site statistically indistinguishable from surface sediment on the seaward reef-flat reflective of rapid deposition. *Acropora* from the lithified rubble rampart at the seaward margin of the reef-island returned an age of 0.48 kyr (**Figure 3.3**).

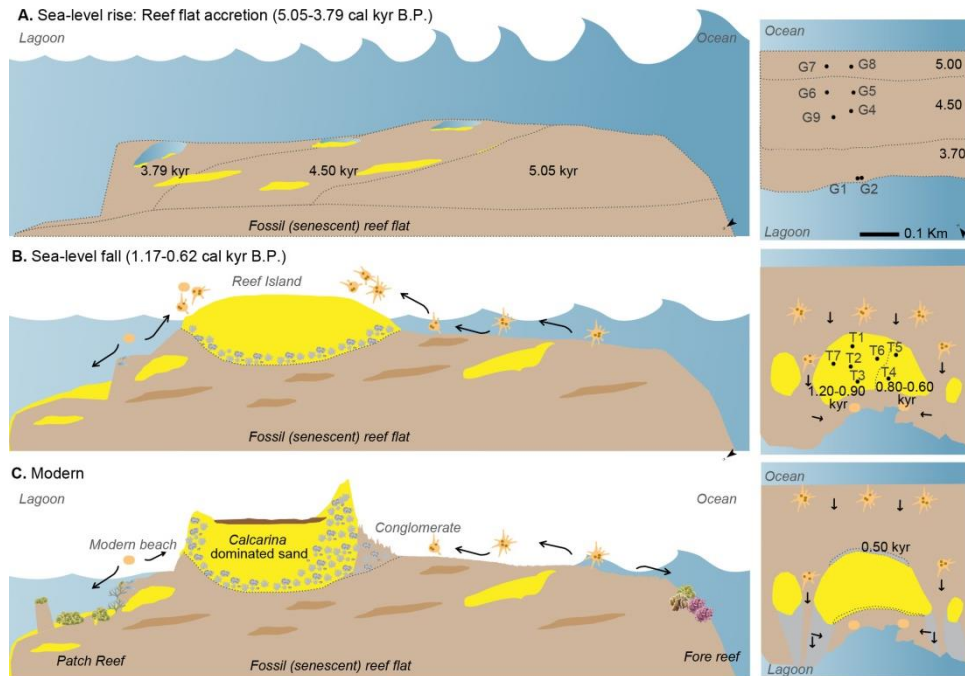


**Figure 3.4** Conceptual model of reef-island formation. A.) As sea level approached highstand values, the reef-flat prograded towards the lagoon (5.05-3.79 cal kyr B.P.). Two and a half millennia of reef infilling and lithification of reef derived sediment by carbonate cements and encrusting foraminifera and coralline algae were required prior to island formation. Arrows depict sediment transport. B.) Rapid island building occurred between 1.17-0.62 cal kyr B.P. Sea level fall enabled habitat conducive for high rates of *Calcarina* sediment production and deposition. C.) With the exception of the island perimeter, the reef-island is bio-geologically disconnected from reef-flat sediment production. *Calcarina* sediment is exported off the reef-flat to the fore reef and lagoon. Living coral is limited to the seaward fore reef and lagoonal perimeter of the reef-flat and patch reefs.

Previous studies document island emergence and building proportional to lateral reef-flat accretion (Woodroffe et al., 1999; Kayanne et al., 2011; Kench et al., 2014b; Yamano et al.,

2014) (**Table 3.2**). In some instances island emergence is delayed up to 3.06 kyr after a reef ceased accreting (Yamano et al., 2000; Kench et al., 2005; Woodroffe et al., 2007; Ford and Kench, 2012). Delayed island formation has been attributed to ecological shifts on the reef surface, consistent with a lag in the attainment of sea level conducive for the production of island-building constituents (e.g. foraminifera and calcareous algae from intertidal reefs and reef-flat environments) (Yamano et al., 2000; Perry et al., 2011). Furthermore, within the Maldives, a prerequisite of reef-island formation is lagoonal (*velu*) infilling of annular (*faro*- ring shaped) reefs (Kench et al., 2005). *Halimeda* dominated island sediments are deposited directly upon lagoonal sediments rather than the reef-flat. This process enables lagoonal infilling and island building to occur simultaneously with reef-flat accretion at smaller faros (<0.5 km<sup>2</sup>), whereas faros larger than >0.5 km<sup>2</sup> may never be fully infilled.

**Table 3.2** Timing of reef-island formation and dominant island constituents

Location	Reef-flat formation (cal kyr B.P.)	Island formation (cal kyr B.P.)	Time lag (kyr)	*Dominant island sediment	Sea level highstand timing	Reference
Pacific						
Bokollap Island, Majuro, RMI	5.05-3.79	1.17-0.62	2.60	Atoll rim (motu): (1) foraminifera sand: <i>Calcarina</i> , (2) coarse gravel	1.13 ± 0.08 m, 1.94-2.26 cal kyr B.P. (RMI estimate)	This study
Laura island, Majuro, RMI	4.17-1.99	1.98-0.65	simultaneous	Atoll rim: (1) foraminifera sand: <i>Calcarina</i> , (2) coarse gravel		(Kayanne et al., 2011)
Jabat Island, RMI	5.38-5.04	4.87-1.82	0.17	Platform reef (motu): (1) cobble size coral with <i>Calcarina</i> dominant sand matrix, (2) coarse gravel		(Kench et al., 2014b)
Tepuka Island, Funafuti atoll Tuvalu	ND	1.10-0.50	ND	Atoll rim (motu): (1) fine to medium foraminifera sand: <i>Baculogypsina</i> , <i>Amphistegina</i> , <i>Calcarina</i> (>50%), (2) coarse grain sand and	ND	(Kench et al., 2014a)

				fine gravel: coralline algae (>40%) & coral (20-30%), (3) coral gravel, coralline algae, & mollusk (>60%)		
Makin, Kiribati	ND	2.50-0.40	ND	Platform reef: Fine to medium foraminifera sand: <i>Baculogypsina sphaerulata</i> , <i>Amphistegina lobifera</i> , <i>Calcarina spengleri</i>	0.4-0.5 m 2.40 cal kyr B.P.	(Woodroffe and Morrison, 2001)
Green Island, GBR, Australia	ND	4.00-2.19	ND	Platform reef (sand cay): foraminifera sand: <i>Amphistegina lessonii</i> , <i>Baculogypsina sphaerulata</i> , & <i>Calcarina hispida</i>	0.5-1.5 m 6.50-4.20 cal kyr B.P. (continental GBR estimate)	Yamano et al. 2000
Warrber Island, Torres Strait, Australia	ND	2.74-2.47	3.06	Platform reef (sand cay): mollusk rich	0.8 m, 5.80 cal kyr B.P.	(Woodroffe et al., 2007)
Mba Island, New Caledonia	ND	4.50-1.37	simultaneous	Platform reef (vegetated sand cay) : medium to coarse sands: coral & <i>Baculogypsina sphaerulata</i>	+1.1 m, 6.50-2.80 cal kyr B.P. (SW New Caledonia)	(Yamano et al., 2014)

Indian Ocean		foraminifera (60%), <i>Halimeda</i> , & mollusk				
West Island, Cocos	4.00- 3.00	3.40-2.00	simultaneous	Atoll rim: coarse foraminifera sand that fines up	0.4-0.8 m, 3.50 cal kyr B.P.	(Woodroffe et al., 1999)
South Maalhosmadul, Maldives	5.50	5.50-2.5	<sup>1</sup> simultaneous, <sup>2</sup> delayed up to 2.50	Lagoon reef-island: (1) fine to medium coral-algal sand, (2) <i>Halimeda</i> sand	0.5 m 4.00-2.00 cal kyr B.P.	(Perry et al., 2013)  (Kench et al., 2005; Gischler et al., 2008)

---

ND = not determined, kyr = 1,000 years, cal kyr B.P. = calibrated 1,000 years before present

<sup>1</sup> islands <0.25 km<sup>2</sup>

<sup>2</sup> islands >0.25 km<sup>2</sup> unvegetated sand cays may be present but islands typically have yet to form

\*Dominant island sediment constituents are numbered sequentially such that the largest number is the basal unit.

At windward Majuro a series of reef cores reveal that infilling of a porous reef-flat and lithification of unconsolidated sediment to form a low-porosity limestone platform was crucial for the accumulation island sediments. To better characterize the role of sediment trapped in the reef-flat framework and ecological shifts of dominant sediment sources we defined four biolithofacies of the windward reef-flat following the methods of Grossman and Fletcher (2004) and Engels et al. (2008). These are: (1) coral framestone (26.8%), (2) bindstone (18.2%), (3) grainstone (44.9%), and (4) unconsolidated sediment (9.1%) (**Figure 3.5**). The coral framestone lithofacies are dominated by in situ branching *Acropora* at the seaward reef-flat, and *Heliopora Coerulea* within grainstone (27.3% coral and 27.4% calcareous algae) at the lagoon reef-flat. Encrustations of foraminifer *Homotrema* are present at the surface of coral (**Figure 3.6A**), and acicular aragonite cements occupy coral pores. With the exception of core G6 (mid seaward reef), corals did not grow above -0.77 - -0.61 m relative to MSL. Bindstone facies consist of coralline algae (*Hydrolithon gardineri* and *Hydrolithon onkodes*) and foraminifera (*Homotrema*) binding rounded coral rubble (*Acropora*, *Heliopora*, *Porites*, *Favosites*, and *Pocillopora*) (**Figure 3.6B**). Minor cements include bladed to acicular aragonite and blocky low magnesium calcite within coral pores, and calcite rim cements within calcareous algae conceptacle chambers.

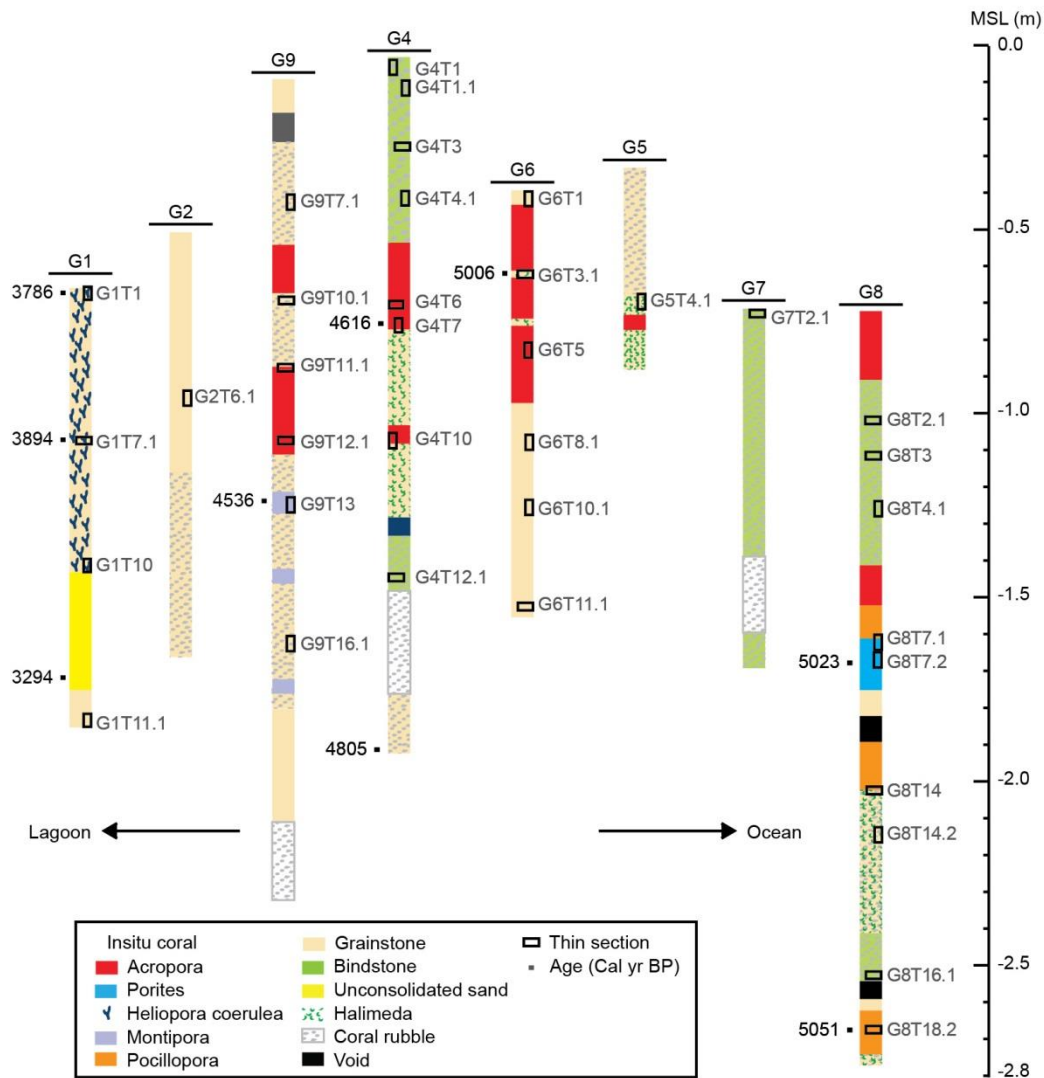


**Figure 3.5** Fossil-reef cores G1-2 were extracted from the lagoonal reef-flat, and cores G4-9 were extracted from the seaward reef-flat. The location of radiocarbon ages (median values; cal kyr B.P.) and thin section samples are noted.

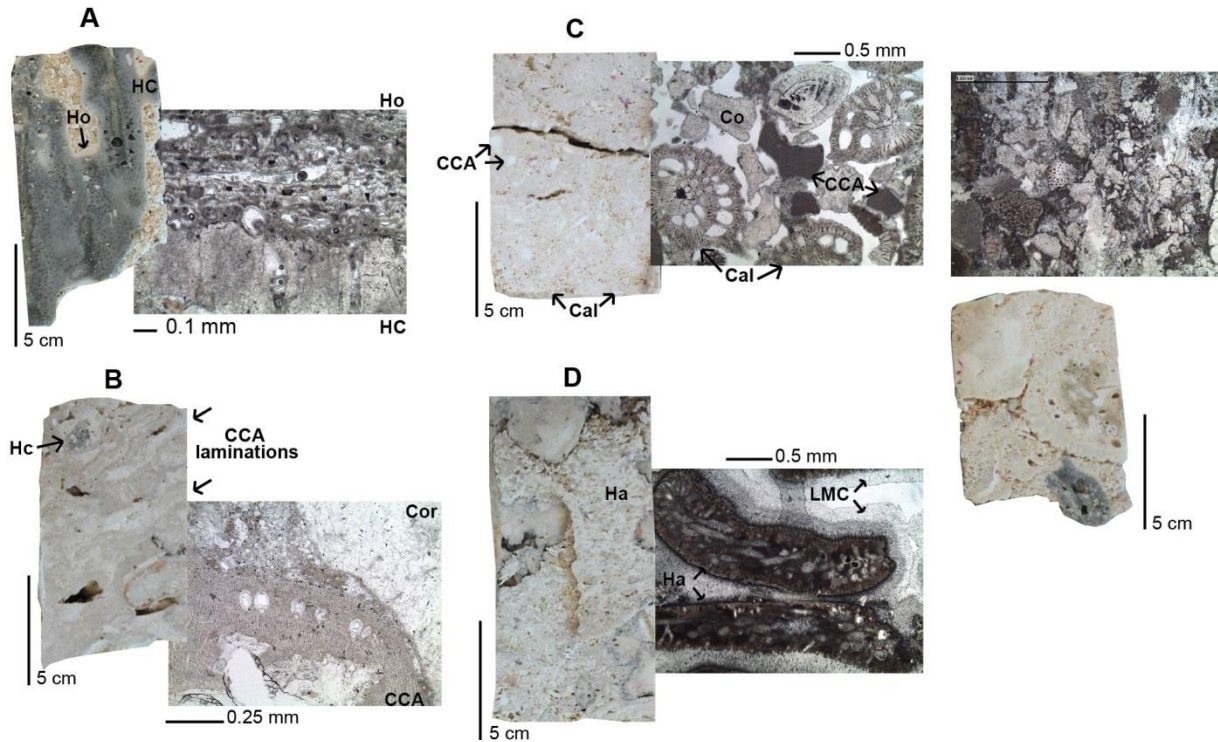


**Figure 3.6** The fossil-reef flat is composed of four biolithofacies: (A) coral framestone, (B) bindstone, (C-E) grainstone, and unconsolidated sediment (not depicted in figure). (C) depicts *Calcarina* rich grainstone, and (E) is composed of *Halimeda* rich grainstone. The figure is labeled such to represent the following: HC: *Heliopora Coerulea*, Ho: *Homotrema* (encrusting foraminifera), Ac: *Acropora*, Cal: *Calcarina* (benthic foraminifera), Ha: *Halimeda*, LMC: low-magnesium calcite, CCA: calcareous red algae, Cor: coral rubble.

The grainstone facies is characterized by *Halimeda* ( $42.0 \pm 13.7\%$ ) subfacies, *Calcarina* (31.8%) subfacies, and rounded coral rubble suspended in highly abraded skeletal fragments (**Table 3.3**). Grainstone facies are typically characterized by heavily rimmed calcite cements, while *Calcarina* grainstone subfacies may be more porous. Unconsolidated sediment facies are composed of rounded coral rubble and fine sand (25.3% *Amphistegina*). Although *Calcarina* is

represented in reef-flat sediment, benthic foraminifera are minor contributors of overall sediment production relative to the modern reef-flat and reef-island. Rather the reef framework was either infilled by *Halimeda*, and fragments of calcareous red algae and coral, or the branching corals such as *Heliopora* (G1) may have acted to slow the flow suspended sediment and aid in deposition. Overtime bioclasts were either lithified by low magnesium calcite cements or bound together by encrusting foraminifera and calcareous algae.

**Table 3.3** Composition of major depositional units at Bokollap island, Windward Majuro

Depositional unit	Cal	Am	O. For	Coral	Ha	CCA	Mol	Ech	UI
Reef-flat surface (modern)	63.20 ± 13.76	3.01 ± 3.65	1.92 ± 1.45	8.67 ± 5.62	4.61 + 2.22	1.51 ± 1.31	5.88 ± 2.59	1.01 ± 3.11	10.2 ± 7.43
Island (1.17-0.62 cal kyr B.P.)	76.11 ± 8.76	3.02 ± 2.42	1.20 ± 0.94	5.14 ± 3.06	0.71 + 0.79	0.11 ± 0.23	2.44 ± 1.93	0.13 ± 0.21	11.06 ± 5.19
Reef-flat sedimentary facies (5.05-3.29 cal kyr B.P.)									
Framestone									
<i>Heliopora</i>	15.00	3.64	5.45	27.27	8.64	27.27	3.64	2.73	6.36
Grainstone									
<i>Halimeda</i>	13.16 ± 10.29	1.77 ± 2.10	8.47 ± 5.19	3.00 ± 1.67	42.01 ± 13.65	8.05 ± 2.72	3.50 ± 1.91	1.90 ± 0.91	18.14 ± 17.46
<i>Calcarina</i>	31.84	4.49	4.49	9.36	6.37	16.10	2.62	0.37	24.34
Coral rubble	6.79	1.51	5.28	4.53	7.55	15.85	3.02	1.51	53.96
Bindstone	13.95	5.44	9.52	1.36	10.88	16.33	1.36	0.34	40.82
Unconsolidated sand	18.47	25.28	5.69	7.10	5.40	0.57	6.25	0.00	31.25

Cal: *Calcarina* (foraminifera), Am: *Amphistegina* (foraminifera), O. For: other foraminifera (*Sorties*, *Homotrema*), Ha: *Halimeda*,

CCA: calcareous red algae, Ech: echinoderm, UI: unidentified bioclasts.

### 3.3.3 Future reef-island resiliency is dependent upon sediment infilling and reef ecology

The biological and geological elements of atoll reef-islands and coral-reef habitats are intimately connected to each other, and to changes in sea level and water quality. Atoll reef-islands are complex, layered accumulations of carbonate sand and gravel that exist because adjacent living reefs and fossil-reef flats act as sediment factories. Thus, for atoll reef-islands to be able to naturally evolve (through migration, and accretion; Kench et al. 2018) with rising sea level and changing hydrodynamic conditions, there needs to be: (1) ecological shifts that enable reactivation of coral growth along the fossil-reef platform to accommodate lagoonal accretion of the reef-flat, and (2) sediment deposition rates comparable to the rate of SLR to foster island building and infilling of the reef-flat.

At Majuro, reef-islands are typically located adjacent to the lagoonal margin of the fossil-reef flat. As sediment is transported from the seaward-foraminifera zone, it is deposited among coalescing coral heads of the lagoonal backreef, infilling the reef-flat. Through this process the atoll platform extends into the lagoon, accommodating island migration depicted by the extension of island spits (**Figure 3.7A**). Platform extension by fringing reef accretion works synergistically with reef-islands as they adjust to modern SLR ( $3.60 \pm 1.22$  mm/yr between 1993-2018; MAJURO-C tide station). Future island resiliency will require the reef-flat expansion towards the lagoon, and increased sediment production and deposition for both infilling the reef-flat, and island building (**Figure 3.7B**). If the growth capacity of the ocean reef ecosystem cannot keep pace with future SLR, then there will be an insufficient supply of sediment (sand, gravel or blocks) to assist in island sediment exchange (erosion and accretion) and platform extension. If the lagoon back reef fails to keep pace with SLR, then lagoonward platform extension will be

impacted. Either of these will limit island resiliency in the face of SLR, potentially contributing to a more rapid loss of island function as SLR enters the exponential phase of rise in coming decades. Thus it is important that management of coastal resources is inclusive of both ocean and lagoon reef systems to improve understanding of their health, sediment production, and ultimately of island resiliency.

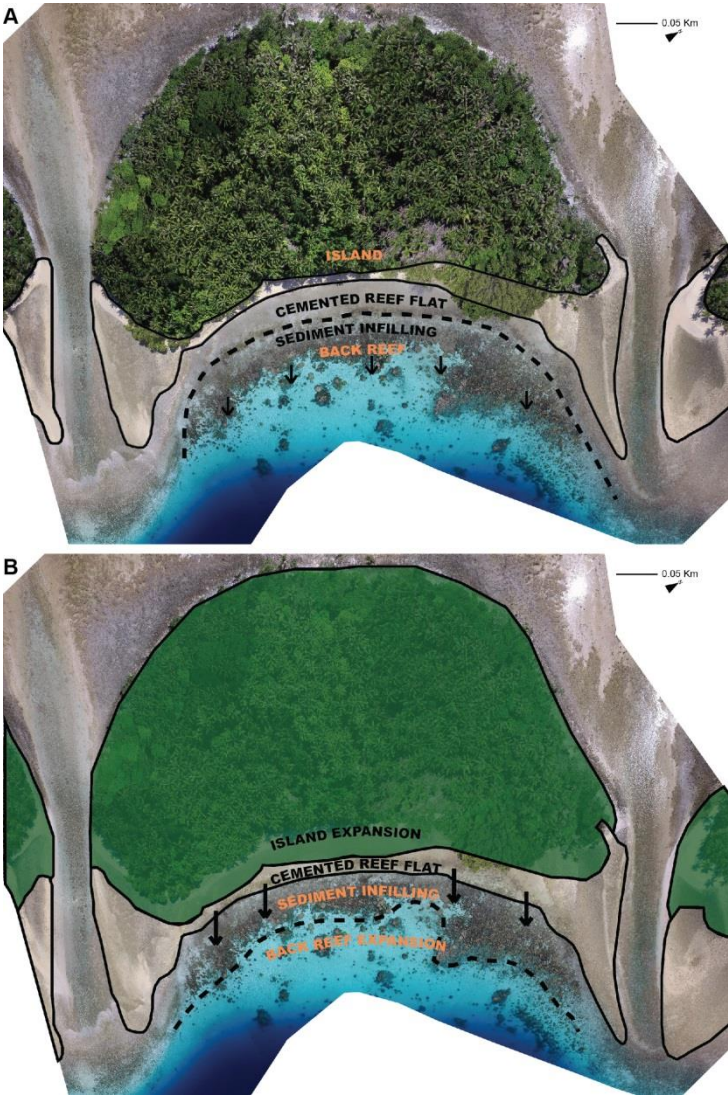


**Figure 3.7** Reef-island extension. A.) Presently, reef-islands are located at the lagoonal extent of the fossil-reef flat. Subaerial sediment deposition and reef infilling of the shallow backreef are indicative of lagoonward island extension. B.) Future island resiliency will require lagoonward expansion of the reef-flat and increased sediment deposition conducive to backreef infilling and island building.

### 3.4 Conclusion

The data presented here illustrates the importance of managing atoll reefs and islands as bio-geologically linked systems. Pacific reef-islands are composed primarily of foraminifera that live within a narrow depth range on tidally emergent reef-flats. Sediment production and deposition are sensitive to sea level change and other environmental shifts. The fossil record at windward Majuro revealed that under elevated sea level *Calcarina* was not a dominant sediment contributor. Rather the coral-algal ecosystem was the largest contributor to reef-flat sediment. Rising or elevated sea level and increasing or increased accommodation space enabled active reef accretion in the lagoonal direction. Branching corals acted to slow and trap suspended sediment under increased hydrodynamic regimes. Collectively these variables enabled reefs to be infilled by sand sized fragments of coral (*Acropora*, *Pocillopora*) and calcareous algae (*Halimeda*, *Hydrolithon gardineri* and *Hydrolithon onkodes*) and coral rubble.

Building upon previous studies (Kench et al., 2005; Kayanne et al., 2011; Perry et al., 2011; Morgan and Kench, 2016; East et al., 2018) we find that the emergence of a high energy windward reef-island required that the reef-flat first be infilled with reef derived detritus and subsequently lithified. Furthermore, falling sea-level and decreased hydrodynamic energy

enabled *Calcarina* foraminifera to replace coral-algal communities as the dominant reef-flat ecosystem. Shortly after *Calcarina* rich reef-flats developed, and *Calcarina* rich reef-islands followed.

As sea level rises in the future, the time scales by which reef-island systems respond to elevated water levels will be highly dependent upon ecosystem shifts of dominant sediment constituents that either foster or inhibit both reef-flat platform extension, and island building. To better elucidate island response to environmental stressors, future studies should focus upon the bio-geological linkages amongst islands of differing dominant sediment constituents (*Halimeda*, coral fragments, mollusk, etc).

## CHAPTER 4. RETHINKING REEF-ISLAND STABILITY IN THE REPUBLIC OF THE MARSHALL ISLANDS

*To Be Submitted To:* Scientific Reports

**Abstract** - Unprecedented rates of sea level rise (SLR) and wave driven flooding threaten the very existence and habitability of atoll nations. Yet geologic reconstructions of island formation during rising mid-Holocene sea level and island persistence in regions where SLR is twice the global average provide more optimistic interpretations of future island viability. To shed light on conflicting interpretations of island habitability, we derive sea level thresholds and time frames to anticipate rapid-island change within the Republic of the Marshall Islands. Here we show that all reef-islands will enter an unstable phase within this century as sea level exceeds late-Holocene sea level threshold values that constrained reef-island emergence and rapid island building. Under the intermediate SLR scenario (1.2 m by 2100) island habitability is further threatened by accelerating SLR (2x local mean) and the loss of potable groundwater by the mid-21<sup>st</sup> century. Impacts are further expedited as the worst case scenario (3.23 m by 2100) depicts island instability, loss of groundwater, exceedance of 1 m of SLR and a tripling in local SLR anticipated by mid-century. SLR threatens the cultural identity of atoll nations and as such will require adaptable planning methods, reflective of multidisciplinary research, and open minded, multi-world views.

## **4.1 Introduction**

Low lying (1-3 m) atoll reef-islands composed largely of unconsolidated sediment and coral rubble (Woodroffe, 2008) provide the only habitable land for atoll islanders. As high-end sea level rise (SLR) projections (~2m) (DeConto and Pollard, 2016) exceed the average elevation of these low reef-islands, unprecedented rates of SLR threaten the very existence of atoll nations within the lifetime of current islanders. Despite accounts of atoll vulnerability, some historical shoreline assessments document islands as dynamic features that have persisted or expanded in regions where historical SLR is as much as twice the global average (Kench et al., 2018). Conflicting interpretations of island viability have resulted from prior research independently assessing the stability (or lack thereof) of islands at three different time scales; 1. The now, 2. The recent past, and 3. The geologic record.

### **4.1.1 The now**

Studies of ‘the now’ document nearly a decade of wave overwash and flooding impacts related to extreme wave events (Becker et al., 2014; Merrifield et al., 2014; Quataert et al., 2015; Storlazzi et al., 2015). Future projections suggest SLR will enable larger wave run up at shorelines during extreme events (Storlazzi et al., 2011). Furthermore with SLR more frequent flooding and overwash may also result from smaller offshore wave heights (Cheriton et al., 2016). Field observations document that salinization of aquifers following a wave-driven flooding event required nearly two years of recovery before becoming potable again (Gingerich et al., 2017). ‘The now’ concludes that the majority of atolls are projected to be uninhabitable by mid-century as potable groundwater on most atoll islands will be permanently unavailable (Storlazzi et al., 2018). Those atolls that function independent of groundwater resources (rely on

rainfall catchments, desalinization facilities, etc), the majority of island and infrastructure will be flooded annually by wave overwash by the end of the century (Storlazzi et al., 2018).

#### **4.1.2 The recent past**

Studies of ‘the recent past’ couples historical tide gauge data, and a limited number (1-3) of available aerial photographs from the last century to characterize change in island area and shoreline position relative to changes in sea level. Analyses of historical aerial imagery documents the majority of atoll islands (88.6%) in the Pacific and Indian Oceans (Duvat, 2018) have remained stable or increased in area ( Tuvalu (Webb and Kench, 2010; Kench et al., 2018), the Republic of the Marshall Islands (Ford and Kench, 2015), French Polynesia (Duvat and Pillet, 2017), Federated States of Micronesia (Webb and Kench, 2010), and Kiribati (Webb and Kench, 2010)). Island persistence and growth is documented despite local relative SLR ranging from  $2.0 \pm 0.6$  (Pingelap, Mokil) to  $5.1 \pm 0.7$  (Funafuti, Tuvalu) mm/yr (Becker et al., 2012; Duvat, 2018). On the basis of the ‘recent past’ it is argued that islands will continue to persist as physical sites for habitation over the next century (Kench et al., 2018) assuming that local sea level rise rates to do not drastically accelerate.

#### **4.1.3 The geologic record**

Studies of ‘the geologic record’ show that atoll reef-islands are among the youngest geological formations in the world (typically less than 5500 cal year BP) (Kench et al., 2005) and reef-island formation is dependent on sea level change, reef growth, and island sediment availability (Woodroffe, 2008; Perry et al., 2011). Following the last ice age, sea level in the equatorial Pacific stood 1-2 m higher than present as recently 2,000-5,000 years ago (Grossman et al., 1998; Dickinson, 2009). Research on the timing of atoll reef-island formation is

inconsistent. Studies document formation during mid-Holocene SLR (pre-highstand) (Kench et al., 2005, 2014b), during the highstand (Kayanne et al., 2011), and as sea level fell in the recent 1,000-2,000 years (post-highstand) (Woodroffe and Morrison, 2001; Mckoy et al., 2010). Islands that formed during mid-Holocene SLR may be more resilient to future SLR (Kench et al., 2005) than those islands that required sea level fall to trigger island emergence because island composition is reflective of sediment sources for adapted to higher water levels and increased hydrodynamic energy.

Among these three time periods there is no scientific consensus on the response of reef-islands to rising sea level (Biribo and Woodroffe, 2013), illustrating the need for improved examination of the vulnerability and resiliency of a nation of islands that spans all three time scales. To inform island resiliency we use geologic evidence of island formation and sea level change to derive place based sea level thresholds and time frames to anticipate rapid island evolution in response to future SLR.

The Republic of the Marshall Islands (RMI) serves as the study site, because the RMI has one of the richest datasets amongst the three time periods. We compare spatial variations of the timing of island formation and reconfiguration in response to mid-late Holocene sea level change across the RMI. Local sea level threshold values are compared to future projections of SLR to assess a timeframe for island destabilization and/or resiliency within the RMI. We assess sea level thresholds within the context of previous studies centered upon the ‘the now’ and ‘the recent past’ to project the timing of island change under future SLR.

## 4.2. Methods

The RMI is composed of 29 atolls and 5 mid-ocean reef platform islands aligned along two nearly parallel chains between 4°34' to 14°43'N and 160°48' to 172°10'E (**Figure 4.1**). Approximately 74% of the total population (53,158 people) of the RMI live on Majuro and Kwajalein atolls (Barton and Nemra, 2012).

### 4.2.1 Modeling island formation

Here we report the methodology employed in this study at windward Majuro, and those methods employed at Laura island, leeward Majuro (Kayanne et al., 2011; Yasukochi et al., 2014), and Jabat Island (Kench et al., 2014b). Two field expeditions between August 4th-8th 2016, and August 8th-13th 2017 to Bokollap Island, windward Majuro supplemented the previously published geologic dataset. Hand held gas powered drills attached to diamond core bits were used to extract 1-2 m cores from the reef-flat at each island. A series of geologic trenches enabled the interpretation of island sedimentology. Topographic surveys of the mid-ocean reef platform and islands were undertaken at windward Majuro using a Leica TC407 total station, and at Jabat island using a laser level and RTK GPS. All surveyed elevations were reduced to mean sea level with reference to the MAJURO-C (<http://www.iocsealevelmonitoring.org/station.php?code=marsh>) or Kwajalein (<https://tidesandcurrents.noaa.gov/stationhome.html?id=1820000>) tide station. Elevations at Bokollap island were further corrected using a locally installed water level installed in the lagoon. Surveyed points were adjusted to geographic coordinates and ellipsoid heights relative to World Geodetic System 1984. Surveyed data points at windward Majuro have a horizontal

accuracy of  $\pm 1.0$  m, and a vertical accuracy of  $\pm 0.03$  m, however the accuracy at the other two study sites was not reported.

A compositional analysis was performed on a minimum of 200 identifiable grains from samples derived from the reef-flat, modern beach, and island trenches to determine origin and relative percentage of biogenic components. Dominant biogenic components included foraminifera (*Calcarina*, *Amphistegina*, *Sortidae*), coral, coralline algae, *Halimeda*, mollusk, and echinoderm fragments. A spine ratio metric was also calculated to account for abrasion of *Calcarina* tests and subsequently track sediment transport. Following Yasukochi et al. (2014) spine ratio was calculated (Equation 1) as follows:

$$\text{SpineRatio}(\%) = \left( \frac{A + B}{A + B + C} \right) \quad (4.1)$$

Grade A had complete spines, grade B had some spines, and grade C had no spines (Yasukochi et al., 2014). Only those *Calcarina* that retained their spines (A or B) were submitted for dating, because these samples are assumed to have been deposited upon the island shortly after removal from the reef-flat. Radiocarbon ages were measured using accelerator mass spectrometers at DirectAMS Radiocarbon Dating Service. Island formation was determined from *Calcarina* foraminifera bulk samples collected at Majuro, while at Jabat both the *Calcarina* and coral-algal sand from gravel units were dated. The timing of reef-flat progradation was determined from radiocarbon dating of in situ corals in geologic cores obtained at each island. At all three study sites radiocarbon ages from distinct reef cores, and stratigraphic units that constrain island emergence and stability were recalibrated for the regional marine reservoir effect using CALIB

version 7.1 (Stuiver et al., 2019) and Marine13 calibration dataset (Stuiver and Braziunas, 1993a; Reimer et al., 2013) (<http://calib.org/calib/calib.html>) (**Table 4.1**). A single  $\Delta R = -30 \pm 25$  years was derived from the comparison of melon-headed whale bones and charcoal specimens removed from the same stratigraphic unit at Laura Island, Majuro atoll (Kayanne et al., 2011).

**Table 4.1:** Reef-island age

Island	Location	Site	<sup>+</sup> MSL (m)	Material dated	Lab ID	<sup>14</sup> C age (yr BP)	Years cal yr BP (2σ)	Median (cal yr BP)	
Windward Majuro	Reef-flat	G1	-0.69	<i>Heliopora coerulea</i>	D-AMS 029828	3800 ± 27	3901-3671	3786	
	Reef-flat	G8	-2.67	<i>Pocillopora</i>	D-AMS 029832	4747 ± 30	5229-4900	5051	
	Island	T1	1.21	<i>Calcarina</i>	D-AMS 020171	1404 ± 28	1081-903	985	
	Island	T1	0.08	<i>Calcarina</i>	D-AMS 020172	1380 ± 29	1059-885	962	
	Island	T2	1.00	<i>Calcarina</i>	D-AMS 020173	1373 ± 25	1049-885	954	
	Island	T2	0.32	<i>Calcarina</i>	D-AMS 020174	1566 ± 23	1251-1068	1170	
	Island	T3	0.95	<i>Calcarina</i>	D-AMS 020175	1322 ± 23	976-795	904	
	Island	T3	-0.43	<i>Calcarina</i>	D-AMS 020176	1518 ± 30	1220-1000	1113	
	Island	T4	1.65	<i>Calcarina</i>	D-AMS 020177	1020 ± 34	686-537	624	
	Island	T4	0.68	<i>Calcarina</i>	D-AMS 020178	1192 ± 24	873-684	767	
	Island	T5	1.52	<i>Calcarina</i>	D-AMS 020179	1086 ± 29	757-615	676	
	Island	T6	2.07	<i>Calcarina</i>	D-AMS 020180	1333 ± 34	1015-793	915	
	Island	T6	0.97	<i>Calcarina</i>	D-AMS 020181	1436 ± 26	1123-926	1017	
	Island	T7	1.40	<i>Calcarina</i>	D-AMS 024740	1276 ± 29	935-755	853	
	Island	T7	-0.24	<i>Calcarina</i>	D-AMS 024741	1466 ± 43	1171-934	1054	
		Beach	LBF37	Beach	<i>Calcarina</i>	D-AMS 020182	modern †(102.86 ± 0.27)	-	-
		Beach	LBF60	Beach	<i>Calcarina</i>	D-AMS 020183	modern †(105.17 ± 0.31)	-	-
	Beach	LBF45	Beach	<i>Calcarina</i>	D-AMS 020184	modern †(103.18 +	-	-	

						0.32)		
	Reef-flat	LrI-14	*NR	<i>Heliopora coerulea</i>	Beta-191716	4080 ± 70	4390-3960	4170
<sup>1</sup> Leeward Majuro	Reef-flat	LrII-5	*NR	<i>Acropora</i>	Beta-191717	3580 ± 100	3800-3290	3520
	Reef-flat	LrIII-1	*NR	<i>Acropora</i>	Beta-191718	2330 ± 60	2150-1820	1990
	Island	N1-140	*NR	<i>Calcarina</i>	Beta-210285	2320 ± 40	1861-2109	1978
	Island	LR-4-105	*NR	<i>Calcarina</i>	Beta-191710	1050 ± 40	548-726	648
	Reef-flat	Wk-29494	-0.17	<i>Porites</i>	Wk-29494	4776 ± 43	4936-5270	5104
	Reef-flat	Wk-29495	-0.53	<i>Porites</i>	Wk-29495	4989 ± 43	5270-5508	5378
	Reef-flat	Wk-29496	-0.74	<i>Porites</i>	Wk-29496	4740 ± 43	4871-5229	5041
<sup>2</sup> Jabat Island	Island	Wk-29475	1.55	coral-algal sand	Wk-29475	4609 ± 42	4776-5023	4870
	Island	Wk-29479	0.77	foraminifera sand	Wk-29479	4399 ± 42	4469-4783	4610
	Island	Wk-29485	0.67	coral-algal sand	Wk-29485	2182 ± 38	1645-1932	1818

<sup>1</sup>Table S1 in Kayanne et al., 2011; <sup>2</sup>Table S1 in Kench et al. 2014

<sup>+</sup>MSL = median elevation values are reported

\*NR = not reported

<sup>†</sup> = fraction of modern <sup>14</sup>C (pMC + 1σ error)

## 4.2.2 Sea level threshold

The RMI sea level history extending from 5300 cal yr BP to present was reconstructed from previously published (J.I. Tracey and Ladd, 1974; Kayanne et al., 2011; Kench et al., 2014b) survey grade microatoll data recovered at four islands within RMI (**Table 4.2**). Intertidal corals such as microatolls are believed to be the most precise sea level indicators with an indicative range as low as 3 cm (Smithers and Woodroffe, 2000). Living microatolls are precisely constrained by modern sea level and as such the age of fossil microatolls and the height of living microatoll corals (HLC) can be used to infer MSL for a specific time in the past.

**Table 4.2:** Reassessment of RMI Holocene sea level curve

Island	Sample name	14C Age	Median age	MSL (m)	Adjusted for HLC (m)	Sample type
<sup>1</sup> Majuro	MJ-Ap-02, MJ-Ap-06,	2350 ± 50, 2460 ± 40	2414	0.36	1.09	microatoll species undefined
<sup>1</sup> Arno	AR-Bk-01, AR-Bk-03, AR-Bk-04 AR-Bk-02	1030 ± 70, 1100 ± 60, 1180 ± 60 1430 ± 50	1110 1020	-0.02 -0.06	0.71 0.67	microatoll species undefined <i>Porites</i> microatoll
<sup>2</sup> Jabat	Wk-29494 Wk-29495	4,776 ± 43 4,989 ± 43	5100 5380	-0.17 -0.53	0.54 0.18	<i>Porites</i> microatoll <i>Porites</i> microatoll
<sup>3</sup> Enewetak	s-1 (GX2626) s-4 (GX2626)	3290 ± 145 2255 ± 130	3160 1910	0.25 0.35	0.98 1.08	<i>Heliopora</i> microatoll <i>Heliopora</i> microatoll

<sup>1</sup>Kayanne et al., 2011; <sup>2</sup>Kench et al. 2014; <sup>3</sup>Tracey & Ladd 1974.

Prior published RMI sea level curves were updated to remove discrepancies amongst marine reservoir values, the confidence interval of reported ages, and lack of survey grade elevation values. Thus, each data point used to construct the revised RMI sea level curve is representative of 1. surveyed elevations reduced to MSL using site specific HLC, and 2. recalibrated radiocarbon ages as described previously for RMI.

Sweet et al., (2017) provide global mean SLR scenarios and associated 1-degree resolution regional sea level estimates and rates given current scientific understanding and assumptions of future greenhouse emissions. This study applied the local SLR projections for Majuro atoll (Sweet et al., 2017) to determine a timeframe of future impacts at RMI. Minimum and maximum sea level threshold values were intersected with the mean sea level value of the low, intermediate, and extreme scenarios to determine a timeframe for island instability for each scenario.

### **4.3 Observations of reef-island formation**

Here we present a detailed chronostratigraphic study for the RMI, and examine island formation in relation to reef-flat development, mid-Holocene sea level change, and hydrodynamic energy. Moving past individual characterizations of islands we seek to propose overarching principles that characterize the depositional history and the timing of windward and leeward reef-islands within a single atoll, and between atoll and reef platform islands. Geologic data collected in this study at Bokollap island (windward Majuro) is supplemented with previously published radiocarbon dates and stratigraphic descriptions from Laura island (leeward Majuro) and Jabat a mid-ocean reef platform island located approximately 230 km west northwest of Majuro atoll (**Figure 4.1**).

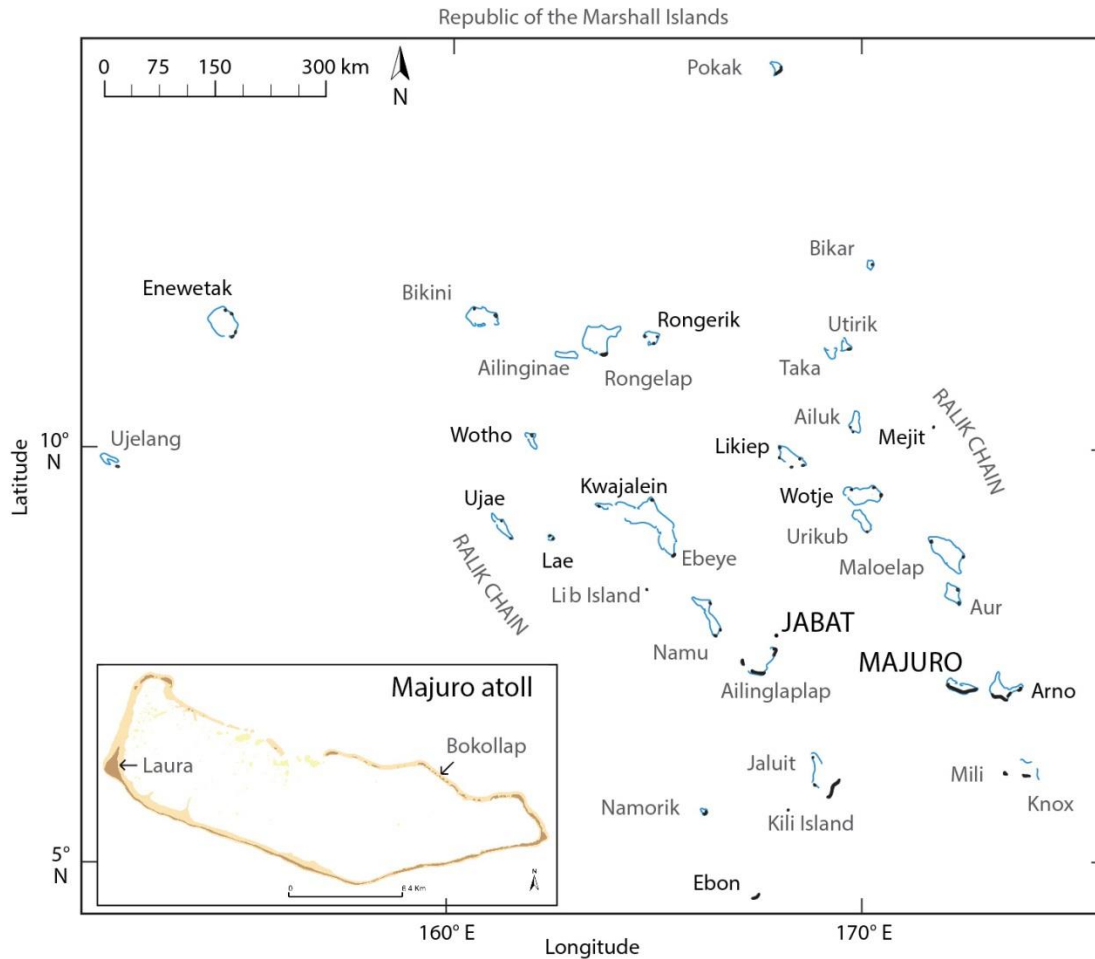


**Figure 4.1:** The Republic of the Marshall Islands. The names of islands mentioned in this study are highlighted in black text. The inset map shows the location of the two reef-islands of interest (Laura and Bokollap) at Majuro atoll.

Previous research at Laura island, a leeward reef-island at Majuro atoll proposed a three phase model of island formation linked to mid-late Holocene sea level change: 1. Active reef progradation, 2. Island emergence, and 3. Island growth (Yasukochi et al., 2014) (**Figure 4.2**). The mid-Holocene highstand has previously been documented at the RMI with peak sea level values of  $+1.13 \pm 0.08$  m approximately 1940-2260 cal yr BP (Kayanne et al., 2011). Following

best practices we present an updated version of the mid-Holocene RMI SLR curve (Figure 2A, see methods). This study finds that the three-phase model for leeward Majuro is valid at all three islands. Despite substantial variability in the timing of each phase both within Majuro and between Majuro and Jabat, island composition and stages of formation are comparable.

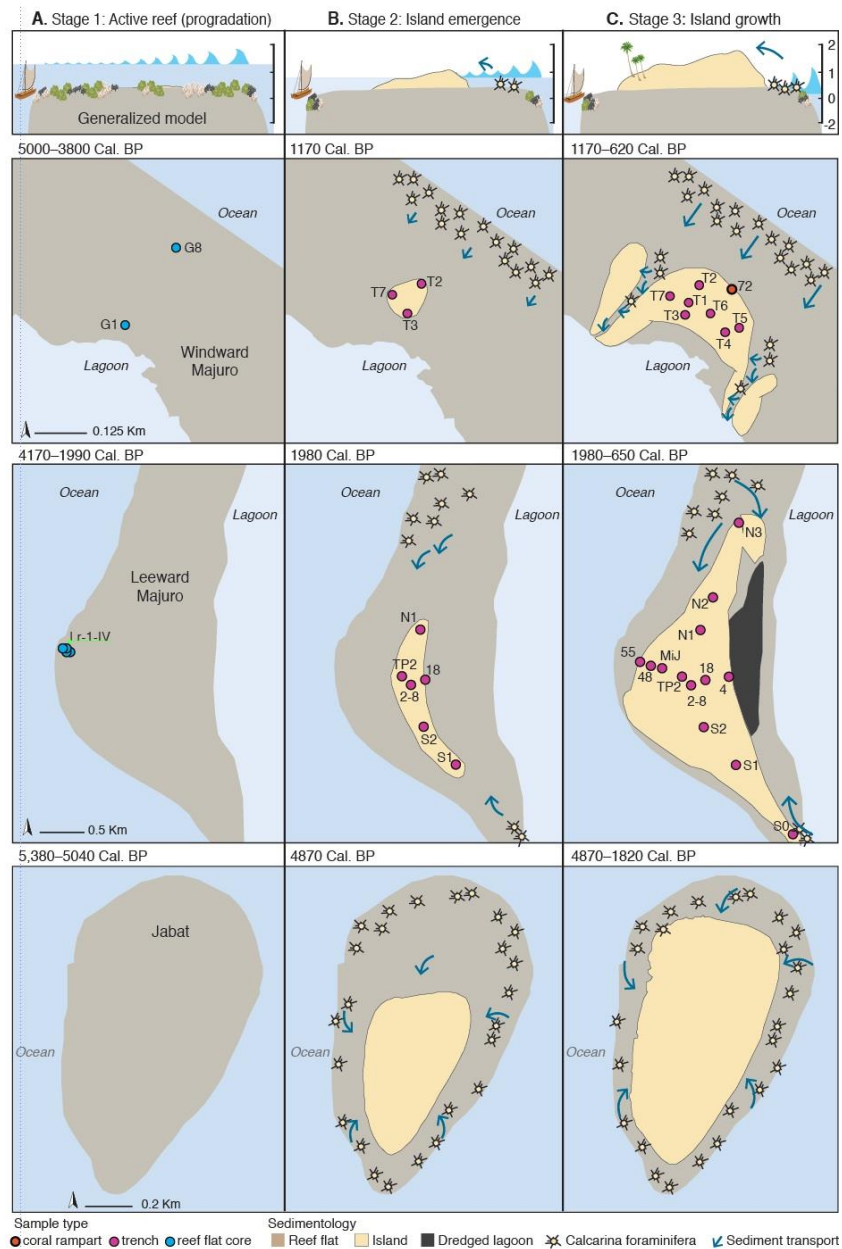


**Figure 4.2:** A four stage, generalized island formation model is based upon geologic data collected at windward Majuro (this study), leeward Majuro (Yasukochi et al., 2014, Figure 7), and Jabat island (Kench et al., 2014). A.) Stage 1, reef-flat progradation as the rate of SLR deaccelerated and limited vertical accretion of reefs. B.) Stage 2, Decreased hydrodynamic energy triggered island building as sediment accumulated on the fossil-reef flat. C.) Stage 3, Rapid island building as *Calcarina* foraminifera replaced coral as the dominant sediment producers along the reef-flat. D.) Stage 4 (not shown) reef-islands stabilized, island building ceased and minimal reconfiguration is limited to island spits and beaches.

As sea level approached the mid-Holocene highstand, decreased accommodation space within the shallow coastal zone limited vertical reef growth triggering reef-flat progradation and the establishment of the limestone basement of reef-islands (**Figure 4.2A**). Lateral reef accretion continued until 5040 cal yr BP at Jabat (Kench et al., 2014b), 1990 cal yr BP at leeward Majuro (Yasukochi et al., 2014), and 3790 cal yr BP at windward Majuro. Closely spaced, geologic reef cores retrieved in this study from Bokollap island (windward Majuro) reveal that the windward reef-flat laterally accreted from the ocean (windward) toward the lagoon. Island emergence was initiated under increased hydrodynamic energy (relative to present) associated with elevated sea level at all three sites (**Figure 4.2B**). Coral gravel accumulated on the reef-flat initiating the formation of an island core prior to the highstand (rising sea level) at Jabat (Kench et al., 2014b), during the highstand at leeward Majuro (Yasukochi et al., 2014), and post highstand (falling sea level) conditions at windward Majuro.

Island growth extended from the island core as decreased wave energy and flow velocities associated with deceleration of SLR and/or sea level fall preferentially transported and deposited very coarse to fine grained sediment (**Figure 4.2C**). Mid-Holocene sea level change resulted in an ecosystem shift where *Calcarina* foraminifera living in turf and macroalgal zones replaced living coral as the dominant reef-flat habitat and island sediment component (41-90% total island sediment) (Kench et al., 2014b; Yasukochi et al., 2014). Furthermore, as reef-flats became intertidal, island growth ceased as the island became decoupled from the reef-flat sediment factory. Here we introduce a phase of island evolution called island stabilization. Despite high sediment production at the reef-flat (Fujita et al., 2009), sea level fall has turned off island building such that many reef-islands are reservoirs of relict, mid- to late- Holocene reef derived sediment with minimal modern sediment deposition limited to spits and beaches.

#### 4.4 Reef-islands will actively evolve under all sea level scenarios this century

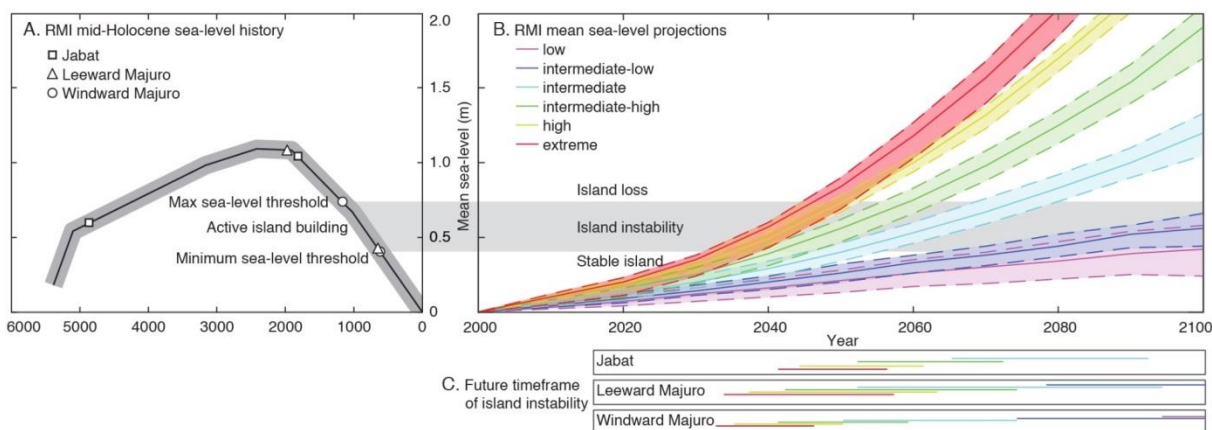
Local sea level thresholds (**Table 4.3**) for mid-Holocene island building at RMI were determined via comparisons amongst the geologic record of reef-islands and the mid-Holocene sea level history (**Figure 4.3A**). The maximum sea level threshold value represents the initiation of mid-Holocene island building, and the minimum sea level threshold value represents island stabilization. Sea level thresholds constrain active island building between 0.6-1.15 m at Jabat, 0.45-1.15 m at leeward Majuro, and 0.40-0.75 m at windward Majuro.

Table 4.3: Sea level threshold values for select islands within the Republic of the Marshall Islands.

Island	Sea level threshold (m)		Future timing of island instability (years AD)		
	Max (island)	Min (island)	Low	Intermediate	Extreme

	initiation)	stabilization)			
Jabat	0.6	1.15	2100+	2070-2090	2040-2060
Leeward Majuro	1.15	0.45	2100+	2050-2090	2030-2060
Windward Majuro	0.40	0.75	2090-	2050-2070	2030-2050
Majuro			2100+		

Leeward Majuro refers to Laura island, and windward Majuro refers to Bokollap island.



**Figure 4.3:** Sea level threshold. A.) Sea level threshold values are determined by comparing the timing of island formation at Jabat island, leeward Majuro, and windward Majuro to the RMI mid-Holocene sea level curve. B.) Mid-Holocene sea level threshold values are compared to future sea level projections (Sweet et al., 2017). Shown here, windward Majuro is currently in a stable island phase, and will experience island instability, followed by island loss as future sea level exceeds threshold values. C.) Local island timeframes of instability predicted for each sea level scenario.

Comparisons of mid-Holocene sea level thresholds to future sea level scenarios (**Figure 4.3B**) for Majuro atoll (Sweet et al., 2017) enable projections of future island instability (**Figure**

**4.3C).** SLR and increased hydrodynamic energy will once again trigger carbonate sediment inputs to reef-islands via a dynamic island building phase related to increased sediment deposition (wave overwash) and shoreline accretion. Assuming no measures are taken to harden shorelines, island loss is anticipated prior to or as sea level exceeds the sea level threshold. Furthermore the methods presented here assume that reef islands will behave the same way during SLR as they did during falling sea level.

Under the most extreme scenario (3.23 m by 2100 (Sweet et al., 2017)) all islands will be erosional by 2060 (Table 4.3). The best case scenario (0.42 m by 2100 (Sweet et al., 2017)) predicts island building will continue beyond 2100. The intermediate scenario (1.2 m by 2100 (Sweet et al., 2017)) predicts that all islands will experience island building by 2070, with a potential for island loss by the end of the century. Of the three islands investigated, windward atoll reef-islands are the most vulnerable to future SLR as reflected by a smaller sea level threshold range, higher modern wave energy, and the greatest reduction in sea level for mid-Holocene island formation. Thus it could be argued that windward islands may be more sensitive to further increases in wave energy associated with future SLR. In addition leeward atoll islands and reef platform islands have lower hydrodynamic energy and larger fossil-reef flats capable of accommodating larger islands both of which may enable sustained island resiliency to future SLR.

## **4.5 Discussion**

### **4.5.1 Sea level thresholds in the context of previous studies**

Previous studies from ‘the recent past’ provide a nearly 70 year record (1943 -2010) of shoreline change and island area variability at 10 of the 34 atoll and mid-ocean reef platform islands (108 reef-islands total) within RMI (Ford, 2012, 2013; Ford and Kench, 2015) (**Table**

**4.4).** During this time, sea level rose between  $1.96 \pm 0.69$  -  $3.60 \pm 1.22$  mm/yr at Kwajalein and Majuro, RMI respectively (<https://tidesandcurrents.noaa.gov/>), which is comparable to a global mean SLR rate of ~3-4 mm/yr (Nerem et al., 2010; Church et al., 2013; Slangen and Jevrejeva, 2017; Vitousek et al., 2017). Thus we conclude that if future SLR follows the low SLR scenario and does not exceed 3 mm/yr by 2100, island stability and or shoreline accretion will continue to be the dominant trend. However accelerated SLR has been documented by satellite altimetry (Nerem et al., 2018), thus it is imperative to look at those SLR projections that incorporate various rates of acceleration. The intermediate and extreme scenarios depict unprecedented rates of SLR twice the local relative long term mean by 2020-2040, and triple the local mean by 2030-2060 (Sweet et al., 2017) (**Figure 4.4**). Although reef-islands have been shown to exhibit a degree of physical resilience (Woodroffe, 2008), it is unclear if these dynamic island landforms will naturally persist under accelerated rates of SLR. Furthermore, analyses of shoreline change since the 1970s have revealed island loss (decreased area) at Wotje , Ebon, and Ujae which may be attributed to SLR or an unresolved shoreline oscillation (Ford, 2013; Ford and Kench, 2015).

**Table 4.4:** Republic of the Marshall Islands shoreline change analysis

Island		% shoreline			Time period (years AD)
		Eroding	Accreting	No change	
<sup>1</sup> Majuro	rural lagoon	19.09	50.73	0.19	1967-2006
	rural ocean	30.68	69.17	11.07	1967-2007
	island average	24.885	59.95	5.63	1967-2007
<sup>2</sup> Jabat	island average	24.36	27.27	48.36	WWII-2010
<sup>2</sup> Ebon	island average	24.36	27.27	48.36	WWII-2010
<sup>2</sup> Lae	island average	10.4	51.73	37.86	WWII-2010
<sup>2</sup> Likiep	island average	13.99	41.85	44.16	WWII-2010
<sup>2</sup> Mejit	island average	26.2	44.74	29.06	WWII-2010
<sup>2</sup> Rongerik	island average	18.12	45.78	36.1	1978-2010
<sup>2</sup> Ujae	island average	33.04	34.24	32.72	WWII-2010

<sup>2</sup> Wotho	island average	12.06	38.86	49.09	WWII-2010
<sup>3</sup> Wotje	ocean	17.28	30.02	52.69	WWII-2010
	lagoon	11.52	47.53	40.96	WWII-2010
	island average	18.19	39.87	41.95	WWII-2010

WWII is defined by Imagery collected between 1943-1945.

<sup>1</sup>Ford 2012; <sup>2</sup>Ford & Kench 2015; <sup>3</sup>Ford 2013

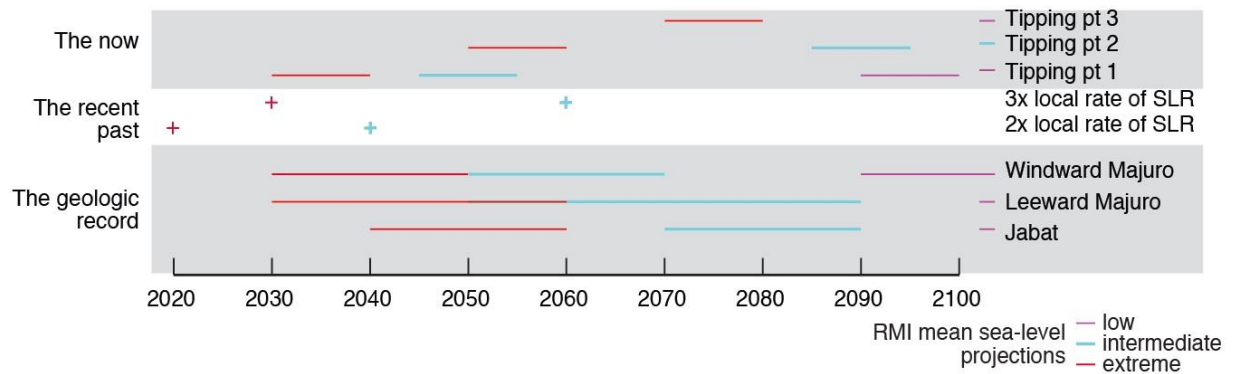


**Figure 4.4:** Exceedance of sea level thresholds provides a time frame for the rapid remobilization of island sediment based upon the geologic record. Comparing the geologic record to previous studies based upon ‘the now’ and ‘the recent past,’ the first half of the century is characterized by exceedance of geologic sea level thresholds and a potential for the permanent loss of potable water (tipping point 1) as the rate of SLR approaches 2-3 times the local long term mean. Assuming no precautions are taken, the second half of the century is characterized by potential island loss (decrease land area) as sea level thresholds, and tipping point 2 are exceeded at all three study site. Sea level exceeds tipping point 3 within this century under the worst case scenario.

Research centered upon ‘the now’ argues that renewed island building due to wave overwash will nonetheless leave islands uninhabitable due to aquifer salinization and damages to agriculture and infrastructure. At Kwajalein atoll, RMI, researchers used wave-driven flood and groundwater models to identify two sea level tipping points (Storlazzi et al., 2018). A 0.4 m of SLR, potable groundwater will no longer be available after two consecutive years of wave overwash because the groundwater aquifer will fail to naturally recover from increased salinity related to marine inundation. A 1.0 m of SLR the majority (50%) of the atoll islands will be flooded annually by wave overwash, compromising the integrity of infrastructure and agriculture.

Assessing the timeframe of sea level thresholds derived in this study within the context of ‘the now’ and ‘the recent past’ we find various outcomes depending upon future SLR scenarios (**Figure 4.4**). The low SLR scenario assumes SLR does not accelerate beyond the historical rate (4 mm/y); rather, impacts will result from the potential loss of potable groundwater and island instability within the last decade (2090-2100). Under the intermediate scenario a doubling of local SLR coupled with the potential loss of potable groundwater is projected for the first half of the century. As sea level exceeds 1 m in the second half of the century, islands may also experience a tripling in the rate of SLR, and island instability across RMI. Only under the worst case scenario is island instability, loss of groundwater, exceedance of 1 m of SLR and a tripling in local SLR anticipated within the first half of this century.

#### **4.5.2 Other considerations for the future stability of reef-islands under elevated sea level**

Sea-level thresholds and future timeframes of instability were derived from the geologic record based upon a number of assumptions. Firstly, we assumed that reef-islands will behave

the same way during SLR as they did as sea level fell during the late-Holocene. During the late-Holocene sea level fell at a rate (-0.50 mm/yr) that is an order of magnitude smaller than the current rate of SLR and two orders of magnitude smaller than the extreme SLR projection by mid-century. Thus it is important to acknowledge that timings of instability based upon the geologic record alone may provide a more conservative approach than also incorporating the ‘the now’ and ‘the recent past.’

All three approaches presented here do not adequately account for future island sediment production and availability. Determining whether islands are continuing to accumulate sediment is essential for their sustainable management (Barry et al., 2007). Growth of carbonate rich reef-islands depends upon the rate and pattern of sediment supply, which are functions of the local reef and reef-flat ecology and hydrodynamic constraints (Woodroffe et al., 2007). It is imperative to improve understandings of the physical and ecological conditions that manifested island building, and ensure continued island maintenance. One of the largest gaps in knowledge in this field is the need for improved understandings of the biogeological linkages between coral reef ecosystems (sediment factories) and atoll reef-islands (sediment reservoirs) (Woodroffe et al., 2007; Dawson and Smithers, 2014). Research at Heron Island, Australia (Scopéltis et al., 2011), Solomon Islands (Saunders, M.I. et al., 2016), Palau (Van Woesik, R. et al., 2015), and Sanya Bay, northern South China Sea (Chen et al., 2018) documents that increased water levels along shallow reefs have created greater accommodation space conducive to increased coral growth and colonization. At RMI renewed coral growth along fossil-reef flats will ultimately result in an ecological shift away from a *Calcarina* and turf algal dominant reef-flat habitat as shallow coral-algal species begin to repopulate. Those islands that are composed primarily of a single sediment constituent such as benthic foraminifera species may be less resilient (most susceptible

to morphologic change) due to higher ecological sensitivity (Perry et al., 2011). Thus the natural resiliency of linked reef-island sediment systems is a function of the ecological sensitivity of dominant sediment producers to environmental and ecological change.

#### **4.5.3 Resiliency of island nations to the rising tide will require shifts in world views**

Future climate change will not only challenge the mindset of atoll islanders but also the world view and values of those living in societies far removed from the rising tide. SLR will challenge host nations through the acceptance and accommodation of islanders who migrate to make a home for their families in foreign lands. There is a growing shift towards in country resettlement (vs. external migration), that is the development and reclaiming of islands as a major adaptation strategy for atoll countries and territories (Webb and Kench, 2010). Because cultural identity of indigenous people is intricately tied to their sense of place many nations are beginning to abandon external migration as a viable option. For example, within the Maldives plans are being made to lease a subset of islands to foreign interests, and couple tourist resorts and natural reserves to generate revenue to support the construction of artificial islands (<https://www.newscientist.com/article/2125198-on-front-line-of-climate-change-as-maldives-fights-rising-seas/>). One such island, Hulhumalé (the city of hope) when completed will be fortified with walls 3 m high, and accommodate 130,000 islanders. Thus SLR impacts are much greater than the loss of remote islands, or disruptions in an islands' ability to naturally evolve with the rising tide. It threatens the cultural identity of sovereign nations. SLR, like all climate related impacts, is a complex physical, social, and dynamic issue that requires adaptable planning methods, multidisciplinary research, and an open minded, multi-world view approach that fosters the ensured existence a peoples identity.

## REFERENCES

- Allen, M.S., 1998, Holocene sea-level change on Aitutaki, Cook Islands: Landscape change and human response: *Journal of Coastal Research*, v. 14, p. 10–22.
- Alley, R.B., and Clark, P.U., 1999, THE DEGLACIATION OF THE NORTHERN HEMISPHERE: A Global Perspective: *Annual Review of Earth and Planetary Sciences*, v. 27, p. 149–182, doi:10.1146/annurev.earth.27.1.149.
- Argus, D.F., Peltier, W.R., Drummond, R., and Moore, A.W., 2014, The Antarctica component of postglacial rebound model ICE-6G\_C (VM5a) based on GPS positioning, exposure age dating of ice thicknesses, and relative sea level histories: *Geophysical Journal International*, v. 198, p. 537–563, doi:10.1093/gji/ggu140.
- Barry, S.J., Cowell, P.J., and Woodroffe, C.D., 2007, A morphodynamic model of reef-island development on atolls: *Sedimentary Geology*, v. 197, p. 47–63, doi:10.1016/j.sedgeo.2006.08.006.
- Barton, J., and Nemra, C., 2012, Republic of the Marshall Islands 2011 Census report:, [http://prism.spc.int/images/census\\_reports/Marshall\\_Islands\\_Census\\_2011-Full.pdf](http://prism.spc.int/images/census_reports/Marshall_Islands_Census_2011-Full.pdf).
- Becker, J., Merrifield, M.A., and Ford, M.R., 2014, Water level effects on breaking wave setup for Pacific Island fringing reefs: *Journal of Geophysical Research: Oceans*, v. 119, p. 914–935, doi:10.1002/2013JC009373.Received.
- Becker, M., Meyssignac, B., Letetrel, C., Llovel, W., Cazenave, A., and Delcroix, T., 2012, Sea level variations at tropical Pacific islands since 1950: *Global and Planetary Change*, v. 80–81, p. 85–98, doi:10.1016/j.gloplacha.2011.09.004.
- Biribo, N., and Woodroffe, C.D., 2013, Historical area and shoreline change of reef islands around Tarawa Atoll, Kiribati: *Sustainability Science*, v. 8, p. 345–362, doi:10.1007/s11625-013-0210-z.
- Bosserelle, C., 2015, Wave Climate Report Majuro.:
- Burley, D., and Addison, D.J., 2015, Tonga and Samoa in Oceanic Prehistory: Contemporary Debates and Personal Perspectives, *in* Cochrane, E.E. and Hunt, T.L. eds., *The Oxford Handbook of Prehistoric Oceania*, New York, Oxford University Press.
- Cai, W. et al., 2015, Increased frequency of extreme La Niña events under greenhouse warming: *Nature Climate Change*, v. 5, p. 132–137, doi:10.1038/nclimate2492.
- Cai, W. et al., 2014, Increasing frequency of extreme El Niño events due to greenhouse warming: *Nature Climate Change*, v. 5, p. 1–6, doi:10.1038/nclimate2100.
- Cai, W. et al., 2012, More extreme swings of the South Pacific convergence zone due to greenhouse warming: *Nature*, v. 488, p. 365–369, doi:10.1038/nature11358.

- Calhoun, R.S., and Fletcher, C.H., 1996, Late Holocene Coastal Plain Stratigraphy and Sea-Level History at Hanalei, Kauai, Hawaiian Islands: *Quaternary Research*, v. 45, p. 47–58, doi:10.1006/qres.1996.0005.
- Chen, T., Roff, G., Mccook, L., Zhao, J., and Li, S., 2018, Recolonization of marginal coral reef flats in response to recent sea-level rise: *Journal of Geophysical Research: Oceans*, v. 123, p. 7618–7628, doi:10.1029/2018JC014534.
- Cheriton, O., Storlazzi, C.D., and Rosenberger, K.J., 2016, Observations and estimates of wave-driven water level extremes at the Marshall: *Journal of Geophysical Research : Oceans*, v. 121, p. 3121–3140, doi:10.1002/2015JC011231.Received.
- Ching, L.L., 2003, KA WA MA MUA, KA WAMA HOPE: University of Hawaii.
- Church, J.A. et al., 2013, Sea level change. In: *Climate Change 2013: The Physical Science Basis. Contribution of Working Group I to the Fifth Assessment Report of the Intergovernmental Panel on Climate Change.*:
- Cobb, K.M., Charles, C.D., Cheng, H., and Edwards, R.L., 2003, El Nino/Southern Oscillation and tropical Pacific climate during the last millennium: *Nature*, v. 424, p. 271–276, doi:10.1038/nature01779.
- Cochrane, E.E., Kane, H., Fletcher, C., Horrocks, M., Mills, J., Barbee, M., Morrison, A.E., and Tautunu, M.M., 2016, Lack of suitable coastal plains likely influenced Lapita (~2800 cal. BP) settlement of Sāmoa: Evidence from south-eastern 'Upolu: *The Holocene*, v. 26, p. 126–135, doi:10.1177/0959683615596841.
- Cochrane, E.E., Rieth, T.M., and Dickinson, W.R., 2013, Plainware ceramics from Samoa: Insights into ceramic chronology, cultural transmission, and selection among colonizing populations: *Journal of Anthropological Archaeology*, v. 32, p. 499–510, doi:10.1016/j.jaa.2013.08.005.
- Conrad, C.P., 2013, The solid earth's influence on sea level: *Bulletin of the Geological Society of America*, v. 125, p. 1027–1052, doi:10.1130/B30764.1.
- Dawson, J.L., and Smithers, S.G., 2014, CARBONATE SEDIMENT PRODUCTION , TRANSPORT , AND SUPPLY TO A CORAL CAY AT RAINE REEF , NORTHERN GREAT BARRIER REEF , AUSTRALIA : A FACIES APPROACH: , p. 1120–1138.
- DeConto, R., and Pollard, D., 2016, Contribution of Antarctica to past and future sea-level rise.: *Nature*, v. 531, p. 591–597.
- Diamond, H.J., Lorrey, A.M., Knapp, K.R., and Levinson, D.H., 2011, Development of an enhanced tropical cyclone tracks database for the southwest Pacific from 1840 to 2010: *International Journal of Climatology*, v. 2250, p. 2240–2250, doi:10.1002/joc.2412.
- Dickinson, W.R., 2014, Beach Ridges as Favored Locales for Human Settlement on Pacific Islands: *Geoarchaeology*, v. 29, p. 249–267, doi:10.1002/gea.21476.

- Dickinson, W.R., 2003, Impact of Mid-Holocene Hydro-Isostatic Highstand in Regional Sea Level on Habitability of Islands in Pacific Oceania: *Journal of Coastal Research*, v. 19, p. 489–502, <http://www.jstor.org/stable/4299192>  
<http://www.jstor.org/page/info/about/policies/terms.jsp>
- Dickinson, W.R., 2009, Pacific atoll living: How long already and until when? *GSA Today*, v. 19, p. 4–10, doi:10.1130/GSATG35A.1.
- Dickinson, W.R., 2001, Paleoshoreline record of relative Holocene sea levels on Pacific islands: *Earth-Science Reviews*, v. 55, p. 191–234, doi:10.1016/S0012-8252(01)00063-0.
- Dickinson, W.R., 2007, Upolu (Samoa): Perspective on Island Subsidence from Volcano Loading: *The Journal of Island and Coastal Archaeology*, v. 2, p. 236–238, doi:10.1080/15564890701520850.
- Dickinson, W.R., Burley, D. V., and Shutler, R., 1994, Impact of hydro-isostatic holocene sea-level change on the geologic context of Island archaeological sites, Northern Ha’apai group, Kingdom of Tonga: *Geoarchaeology*, v. 9, p. 85–111.
- Dickinson, W.R., and Green, R.C., 1998, Geoarchaeological context of Holocene subsidence at the Ferry Berth Lapita Site, Mulifanua, Upolu, Samoa: *Geoarchaeology*, v. 13, p. 239–263, doi:10.1002/(SICI)1520-6548(199802)13:3<239::AID-GEA1>3.0.CO;2-5.
- Duvat, V.K.E., 2018, A global assessment of atoll island planform changes over the past decades: *WIREs Climate Change*, p. 1–16, doi:10.1002/wcc.557.
- Duvat, V.K.E., and Pillet, V., 2017, Shoreline changes in reef islands of the Central Pacific: Takapoto Atoll, Northern Tuamotu, French Polynesia: *Geomorphology*, v. 282, p. 96–118, doi:10.1016/j.geomorph.2017.01.002.
- East, H.K., Perry, C.T., Kench, P.S., Liang, Y., and Gulliver, P., 2018, Coral Reef Island Initiation and Development Under Higher Than Present Sea Levels: *Geophysical Research Letters*, p. 265–274, doi:10.1029/2018GL079589.
- Emery, K.O., Tracey, J.I., and Ladd, H.S., 1954, *Geology of Bikini and Nearby Atolls - Part 1: Geology*: Geological Survey professional paper 260, v. A, p. 1–329.
- Engels, M.S., Fletcher, C.H., Field, M., Conger, C.L., and Bochicchio, C., 2008, Demise of reef-flat carbonate accumulation with late Holocene sea-level fall: Evidence from Molokai, Hawaii: *Coral Reefs*, v. 27, p. 991–996, doi:10.1007/s00338-008-0410-7.
- Fletcher, C.H., and Jones, A.T., 1996, Sea-level highstand recorded in Holocene shoreline deposits on Oahu, Hawaii.: *Journal of Sedimentary Research*, v. 66, p. 632–641, doi:10.1306/D42683CE-2B26-11D7-8648000102C1865D.
- Folk, R.L., and Ward, W.C., 1957, Brazos River bar: a study in the significance of grain size parameters: *Journal of Sedimentary Research*, v. 27, p. 3–26.

- Ford, M., 2013, Shoreline changes interpreted from multi-temporal aerial photographs and high resolution satellite images: Wotje Atoll, Marshall Islands: *Remote Sensing of Environment*, v. 135, p. 130–140, doi:10.1016/j.rse.2013.03.027.
- Ford, M., 2012, Shoreline Changes on an Urban Atoll in the Central Pacific Ocean: Majuro Atoll, Marshall Islands: *Journal of Coastal Research*, v. 279, p. 11–22, doi:10.2112/JCOASTRES-D-11-00008.1.
- Ford, M.R., and Kench, P.S., 2015, Anthropocene Multi-decadal shoreline changes in response to sea level rise in the Marshall Islands: v. 11, p. 14–24.
- Ford, M.R., and Kench, P.S., 2012, The durability of bioclastic sediments and implications for coral reef deposit formation: *Sedimentology*, v. 59, p. 830–842, doi:10.1111/j.1365-3091.2011.01281.x.
- Fujita, K., Osawa, Y., Kayanne, H., Ide, Y., and Yamano, H., 2009, Distribution and sediment production of large benthic foraminifers on reef flats of the Majuro Atoll, Marshall Islands: *Coral Reefs*, v. 28, p. 29–45, doi:10.1007/s00338-008-0441-0.
- Gingerich, S.B., Voss, C.I., and Johnson, A.G., 2017, Seawater-flooding events and impact on freshwater lenses of low-lying islands : Controlling factors , basic management and mitigation: *Journal of Hydrology*, v. 551, p. 676–688.
- Gischler, E., Hudson, J.H., and Pisera, A., 2008, Late Quaternary reef growth and sea level in the Maldives (Indian Ocean): *Marine Geology*, v. 250, p. 104–113, doi:10.1016/j.margeo.2008.01.004.
- Goff, J., Lamarche, G., Pelletier, B., Chagué-Goff, C., and Strotz, L., 2011, Predecessors to the 2009 South Pacific tsunami in the Wallis and Futuna archipelago: *Earth-Science Reviews*, v. 107, p. 91–106, doi:10.1016/j.earscirev.2010.11.003.
- Goodwin, I.D., and Grossman, E.E., 2003, Middle to late Holocene coastal evolution along the south coast of Upolu Island, Samoa: *Marine Geology*, v. 202, p. 1–16, doi:10.1016/S0025-3227(03)00284-6.
- Goto, K., Miyagi, K., Kawamata, H., and Imamura, F., 2010, Discrimination of boulders deposited by tsunamis and storm waves at Ishigaki Island, Japan: *Marine Geology*, v. 269, p. 34–45, doi:10.1016/j.margeo.2009.12.004.
- Grossman, E.E., and Fletcher, I.C.H., 2004, Holocene reef development where wave energy reduces accommodation space, Kailua Bay, Windward Oahu, Hawaii, U.S.A: *Journal of Sedimentary Research*, v. 74, p. 49–63, doi:10.1306/070203740049.
- Grossman, E.E., Fletcher, C.H., and Richmond, B.M., 1998, The Holocene sea-level highstand in the equatorial Pacific: Analysis of the insular paleosea-level database: *Coral Reefs*, v. 17, p. 309–327, doi:10.1007/s003380050132.
- Harney, J.N., Grossman, E.E., Richmond, B.M., and Fletcher, C.H., 2000, Age and composition

- of carbonate shoreface sediments, Kailua Bay, Oahu, Hawaii: *Coral Reefs*, v. 19, p. 141–154, doi:10.1007/s003380000085.
- Hongo, C., and Kayanne, H., 2009, Holocene coral reef development under windward and leeward locations at Ishigaki Island, Ryukyu Islands, Japan: *Sedimentary Geology*, v. 214, p. 62–73, doi:10.1016/j.sedgeo.2008.01.011.
- Humblet, M., Hongo, C., and Sugihara, K., 2015, An identification guide to some major Quaternary fossil reef-building coral genera (*Acropora*, *Isopora*, *Montipora*, and *Porites*): *Island Arc*, v. 24, p. 16–30, doi:10.1111/iar.12077.
- J.I. Tracey, J., and Ladd, H.S., 1974, Quaternary History of Eniwetok and Bikini Atolls, Marshall Islands, in *Proceedings of the Second International Coral Reef Symposium 2*. Great Barrier Reef Committee, Brisbane, p. 537–550.
- Jaffe, B., Buckley, M., Richmond, B., Strotz, L., Etienne, S., Clark, K., Watt, S., Gelfenbaum, G., and Goff, J., 2011, Flow speed estimated by inverse modeling of sandy sediment deposited by the 29 September 2009 tsunami near Satitua, east Upolu, Samoa: *Earth-Science Reviews*, v. 107, p. 23–37, doi:10.1016/j.earscirev.2011.03.009.
- Kahn, J.G., Nickelsen, C., Stevenson, J., Porch, N., Dotte-Sarout, E., Christensen, C.C., May, L., Athens, J.S., and Kirch, P. V., 2014, Mid- to late Holocene landscape change and anthropogenic transformations on Mo’orea, Society Islands: A multi-proxy approach: *The Holocene*, v. 25, p. 333–347, doi:10.1177/0959683614558649.
- Kame`eleihiwa, L., 1992, *Native Land and Foreign Desires: Pehea la E Pono Ai?* Honolulu.
- Kane, H.H., Fletcher, C.H., Frazer, L.N., and Barbee, M.M., 2015, Critical elevation levels for flooding due to sea-level rise in Hawai‘i: *Regional Environmental Change*, v. 15, p. 1679–1687, doi:10.1007/s10113-014-0725-6.
- Kayanne, H., Yasukochi, T., Yamaguchi, T., Yamano, H., and Yoneda, M., 2011, Rapid settlement of Majuro Atoll, central Pacific, following its emergence at 2000 years Cal BP: *Geophysical Research Letters*, v. 38, p. 1–5, doi:10.1029/2011GL049163.
- Kench, P.S., Chan, J., Owen, S.D., and McLean, R.F., 2014a, The geomorphology, development and temporal dynamics of Tepuka Island, Funafuti atoll, Tuvalu: *Geomorphology*, v. 222, p. 46–58, doi:10.1016/j.geomorph.2014.03.043.
- Kench, P.S., Ford, M.R., and Owen, S.D., 2018, Patterns of island change and persistence offer alternate adaptation pathways for atoll nations: *Nature Communications*, v. 9, p. 605, doi:10.1038/s41467-018-02954-1.
- Kench, P.S., McLean, R.F., and Nichol, S.L., 2005, New model of reef-island evolution: Maldives, Indian Ocean: *Geology*, v. 33, p. 145–148, doi:10.1130/G21066.1.
- Kench, P.S., Owen, S., and Ford, M.R., 2014b, Evidence for coral island formation during rising sea level in the central Pacific Ocean: *Geophysical Research Letters*, p. 1–8,

doi:10.1002/2013GL059000.Received.

- Kench, P.S., Owen, S.D., and Ford, M.R., 2014c, Evidence for coral island formation during rising sea level in the central Pacific Ocean: *Geophysical Research Letters*, v. 41, p. 820–827, doi:10.1002/2013GL059000.
- Kendall, R.A., Mitrovica, J.X., and Milne, G.A., 2005, On post-glacial sea level - II. Numerical formulation and comparative results on spherically symmetric models: *Geophysical Journal International*, v. 161, p. 679–706, doi:10.1111/j.1365-246X.2005.02553.x.
- Kirch, P. V., 1983, Man's Role in Modifying Tropical and Subtropical Polynesian Ecosystems: *Archaeology in Oceania*, v. 18, p. 26–31.
- Kirch, P. V., 1993, The To'aga site: Modelling morphodynamics of the land-sea interface, *in* Kirch, P. V. and Hunt, T.L. eds., *The To'aga Site: Three Millennia of Polynesian Occupation in the Manu'a Islands, American Samoa*, Berkeley, University of California, p. 31–42.
- Kirch, P. V., and Yen, D.E., 1982, Tikopia: The prehistory and ecology of a Polynesian outlier: *Bernice P. Bishop Mus. Bull*, v. 238.
- Lambeck, K., Esat, T.M., and Potter, E.-K., 2002, Links between climate and sea levels for the past three million years.: *Nature*, v. 419, p. 199–206, doi:10.1038/nature01089.
- Lambeck, K., Rouby, H., Purcell, A., Sun, Y., and Sambridge, M., 2014, Sea level and global ice volumes from the Last Glacial Maximum to the Holocene: *Proceedings of the National Academy of Sciences*, v. 111, p. 15296–15303, doi:10.1073/pnas.1411762111.
- Mauz, B., Vacchi, M., Green, A., Hoffmann, G., and Cooper, A., 2015, Beachrock: A tool for reconstructing relative sea level in the far-field: *Marine Geology*, v. 362, p. 1–16, doi:10.1016/j.margeo.2015.01.009.
- Mayewski, P.A., Rohling, E., Curtstager, J., Karlén, W., Maasch, K., Davidmeeker, L., Meyerson, E., Gasse, F., Vankreveld, S., and Holmgren, K., 2004, Holocene climate variability: *Quaternary Research*, v. 62, p. 243–255, doi:10.1016/j.yqres.2004.07.001.
- McAdoo, B.G., Ah-Leong, J.S., Bell, L., Ifopo, P., Ward, J., Lovell, E., and Skelton, P., 2011, Coral reefs as buffers during the 2009 South Pacific tsunami, Upolu Island, Samoa: *Earth-Science Reviews*, v. 107, p. 147–155, doi:10.1016/j.earscirev.2010.11.005.
- Mckoy, H., Kennedy, D.M., and Kench, P.S., 2010, Sand cay evolution on reef platforms , Mamanuca Islands , Fiji: *Marine Geology*, v. 269, p. 61–73, doi:10.1016/j.margeo.2009.12.006.
- Merrifield, M.A., Becker, J.M., Ford, M., and Yao, Y., 2014, Observations and estimates of wave-driven water level extremes at the Marshall Islands: , p. 7245–7253, doi:10.1002/2014GL061005.Abstract.
- Mitrovica, J.X., and Milne, G.A., 2002, On the origin of late Holocene sea-level highstands

- within equatorial ocean basins: *Quaternary Science Reviews*, v. 21, p. 2179–2190, doi:10.1016/S0277-3791(02)00080-X.
- Mitrovica, J.X., and Peltier, W.R., 1991, On Postglacial Geoid Subsidence Over the Equatorial Oceans: *Journal of Geophysical Research*, v. 96, p. 20053–20071, doi:10.1029/91JB01284.
- Moberly, R., and Chamberlain, T., 1964, Hawaiian beach systems. *HIG Rep. 64-2*. Hawaii Institute of Geophysics, University of Hawaii.:
- Moore, J.G., Ingram, B.L., Ludwig, K.R., and Clague, D.A., 1996, Coral ages and island subsidence, Hilo drill hole: *Journal of Geophysical Research: Solid Earth*, v. 101, p. 11599–11605, doi:10.1029/95JB03215.
- Morgan, K.M., and Kench, P.S., 2016, Reef to island sediment connections on a Maldivian carbonate platform : using benthic ecology and biosedimentary depositional facies to examine island-building potential: v. 1825, p. 1815–1825, doi:10.1002/esp.3946.
- Muhs, D.R., and Szabo, B.J., 1994, New uranium-series ages of the Waimanalo Limestone, Oahu, Hawaii: Implications for sea level during the last interglacial period: *Marine Geology*, v. 118, p. 315–326, doi:10.1016/0025-3227(94)90091-4.
- Nerem, R.S., Beckley, B.D., Fasullo, J.T., Hamlington, B.D., Masters, D., and Mitchum, G.T., 2018, Climate-change–driven accelerated sea-level rise detected in the altimeter era: *Proceedings of the National Academy of Sciences*, v. 0, p. 201717312, doi:10.1073/pnas.1717312115.
- Nerem, R.S., Chambers, D.P., Choe, C., and Mitchum, G.T., 2010, Estimating mean sea level change from the TOPEX and Jason altimeter missions: *Marine Geodesy*, v. 33, p. 435–446.
- Peltier, W.R., and Fairbanks, R.G., 2006, Global glacial ice volume and Last Glacial Maximum duration from an extended Barbados sea level record: *Quaternary Science Reviews*, v. 25, p. 3322–3337, doi:10.1016/j.quascirev.2006.04.010.
- Perry, C.T., Kench, P.S., Smithers, S.G., and Riegl, B., 2011, Implications of reef ecosystem change for the stability and maintenance of coral reef islands: , p. 3679–3696, doi:10.1111/j.1365-2486.2011.02523.x.
- Perry, C.T., Kench, P.S., Smithers, S.G., Yamano, H., O’Leary, M.J., and Gulliver, P., 2013, Time scales and modes of reef lagoon infilling in the Maldives and controls on the onset of reef island formation: *Geology*, v. 41, p. 1111–1114, doi:10.1130/G34690.1.
- Petchev, F., 2001, Radiocarbon determinations from the Mulifanua Lapita site, Upolu, western Samoa.: *Radiocarbon*, v. 43, p. 63–68, <http://scholar.google.com/scholar?hl=en&btnG=Search&q=intitle:Radiocarbon+determinations+from+the+mulifanua+lapita+site,+upolu,+western+samoa#0>.
- Pirazzoli, P.A., and Montaggioni, L.F., 1988, Holocene sea-level changes in French Polynesia: *Palaeogeography, Palaeoclimatology, Palaeoecology*, v. 68, p. 153–175.

- Quataert, E., Storlazzi, C., Rooijen, A., Cheriton, O., and Dongeren, A., 2015, The influence of coral reefs and climate change on wave-driven flooding of tropical coastlines: , p. 6407–6415, doi:10.1002/2015GL064861.Received.
- Quintus, S., Clark, J.T., Day, S.S., and Schwert, D.P., 2015, Landscape Evolution and Human Settlement Patterns on Ofu Island, Manu'a Group, American Samoa: Asian Perspectives, v. 54, p. 208–237.
- Rearic, D.M., 1990, Survey of Cyclone Ofa Damage to the Northern Coast of Upolu Western Samoa. SOPAC Technical Report 104. SOPAC Technical Secretariat, Suva, Fiji. 37 pp., <http://ict.sopac.org/VirLib/TR0104.pdf>.
- Reimer, P.J. et al., 2013, IntCal13 and Marine13 Radiocarbon Age Calibration Curves 0–50,000 Years cal BP: Radiocarbon, v. 55, p. 1869–1887, doi:10.2458/azu\_js\_rc.55.16947.
- Resig, J.M., 2004, Age and preservation of Amphistegina (foraminifera) in Hawaiian beach sand: Implication for sand turnover rate and resource renewal: Marine Micropaleontology, v. 50, p. 225–236, doi:10.1016/S0377-8398(03)00073-2.
- Richmond, B.M., Buckley, M., Etienne, S., Chagué-Goff, C., Clark, K., Goff, J., Dominey-Howes, D., and Strotz, L., 2011, Deposits, flow characteristics, and landscape change resulting from the September 2009 South Pacific tsunami in the Samoan islands: Earth-Science Reviews, v. 107, p. 38–51, doi:10.1016/j.earscirev.2011.03.008.
- Rieth, T.M., Morrison, A.E., and Addison, D.J., 2008, The Temporal and Spatial Patterning of the Initial Settlement of Sāmoa: The Journal of Island and Coastal Archaeology, v. 3, p. 214–239, doi:10.1080/15564890802128975.
- Saunders, M.I., Albert, S., Roelfsema, C.M., Leon, J.X., Woodroffe, C.D., Phinn, S.R., and Mumby, P.J., 2016, Tectonic subsidence provides insight into possible coral reef futures under rapid sea-level rise: Coral Reefs, v. 35, p. 155–167.
- Scopéltis, J., Andréfouët, S., Phinn, S., Done, T., and Chabanet, P., 2011, Coral colonization of a shallow reef flat in response to rising sea level: quantification from 35 years of remote sensing data at Heron Island, Australia.: Coral Reefs, v. 30, p. 951–965.
- Slangen, A.B.A., and Jevrejeva, F.A.S., 2017, A Review of Recent Updates of Sea-Level Projections at Global and Regional Scales: Surveys in Geophysics, v. 38, p. 385–406, doi:10.1007/s10712-016-9374-2.
- Smithers, S.G., and Woodroffe, C.D., 2000, Microatolls as sea-level indicators on a mid-ocean atoll: Marine Geology, v. 168, p. 61–78.
- Spada, G., Bamber, J.L., and Hurkmans, R., 2013, The gravitationally consistent sea-level fingerprint of future terrestrial ice loss: Geophysical Research Letters, v. 40, p. 482–486.
- Spriggs, M., 1986, Landscape, land use, and political transformation in southern Malanesia, *in* Island Societies: Archaeological Approaches to Evolution and Transformation, p. 6–19.

- Storlazzi, C.D. et al., 2018, Most atolls will be uninhabitable by the mid-21st century because of sea-level rise exacerbating wave-driven flooding: *Science Advances*, v. 4, p. 1–10, doi:10.1126/sciadv.aap9741.
- Storlazzi, C.D., Elias, E.P.L., and Berkowitz, P., 2015, Many Atolls May be Uninhabitable Within Decades Due to Climate Change: Nature Publishing Group, p. 1–9, doi:10.1038/srep14546.
- Storlazzi, C.D., Elias, E., Field, M.E., and Presto, M.K., 2011, Numerical modeling of the impact of sea-level rise on fringing coral reef hydrodynamics and sediment transport: *Coral Reefs*, v. 30, p. 83–96, doi:10.1007/s00338-011-0723-9.
- Stuiver, M., and Braziunas, T.F., 1993a, Modeling atmospheric 14C influences and 14C ages of marine samples back to 10,000 BC: *Radiocarbon*, v. 35, p. 137–189.
- Stuiver, M., and Braziunas, T.F., 1993b, Modeling Atmospheric 14C Influences and 14C Ages of Marine Samples to 10,000 BC: *Radiocarbon*, v. 35, p. 137–189.
- Stuiver, M., Reimer, P.J., and Reimer, R.W., 2019, CALIB 7.1.: <http://calib.org/calib/>, accessed 2019-4-2.
- Sweet, W., Kopp, R., Weaver, C., Obesekera, J., Horton, R., Thieler, E., and Zervas, C., 2017, Global and Regional Sea Level Rise Scenarios for the United States. NOAA Technical Report NOS CO-OPS 083.:
- Terry, J.P., Kostaschuk, R.A., and Garimella, S., 2006, Sediment deposition rate in the Falefa River basin, Upolu Island, Samoa: *Journal of Environmental Radioactivity*, v. 86, p. 45–63, doi:10.1016/j.jenvrad.2005.07.004.
- Vernon, J.E.N., 2000, *Corals of the World* (M. Stafford-Smith, Ed.): Australian Institute of Marine Science.
- Vitousek, S., Barnar, P.L., Storlazzi, C.D., Fletcher, C.H., and Frazer, N., 2017, Doubling of coastal flooding frequency within decades due to sea-level rise: *Scientific Reports*, v. 7, p. 1–9, doi:10.1038/s41598-017-01362-7.
- Webb, A.P., and Kench, P.S., 2010, The dynamic response of reef islands to sea-level rise: Evidence from multi-decadal analysis of island change in the Central Pacific: *Global and Planetary Change*, v. 72, p. 234–246, doi:10.1016/j.gloplacha.2010.05.003.
- Wentworth, C.K., 1922, A scale of grade and class terms for clastic sediments: *Journal of Geology*, v. 30, p. 377–392.
- Van Woesik, R., Golbuu, Y., and Roff, G., 2015, Keep up or drown: adjustment of western Pacific coral reefs to sea-level rise in the 21st century: *Royal Society Open Science*, v. 2, p. 150181, doi:http://dx.doi.org/10.1098/rsos.150181.
- Woodroffe, C.D., 2008, Reef-island topography and the vulnerability of atolls to sea-level rise:

- Global and Planetary Change, v. 62, p. 77–96, doi:10.1016/j.gloplacha.2007.11.001.
- Woodroffe, C.D., McGregor, H. V., Lambeck, K., Smithers, S.G., and Fink, D., 2012, Mid-Pacific microatolls record sea-level stability over the past 5000 yr: *Geology*, v. 40, p. 951–954, doi:10.1130/G33344.1.
- Woodroffe, C.D., McLean, R.F., Smithers, S.G., and Lawson, E.M., 1999, Atoll reef-island formation and response to sea-level change: West Island, Cocos (Keeling) Islands: *Marine Geology*, v. 160, p. 85–104, doi:10.1016/S0025-3227(99)00009-2.
- Woodroffe, C.D., and Morrison, R.J., 2001, Reef-island accretion and soil development on Makin, Kiribati, central Pacific: *Catena*, v. 44, p. 245–261, doi:10.1016/S0341-8162(01)00135-7.
- Woodroffe, C.D., Samosorn, B., Hua, Q., and Hart, D.E., 2007, Incremental accretion of a sandy reef island over the past 3000 years indicated by component-specific radiocarbon dating: *Geophysical Research Letters*, v. 34, p. 1–5, doi:10.1029/2006GL028875.
- Yamaguchi, T., Kayanne, H., and Yamano, H., 2009, Archaeological Investigation of the Landscape History of an Oceanic Atoll: Majuro, Marshall Islands: *Pacific Science*, v. 63, p. 537–565, doi:10.2984/049.063.0405.
- Yamano, H., Cabioch, G., Chevillon, C., and Join, J.-L., 2014, Late Holocene sea-level change and reef-island evolution in New Caledonia: *Geomorphology*, v. 222, p. 39–45, doi:10.1016/j.geomorph.2014.03.002.
- Yamano, H., Miyajima, T., and Koike, I., 2000, Importance of foraminifera for the formation and maintenance of a coral sand cay: Green Island, Australia: *Coral Reefs*, v. 19, p. 51–58, doi:10.1007/s003380050226.
- Yasukochi, T., Kayanne, H., Yamaguchi, T., and Yamano, H., 2014, Geomorphology Sedimentary facies and Holocene depositional processes of Laura Island , Majuro Atoll: *Geomorphology*, v. 222, p. 59–67, doi:10.1016/j.geomorph.2014.04.017.

## Appendix 1. Carbonate Identification

Here I have created a Carbonate ID work book based upon thin section images of cores, and photographs of the modern environment at Majuro atoll. Jodi Harney created something similar from her work in Hawai'i. It was her workbook that started my fascination with fossil carbonates. I hope you find this workbook as helpful as Jodi's workbook was for me.

Me ke aloha,  
Haunani

At Majuro we classified 4 biolithofacies within the fossil reef flat: coral framestone, bindstone, grainstone, and unconsolidated sediment.

### **Coral framestone** (Plates 1-7)

The coral framestone lithofacies is dominated by in situ branching *Acropora* at the seaward reef flat, and *Heliopora Coerulea* within grainstone (27.27% coral and 27.37% calcareous agae) at the lagoon reef flat. Encrustations of foraminifer *Homotrema* are present at the surface of coral (**Figure 3.4A**), and secondary acicular aragonite cements occupy coral pores. With the exception of core G6 (mid seaward reef), corals did not grow above -0.77 - -00.61 m relative to MSL.

### **Bindstone** (Plates 8-13)

Bindstone facies consist of coralline algae (*Hydrolithon gardineri* and *Hydrolithon onkodes*) and foraminifera (*Homotrema*) binding rounded coral rubble (*Acropora*, *Heliopora*, *Porites*, *Favid*, and *Pocillopora*) (**Figure 3.4B**). Minor cements include bladed to acicular aragonite and blocky calcite within coral pores, and calcite rim cements within calcareous algae conceptacle chambers.

### **Grainstone** (Plates 14-16)

The grainstone facies is characterized by *Halimeda* (42.01 ± 13.65%) subfacies, *Calcarina* (31.84%) subfacies, and fine grained, highly abraded skeletal fragments and micrite surrounding rounded coral rubble (**Table 3.3**). Grainstone facies are typically characterized by heavily rimmed calcite cements, while *Calcarina* grainstone subfacies may be more porous.

Unconsolidated sediment facies are composed of rounded coral rubble and fine sand (25.28% *Amphistegina*). Although *Calcarina* is represented in reef flat sediment, benthic foraminifera are minor contributors of overall sediment production relative to the modern reef flat and reef island. Rather the reef framework was either infilled by *Halimeda*, and fragments of calcareous red algae and coral, or the branching corals such as *Heliopora* (G1) may have acted to slow the flow suspended sediment and aid in deposition. Overtime bioclasts were either lithified by low magnesium calcite cements or bound together by encrusting foraminifera and calcareous algae.

**Plate 1**

**Framestone**



Grainstone

branching

***Acropora* (Ac)**

*Acropora* are a dominant species on the seaward reef flat between 1-6 m. *Acropora* can be described based upon morphology.



submassive

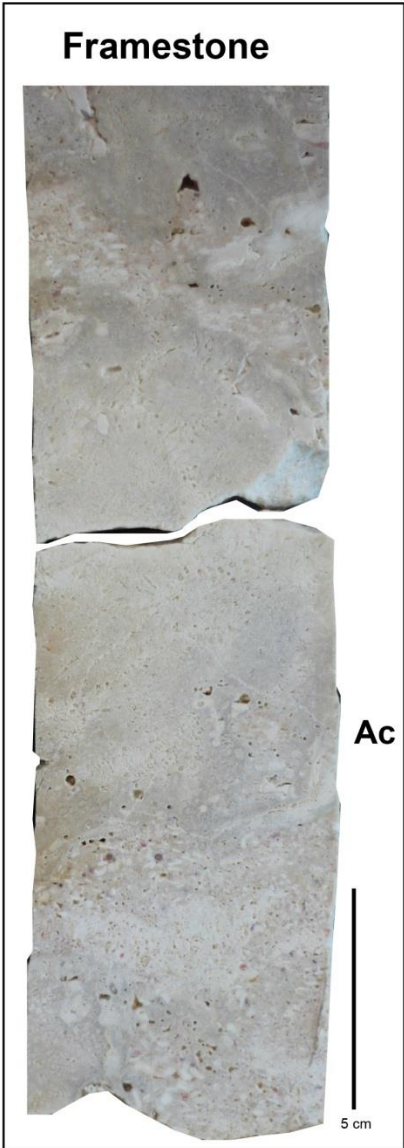


digitate



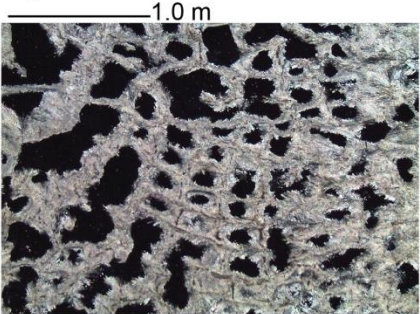
table

Plate 2

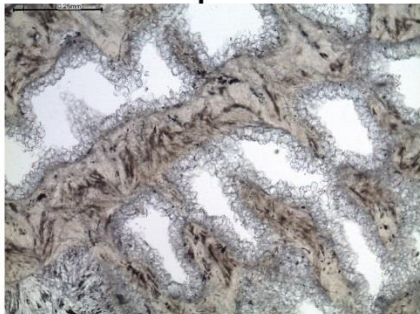


**Acropora (Ac)**

Depicted below is the interstitial space (space between the branches) of *Acropora*.



Acicular aragonite needles extend from the coral skeleton into coral pores.



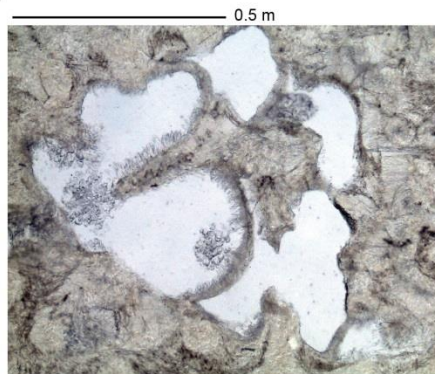
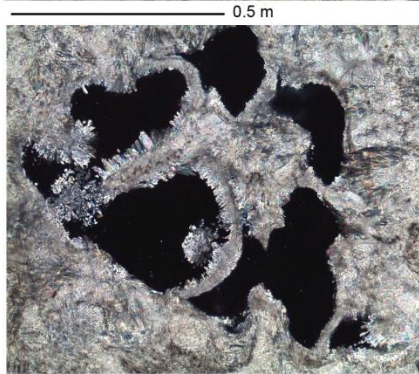
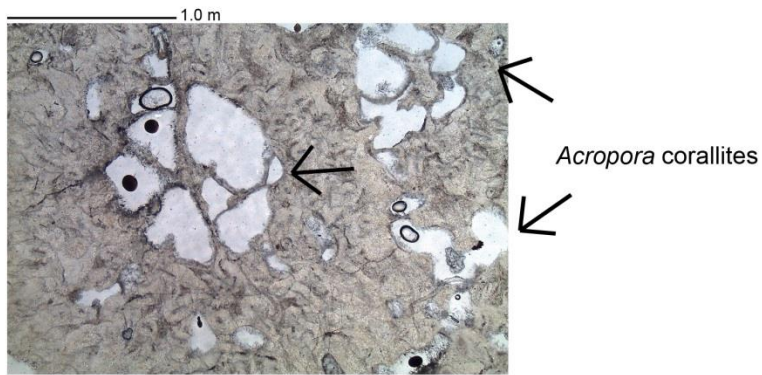
Blocky rimmed cements line coral pores.



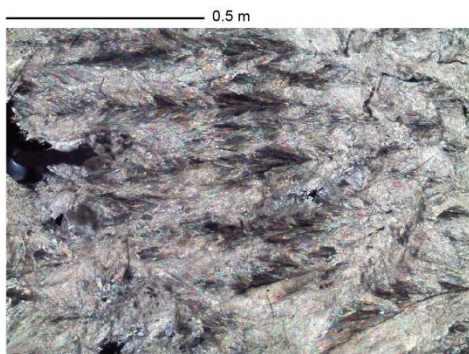
Acicular aragonite needles completely infilling coral pores.

Plate 3

**Acropora (Ac)**

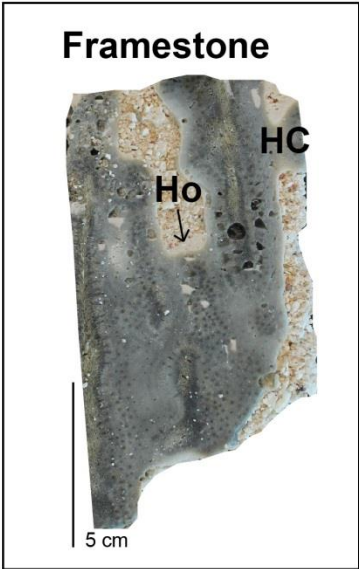


*Acropora* corallites with minimal acicular aragonite cements. Cross polar light (left), plain light (right).



Aragonite cement can be seen within the coral skeleton. Cross polar light (left), plain light (right).

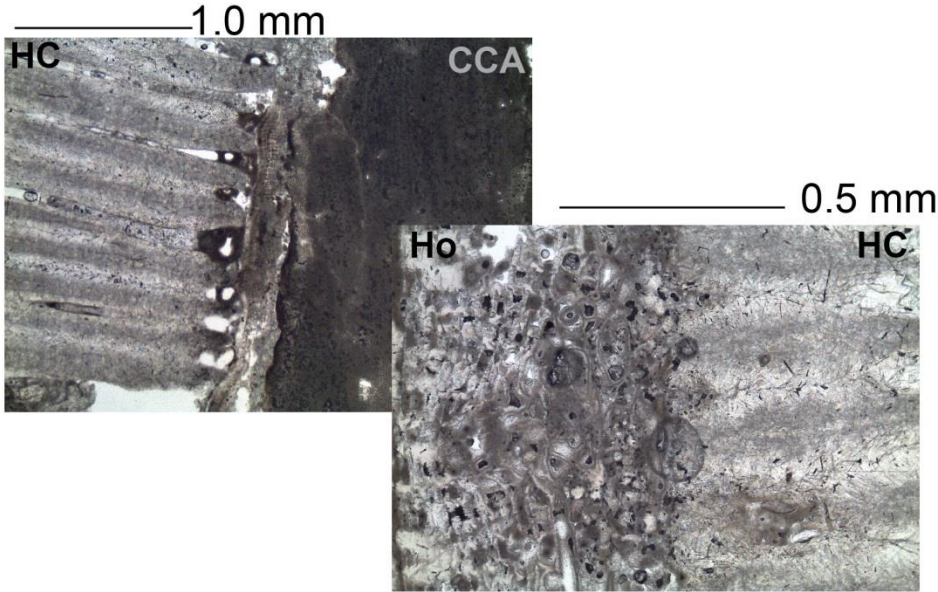
Plate 4



***Heliopora Coerulea* (HC)**



*Heliopora Coerulea* photographed along the seaward reef slope at Bokollap Island.

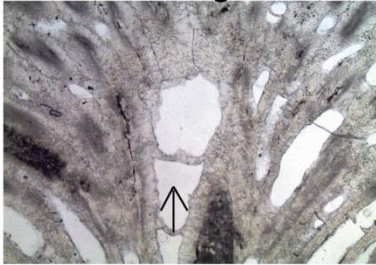


Coral surface is characterized by **Ho**: *Homotrema* (encrusting foraminifera) and **CCA**: Calcareous red algae.

Plate 5

*Heliopora Coerulea* (HC)

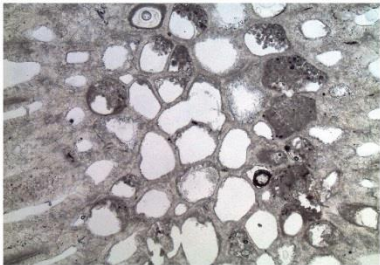
branching coral



1.0 mm

arrow denotes growth direction

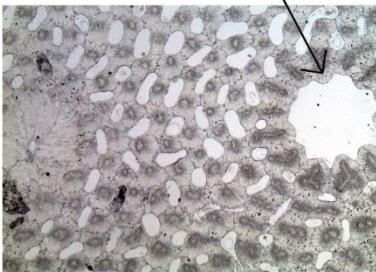
Interbranch space



1.0 mm

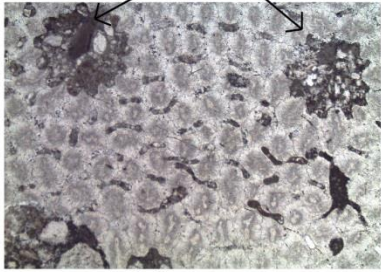
corallites

no secondary cement



1.0 mm

micrite



1.0 mm

acicular aragonite



0.1 mm

XPL

aragonite mesh of needles

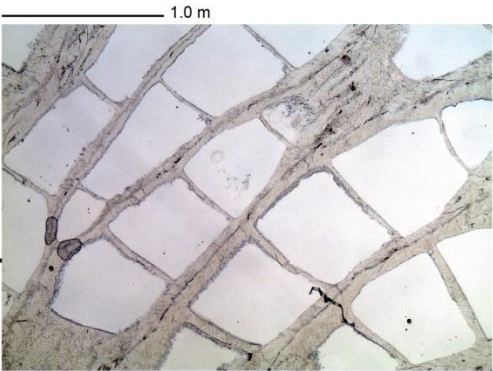


1.0 mm

Plate 6



*Pocillopora* observed on the seaward reef flat.



Acicular cements extending from the coral skeleton.

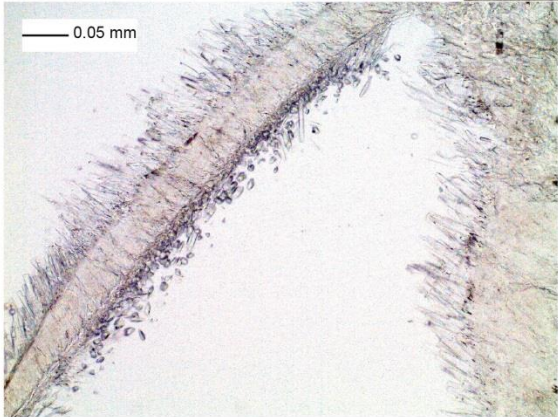
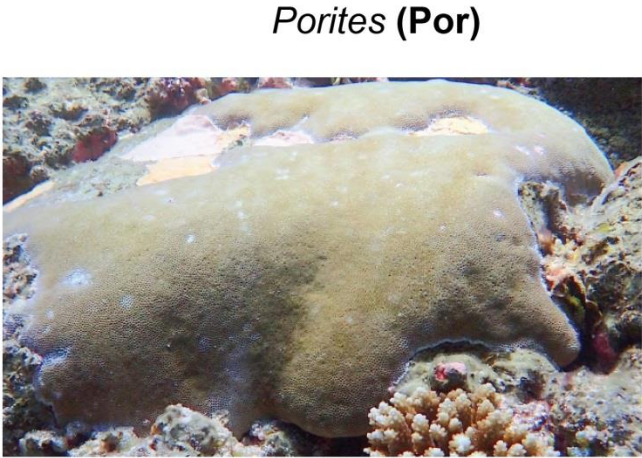
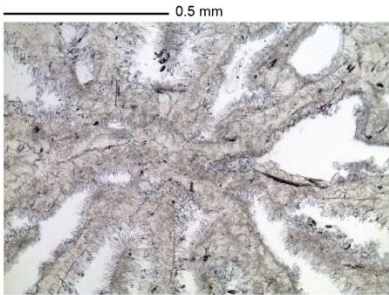
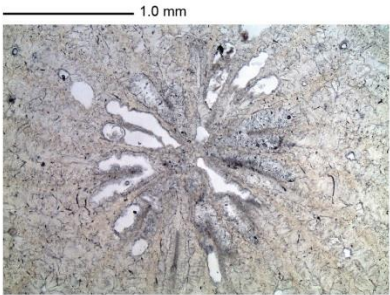


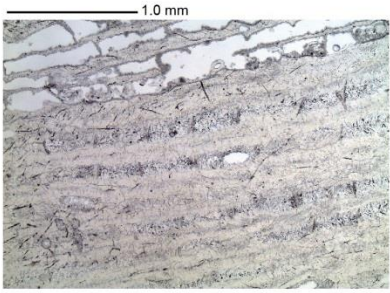
Plate 7



*Porites* (massive) observed at 5 m depth along the seaward reef flat.



*Porites* corallites infilled with minimal acicular aragonite cements.



Acicular cements observed within coral skeleton and within pores (voids).

**Plate 8**

**Calcareous red algae (CCA)**  
*Hydrolithon gardineri* & *Hydrolithon onkodes*



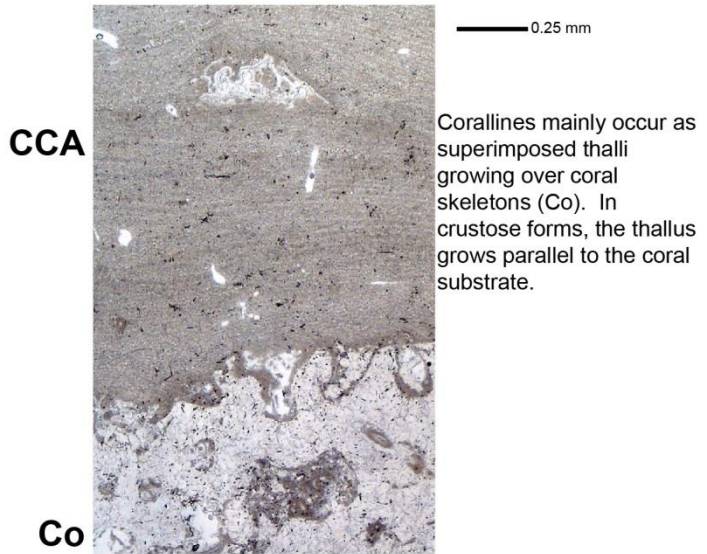
Spur and groove system dissecting modern algal ridge. Top image looks out to see, Bottom image looks northwest. Both photos were taken at low tide.



Plate 9



Crustose coralline algae (CCA)  
*Hydrolithon gardineri* & *Hydrolithon onkodes*



Bindstone facies consist of crusts of coralline algae (*Hydrolithon gardineri* and *Hydrolithon onkodes*) and, or fencrusting foraminifera (*Homotrema*) binding rounded coral gravel.



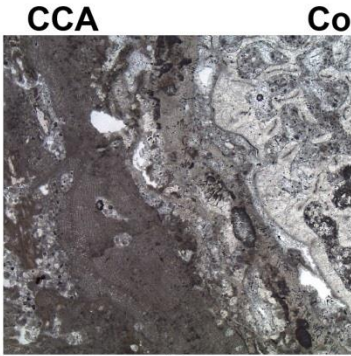
**Plate 10**

**Calcareous red algae (CCA)**  
*Hydrolithon gardineri* & *Hydrolithon onkodes*



**CCA**

0.1 mm

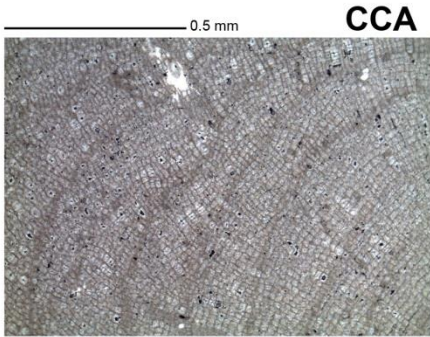


**CCA**

**Co**

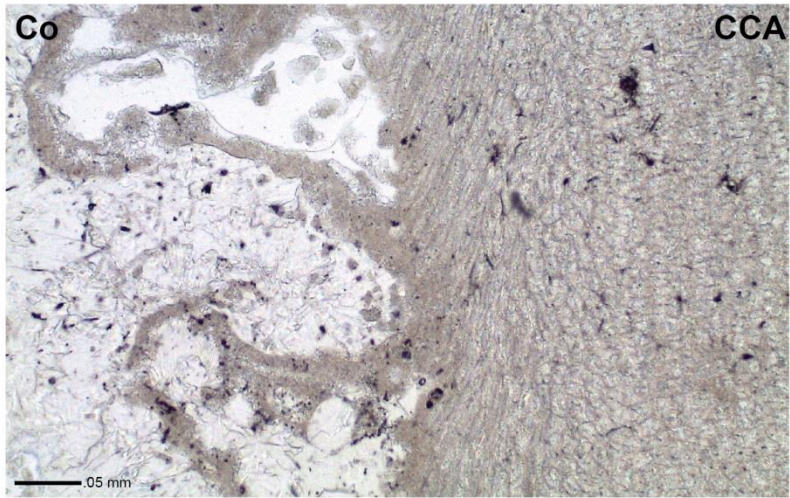
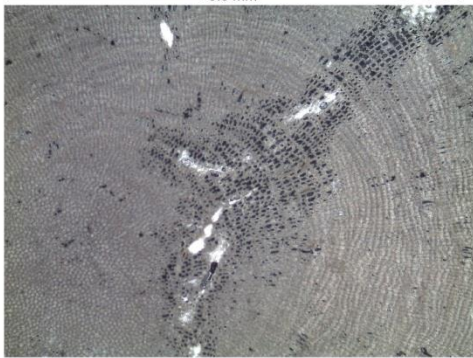
1.0 mm  
0.5 mm

**CCA**



**CCA**

0.5 mm

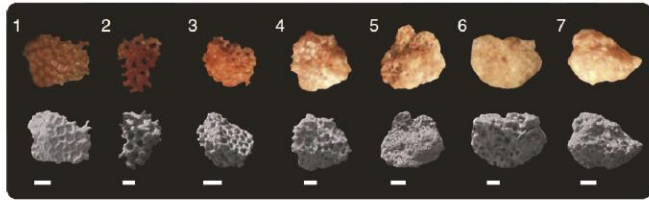


**Co**

**CCA**

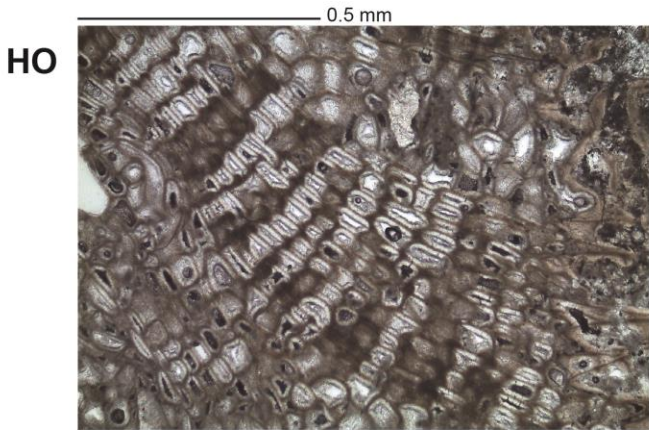
.05 mm

**Plate 11**  
**Encrusting foraminifera**  
*Homotrema* (HO)

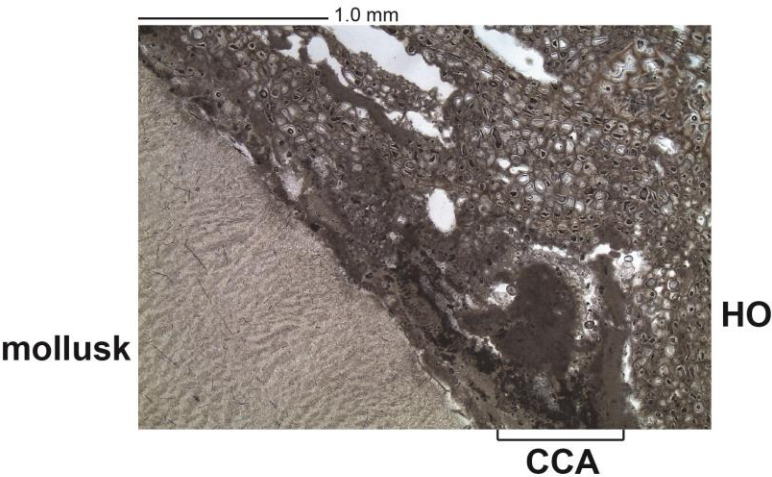


Modern samples of *Homotrema*. Increasing abrasion from sample 1-7. These samples were found in minor (<1%) of unconsolidated beach and island sediment. Figure above taken from Plate 1 in:

Pilarczyk, J.E., Goff, J., Mountjoy, J., Lamarche, G., Pelletier, B., Horton, B.P. 2014. Sediment transport trends from a tropical lagoon as indicated by *Homotrema rubra* taphonomy: wasilis Island Polynesia. *Marine Micropaleontology* 109: 21-29.

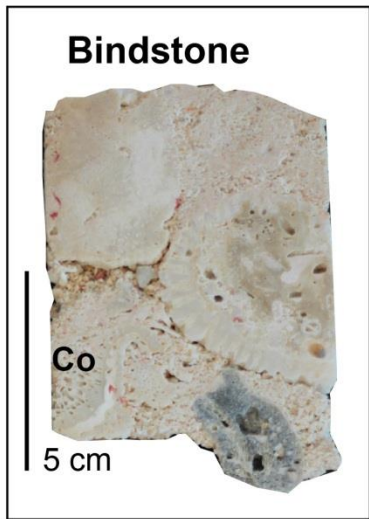


*Homotrema* foraminifera preserved in the fossil record are typically found encrusting coral and coral rubble.

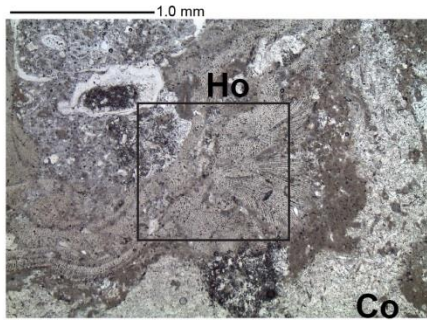


Abundant foraminifera with intermittent coralline algae laminae encrusts a mollusk

Plate 12



***Homotrema* (HO)**  
Encrusting foraminifera



0.25 mm

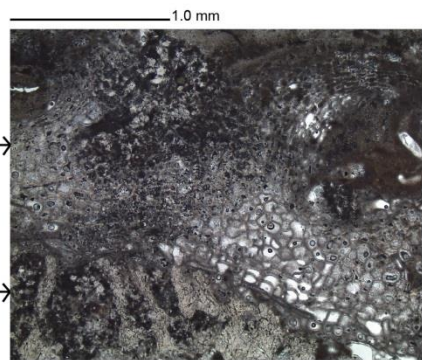
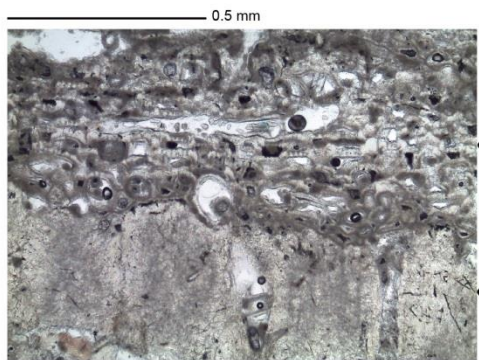
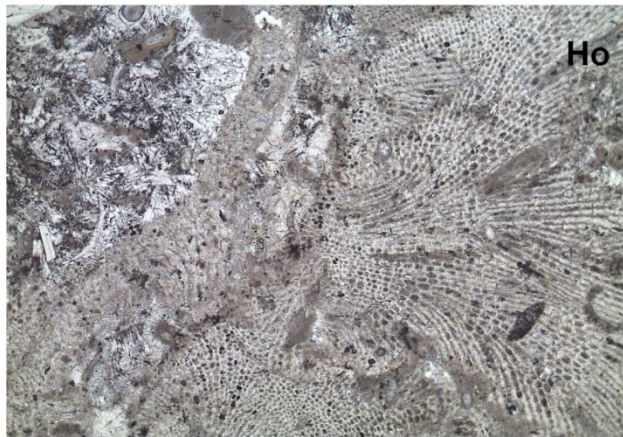
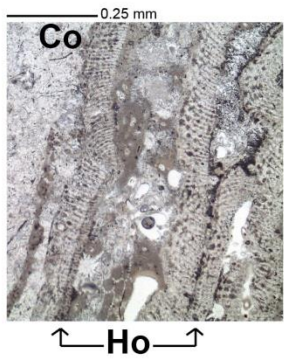
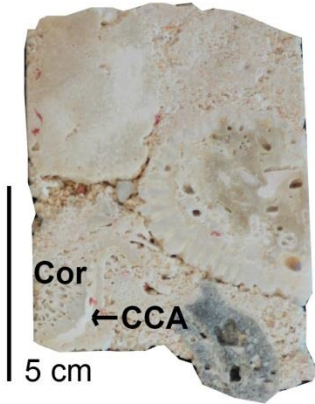


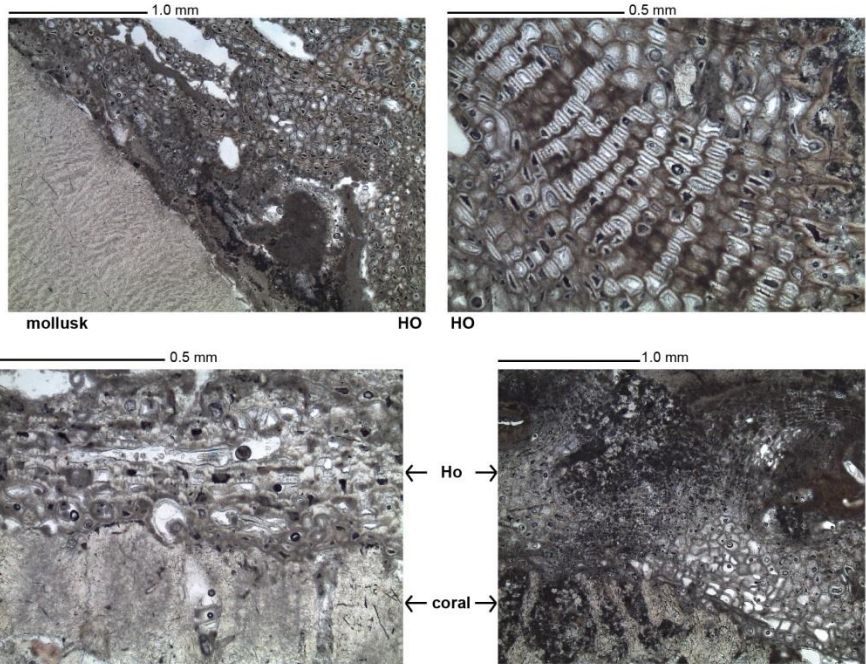
**Plate 13**

**Bindstone**



Note the difference in skeleton structure and organization between foraminifera and crustose coralline alge.

*Homotrema* (HO)  
encrusting foraminifera (below)



Crustose coralline algae (below)

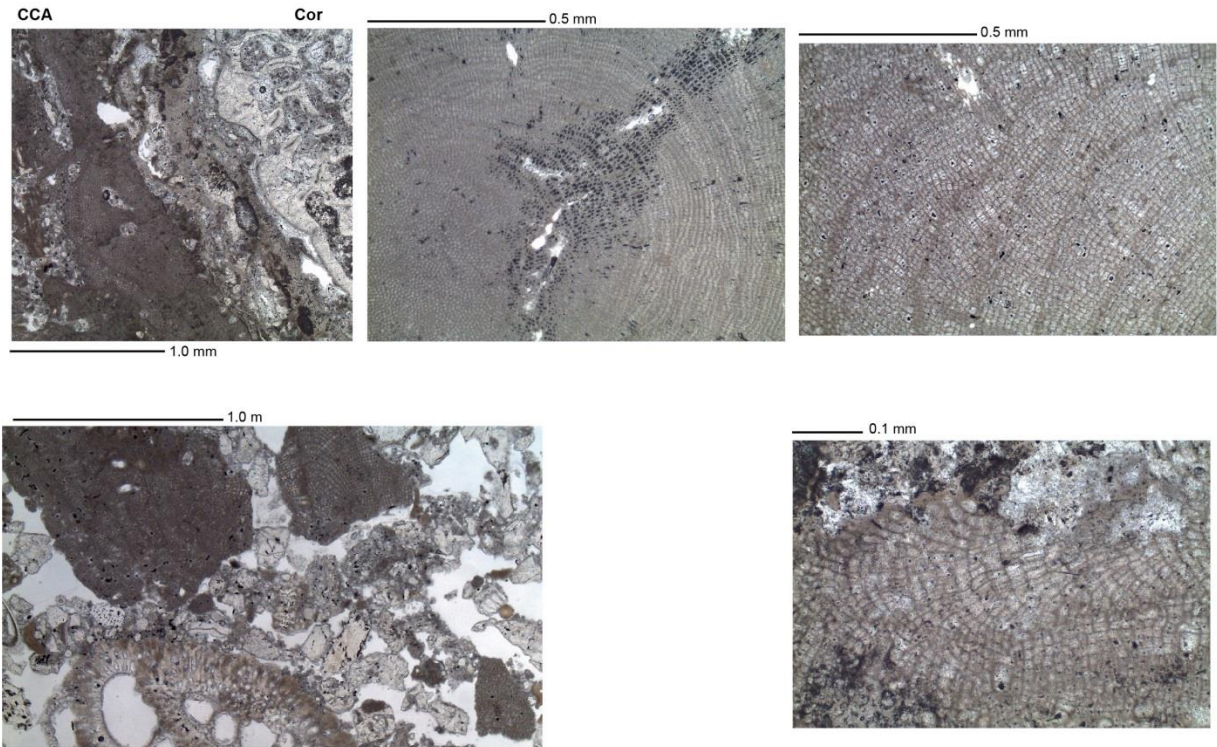
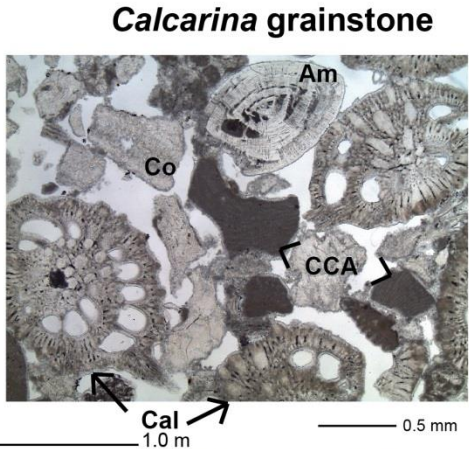
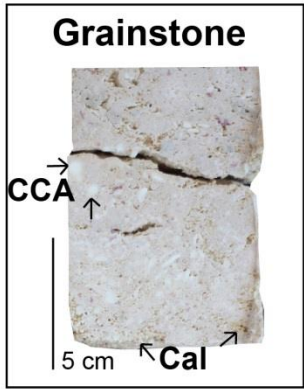
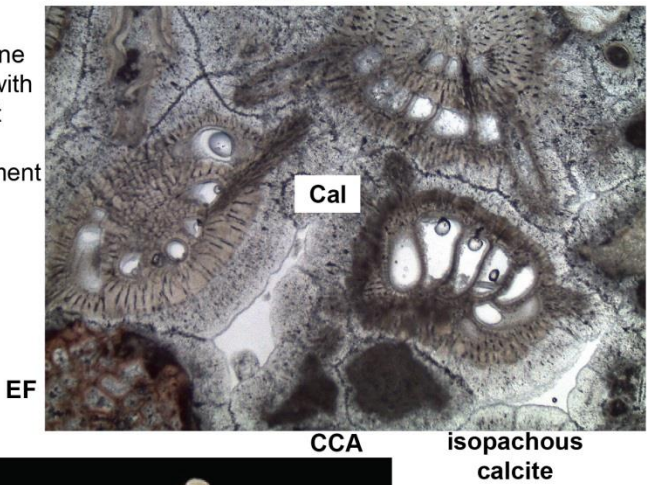


Plate 14



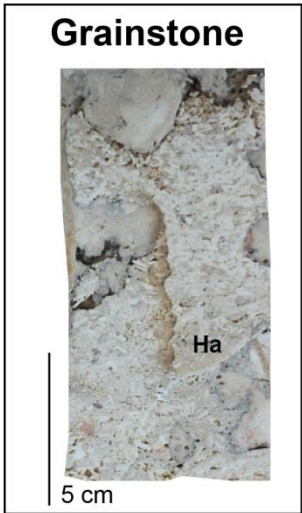
*Calcarina* rich grainstone with spines still intact with minimal calcite cement (top right) and thick isopachous calcite cement (right).



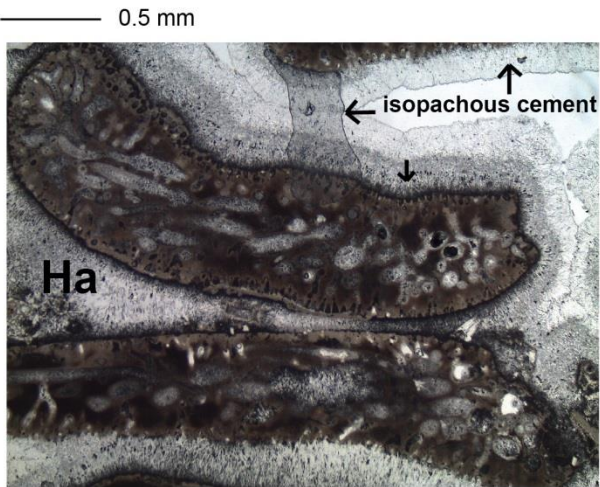
*Calcarina* (whole specimens) with spines still intact (left).

Co: coral, CCA: crustose coralline algae, Cal: *Calcarina*, Ha: *Halimeda*, EF: encrusting foraminifera, Am: Amphistegina foraminifera

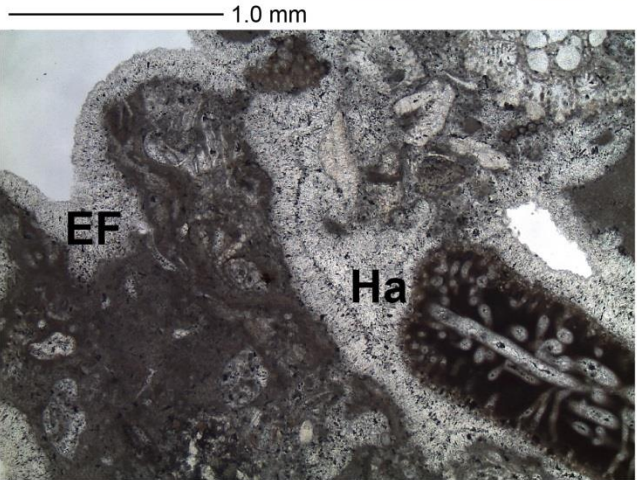
Plate 15



*Halimeda* grainstone



Bioclasts are surrounded by an isopachous calcite cement fringe.



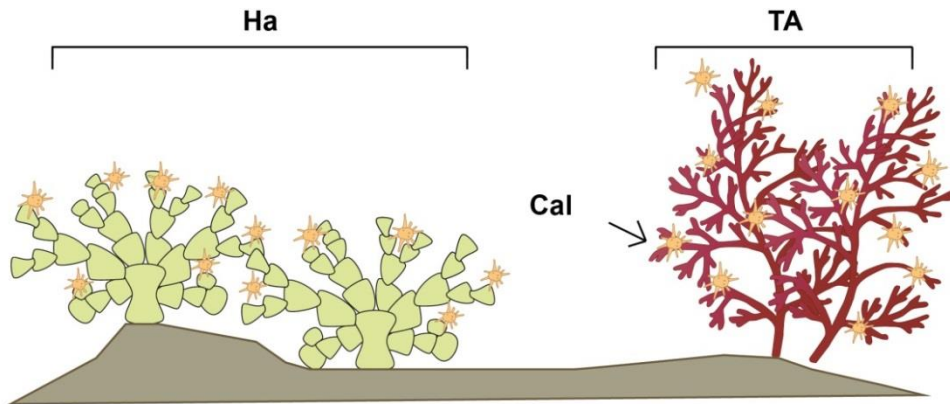
Ha: *Halimeda*,  
EF: encrusting foraminifera

Plate 16

***Halimeda* grainstone**



*Halimeda* (Ha) observed along the shallow (<5 m) seaward reef slope amongst crustose coralline algae (CCA), and *Heliopora Coerulea* (HC) coral.



*Calcarina* (Cal) foraminifera attach themselves to the surface of *Halimeda* (Ha) and turf algae (TA). Along the modern reef flat *Halimeda* is only observed within the shallow channels found between islands. Under higher sea-level *Halimeda* was more abundant along the main reef flat.